

CUBIPOD[®] MANUAL 2016

JOSEP R. MEDINA |
M. ESTHER GÓMEZ-MARTÍN



Cubipod¹ 'O cpwcn'4238

Josep R. Medina
M. Esther Gómez-Martín

EDITORIAL
UNIVERSITAT POLITÈCNICA DE VALÈNCIA

UPV Scientia; Serie Civil Engineering
Cubipod® Manual 2016

Cite this book as: MEDINA, J.R. and GÓMEZ-MARTÍN, M.E., (2016).
Cubipod® Manual 2016. Valencia: Universitat Politècnica de València

The contents of this publication have been evaluated by a double –blind system as can be consulted on the following page
<http://www.upv.es/entidades/AEUPV/info/891747normalc.html>

© Josep Ramon Medina Folgado
María Esther Gómez-Martín

© 2016, Editorial Universitat Politècnica de València
distribution: Telf.: +34 963 877 012 / www.lalibreria.upv.es / Ref.:6350_01_01_01

ISBN: 978-84-9048-538-5 (print version)

All rights reserved. No part of this book may be reprinted or reproduced or distributed in any form or by any electronic, mechanical or other means, now known or hereafter invented, including photocopying and recording, or in any information storage or retrieval system, without permission in writing from the publishers

Contents

Contents	i
Preface	v
Chapter 1. Introduction	1
1.1. Introduction	1
1.2. Mound breakwaters	4
1.3. Quarry materials supply	7
1.4. Concrete supply	9
1.5. Construction, Manufacturing, stacking and placement	12
1.6. Construction costs of Cubipod [®] armors	15
Chapter 2. Hydraulic stability of the armor layer	21
2.1. Introduction	21
2.2. Trunk hydraulic stability of double-layer Cubipod [®] armors ($K_D=28$)	24
2.3. Trunk hydraulic stability of single-layer Cubipod [®] armors ($K_D=12$)	29
2.4. Roundhead hydraulic stability of double-layer Cubipod [®] armors ($K_D=7$)	33

2.5.	Roundhead hydraulic stability of single-layer Cubipod [®] armors ($K_D=5$).....	36
2.6.	Cubipod [®] armors in depth-limited breaking wave conditions.....	40
Chapter 3.	Overtopping and forces on crown wall.....	45
3.1.	Introduction	45
3.2.	Overtopping on double-layer Cubipod [®] armors ($\gamma_f=0.44$).....	48
3.3.	Overtopping on single-layer Cubipod [®] armors ($\gamma_f=0.46$).....	50
3.4.	Forces on the crown wall. Single- and double-layer armors	53
3.5.	Wave reflection. Single- and double-layer armors	58
Chapter 4.	Structural integrity of Cubipod [®] armor units	63
4.1.	Introduction	63
4.2.	Prototype fall tests: Free-fall and extreme free-fall tests	66
4.3.	Concrete to manufacture Cubipods. Tensile strength	69
Chapter 5.	Manufacture, handling and stacking of Cubipods	73
5.1.	Introduction	73
5.2.	Molds and manufacturing of Cubipods in the block yard.....	77
5.3.	Stacking Cubipods. Block yard design.....	80
Chapter 6.	Cubipod [®] placement in the armor	85
6.1.	Introduction	85
6.2.	Toe berm and scour protection	88
6.3.	Placing Cubipod [®] units in the trunk armor.....	91
6.4.	Placing Cubipod [®] units in the roundhead.....	94
6.5.	Transitions for changes in armor thickness	97
Chapter 7.	Example.....	101
7.1.	Introduction	101
7.2.	Design conditions	102

7.3.	Preliminary design and calculations using <i>Cubipod</i> [®] <i>Manual 2016</i>	103
7.4.	Hydraulic stability of armored trunks.....	104
7.5.	Overtopping and breakwater crest design	106
7.6.	Design of toe berm	109
7.7.	Design of core and filter layers	111
7.8.	Design of crown wall	112
7.9.	Estimated construction costs and optimum alternative	119
7.10.	Roundhead design	123
7.11.	<i>Cubipod</i> [®] armor design in breaking conditions.....	128
7.12.	Small-scale tests for validation and design optimization	130
NOTATIONS.....		135
REFERENCES		141
FIGURES.....		145
TABLES.....		149

Preface

This manual serves to guide civil engineers in the preliminary design of mound breakwaters, focusing attention on economic, environmental and logistic factors to be considered when designing Cubipod[®] armors. The Cubipod[®] is a robust precast armor unit which can be used for single- and double-layer armoring. Efficiently manufactured with vertical molds, Cubipods are easy to handle and place with pressure clamps, and may be re-used. Economic savings and logistic efficiency are the greatest advantages of Cubipod[®] armoring when compared to other concrete armor units. SATO (OHL Group) is the exclusive licensee of the Cubipod[®] registered trademark and the patent.

The *Universitat Politècnica de València* (UPV) filed the Cubipod[®] armor unit patent at the Spanish Patent and Trademark Office (SPTO) in 2005 and the Patent Cooperation Treaty (PCT) in 2006. During 2005 and 2006, the inventors of the Cubipod[®] and authors of the *Cubipod[®] Manual 2016* carried out preliminary research in the Laboratory of Ports and Coasts (LPC) at the UPV, revealing the extraordinary hydraulic performance of Cubipod[®] armors, compared to the cube armors frequently used on the coasts of Spain. The patent was licensed exclusively to SATO-OHL in 2007 and the research project CUBIPOD (2007-2010), partially funded by CDTI (Spanish Ministry of Economy and Competitiveness), served to combine the efforts of engineers and technicians from SATO and researchers from the LPC-UPV and other institutions for the full development of the Cubipod[®] unit. SATO-OHL technicians designed an efficient vertical mold to manufacture Cubipod[®] units, whose corresponding patent was filed at the SPTO in 2007. A complete series of studies, prototype drop tests, along with 2D and 3D small-scale physical experiments, were carried out to characterize the hydraulic stability of single- and double-layer Cubipod[®] armors. In addition to SATO-OHL and LPC-UPV, other institutions collaborated in essential tasks, namely *Universidad de Alicante* (UA), *Instituto de Hidrodinámica Aplicada* (INHA), *Instituto de Hidráulica Ambiental de Cantabria* (IH Cantabria), and Aalborg University (AAU).

SATO-OHL also provided funding for the research projects CLIOMARS (2009-2011) and MMONOCAPA (2013-2014) as well as for specific studies and small-scale tests corresponding to breakwaters in which Cubipods were used (San Andrés Breakwater-Málaga, Western Breakwater-Langosteira, etc.). In addition to SATO-OHL and LPC-UPV, other institutions with different test facilities, specifically *Universidad Politécnica de Madrid* (UPM), *Centro de Estudios de Puertos y Costas* (CEPYC), *IH Cantabria*, *INHA* and *Universidade da Coruña* (UDC), provided relevant contributions. Not only have these researchers collaborated with SATO-OHL to improve the characterization of Cubipod[®] armors, but also engineers from *Puertos del Estado* (Spanish Ministry of Public Works and Transport), consulting companies, port authorities (Alicante, Málaga, A Coruña, etc.), and consortiums responsible for the construction of Cubipod[®]

armored breakwaters, such as those of the ports of A Coruña and Las Palmas de Gran Canaria in Spain.

The results of this research and development have been applied to the construction of several Cubipod[®] armored breakwaters along the Spanish Atlantic and Mediterranean coasts. Results have also been presented in three PhD thesis, published in more than forty papers in technical journals and discussed in national and international coastal engineering congresses. The most relevant publications are listed in the References of this *Cubipod[®] Manual 2016*. Regarding to the contents of the present manual, the following civil engineers and researchers deserve special mention for their relevant contribution to the research, development and design of Cubipod[®] armors: Moisés Santos, Rafael Torres, Antonio Corredor, Carlos Fermín Menéndez, Eva Smolka, Vicente Pardo and Jorge Molines. Debra Westall revised the manuscript.

Chapter 1

Introduction

1.1. Introduction

The *Cubipod[®] Manual 2016* provides the basic criteria to design and construct mound breakwaters protected with single- and double layer Cubipod[®] armors. This Introduction describes the main characteristics of rubble-mound breakwaters and Cubipod[®] armoring.

The economic cost of a mound breakwater depends on the environmental conditions and one key factor: the rock or artificial concrete units used for the armor layer. Each geometrical shape (cube, Cubipod[®], Tetrapod, Dolo, Xbloc[®], etc.) requires a specific placement pattern (random, uniform, interlocked, etc.) and each can be placed or not in a single- or double-layer. Each armor unit and placement pattern requires a given armor porosity with different breakwater performance (hydraulic stability, overtopping rates, etc.). A concrete armor unit with higher hydraulic stability (higher stability coefficient, K_D) should be smaller to withstand the design storm, reducing concrete consumption and size of cranes and handling equipment as well as stones in the filter layer.

Cubipod[®] is a massive armor unit belonging to the cube family; Cubipod[®] has a robust design for structural integrity (140-tonne Cubipod[®] units can be manufactured with $f_{ck}[f_{ct,k}]=30[2.0]$ MPa concrete). Cubipods are placed randomly in single- or double-layer armors, and they tend to self-position on the slope with homogeneous armor porosity. Double-layer Cubipod[®] armors show a high hydraulic stability ($K_D=28$); they are especially appropriate to withstand rough seas or relevant design uncertainties (differential settlements, construction quality control, etc.). The double-layer Cubipod[®]

armor is an adequate design alternative for the most adverse construction or environmental conditions given its high hydraulic stability together with its self-arrangement and self-repairing performance. Figure 1.1 shows the double-layer 6-tonne Cubipod[®] armor placed in the San Andrés Breakwater of the Port of Málaga (Spain).

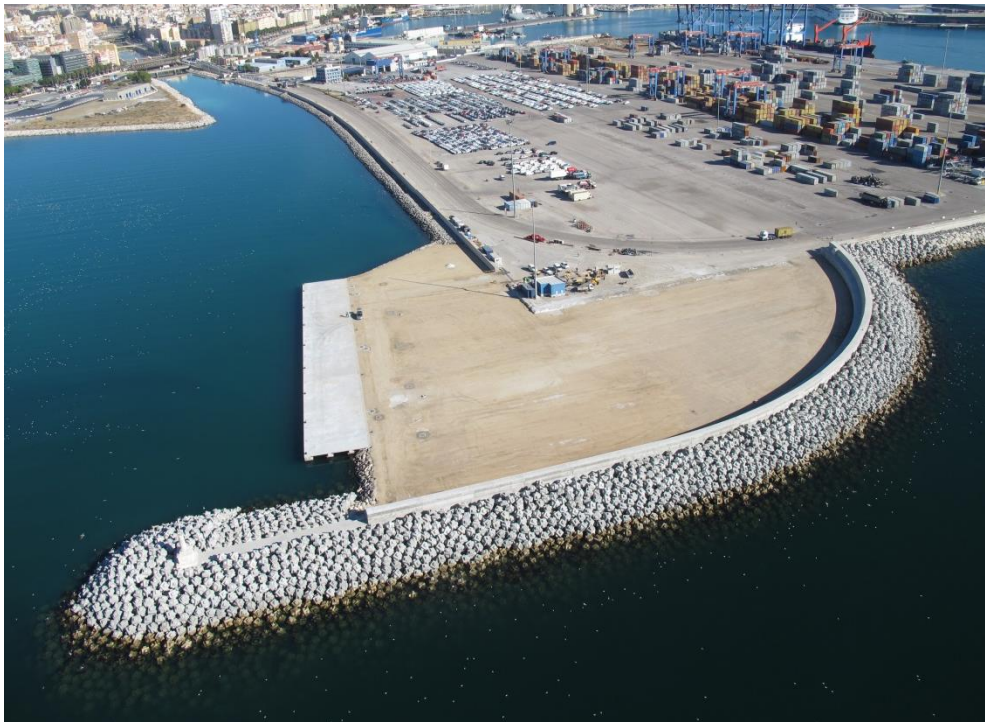


Figure 1.1 Six-tonne Cubipod[®] units in the San Andrés Breakwater of the Port of Málaga (Spain).

A single-layer Cubipod[®] armor ($K_D=12$) has a higher hydraulic stability in the trunk than a conventional double-layer cube armor ($K_D=6$), but a lower hydraulic stability than the double-layer Cubipod[®] armor ($K_D=28$). However, the single-layer Cubipod armor reduces by one-third the concrete required for the double-layer Cubipod[®] armor. For breakwaters which must withstand very rough wave storms ($H_{sd}[m]>12$), single-layer Cubipod armors usually require another single-layer Cubipod[®] armor as a secondary cover layer (using concrete units with a 5-10% mass of units in the first cover layer); the clear advantage of the single-layer is neutralized in these conditions. Figure 1.2 shows a single-layer 25-tonne Cubipod[®] armor, with a 2-tonne quarry-stone underlayer, placed in the Western Breakwater of the Outer Port of A Coruña at Punta Langosteira (Spain).



Figure 1.2 Twenty five-tonne Cubipod[®] units in the Western Breakwater of the Outer Port of A Coruña at Punta Langosteira (Spain).

Compared to slender or bulky interlocking units, the Cubipod[®] is much more robust; much larger units can be manufactured with concrete having lower characteristic compressive and tensile strengths (cheaper concrete). Cubipod[®] manufacturing (2 to 3.5 units/day) and unit stacking (multiple levels) are much more efficient, while its handling is safer and easier using pressure clamps instead of slings. The hydraulic stability of single-layer Cubipod[®] armors is slightly lower than that of armors with interlocking bulky units ($K_D=12 < 15$ or 16) and the recommended slope is less pronounced ($H/V=1.5 < 1.33$); however, the packing density ($\Phi=0.59$) is lower than most interlocking units. Compared to single-layer interlocked armors, Cubipod[®] armors usually require between -3% and +18% additional concrete, depending on the slope and unit used for comparison. This slight disadvantage in the required volume of concrete becomes a clear advantage when taking into account the quality of concrete required as well as the handling and placement of units. Slender and bulky units require concrete with a much higher characteristic tensile strength (much higher cement to volume ratio) than massive concrete armor units such as Cubipods or conventional cubes.

Compared to conventional cubic blocks, Cubipod[®] units are quite similar in terms of robustness, manufacturing, handling with pressure clamps and stacking in the block yard. Cubipods can be used in single- and double-layer armoring, these units are not prone to Heterogeneous Packing (HeP) failure mode and its hydraulic stability is much higher than cube armors. Unlike conventional cubic blocks, which tend to position one face parallel to the slope (favoring sliding) and several faces parallel to those of neighboring units, Cubipods arrange themselves in random orientations and with homogene-

ous armor porosity. For breakwaters designed to withstand low intensity design storms ($5 < H_{sd}[m] < 8$), single-layer ($K_D=12$) and double-layer ($K_D=28$) Cubipod[®] armors reduce concrete consumption by 60% and 40%, respectively. The economic savings are higher for breakwaters under intense design storms ($H_{sd}[m] > 8$) because, in addition to concrete savings in the first cover layer, no concrete is required for the secondary cover layer (depending on the type of quarry stone available at the construction site). Figure 1.3 shows 15-tonne cube and 16-tonne Cubipod[®] units, stacked in the SATO block yard at the Port of Alicante, ready to be used in the prototype drop tests carried out in April 2008 during the CUBIPOD Project (2007-2009).



Figure 1.3 Fifteen-tonne cube and sixteen-tonne Cubipod[®] units in the Port of Alicante (Spain).

1.2. Mound breakwaters

Mound breakwaters are sloping structures composed of layers of stones, protected with a cover layer of selected armor units made up of either natural quarry stones or special concrete units. These sloping structures cause waves to break on the slope, sheltering coastal areas or protecting the shoreline. The armor or primary cover layer, made of large quarry stones or precast concrete units, must withstand the forces generated by

waves breaking on the slope during wave storms. The *Cubipod[®] Manual 2016* focuses on mound breakwaters protected with Cubipod[®] armors.

In addition to the armor layer, mound breakwaters have a core made of heterogeneous and small stones (typically from 1 to 50 kg) which is the most voluminous part of the breakwater. The core must not only reduce wave transmission through the breakwater during service time, but it must also provide a work platform for the terrestrial equipment (cranes, trucks, etc.) during the construction phase. The materials required for the core are usually selected after a sound analysis of both the quarries available at the construction site and the logistics of materials supply; logistics and construction costs are highly dependent on a reliable source of materials.

The armor layer (large quarry stones or concrete units) must not be placed directly on the core because smaller stones escape through the voids of the armor layer. A secondary cover layer and perhaps an additional underlayer, following the filter criterion, should be placed between the armor and the core. These layers of stones or concrete units, with increasing size from the core to the armor, prevent smaller stones from the core being dragged out by wave currents during storms. The filter criterion commonly used for mound breakwaters is simple: the size of the units in the upper layer should not exceed 2.5 times the size of units in the underlayer (mass relation $W/10$ to $W/20$). If this filter criterion is applied, smaller stones from the underlayers are not able to pass through the voids in the outer layers, and the layers remain stable during wave storms. Figure 1.4 shows a typical cross section of a mound breakwater protected by a single Cubipod[®] layer.

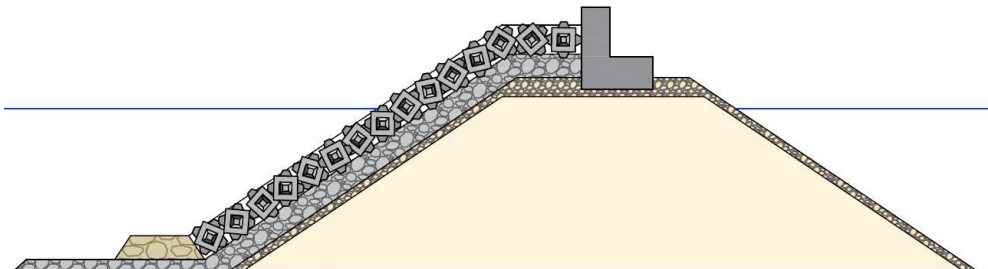


Figure 1.4 Mound breakwater protected by a single-layer Cubipod[®] armor.

The secondary cover layer and filter layer must follow the filter criterion ($W/10$ to $W/20$). Stone filter layers must be at least one meter thick and double the equivalent cube size or nominal diameter ($e_i[m] > \max[1.0, 2D_{n50i} = (W_i/\rho_i)^{1/3}]$). For breakwaters to withstand very rough wave storms ($H_{sd}[m] > 12$), it may be necessary to use a single layer of Cubipod[®] concrete units as a secondary cover layer, when very large quarry stones are not available; in this case, the recommended unit mass is $W_1 = W_0/15$, where W_0 is the mass of the Cubipods in the armor and W_1 is the mass of the Cubipods in the secondary cover layer.

Cubipods are designed to enhance the friction with the underlayer. The size of the protrusions on Cubipod[®] armor units (unit mass W_0) is similar to that of the voids in a layer of quarry stones, thus fulfilling the filter criterion (unit mass $W_1=W_0/15$). The higher friction between layers is achieved when a layer of Cubipod[®] units is placed on a layer of randomly-placed stones; to maximize the friction between layers, ordering the stones in the secondary cover layer is not recommended.

When precast concrete units are used for the armor layer, a toe berm is necessary for an adequate support and a precise placement of the first row of concrete units. A correct toe berm design and construction is relevant in single-layer armoring because the placement of the first row of concrete units affects the upper rows. In the case of interlocking units, the placement of the first row is critical and must follow strict placement criteria to guarantee the prescribed interlocking. Cubipod[®] units show a self-arranging behavior on the slope and tend to achieve homogeneous armor porosity (see Gómez-Martín, 2015). In any case, it is always recommended to place the first row of Cubipods with low error positioning to obtain homogeneous armors.

If the breakwater is placed on a sandy sea bottom with a high risk of scouring, a scour apron and a toe berm are necessary. The construction of the new breakwater tends to create new wave-induced currents along the breakwater which favor scouring near the toe of the structure. If the geotechnical conditions are poor (low bearing capacity, high liquefaction potential, etc.), it may be necessary to dredge the sea bottom and change material, to construct bottom wide berm structures, to pre-load the soil or to make use of other techniques. These techniques increase bearing capacity, reduce long-term settlements and prevent geotechnical failure modes.

Finally, the design process should also take into account the minimum core crest width for an efficient use of the terrestrial construction equipment (cranes, trucks, etc.). It is common to design a crown wall on the breakwater crest to reduce the consumption of materials, to improve accessibility to the breakwater or to reduce overtopping rates. The crown wall is the last element of the mound breakwater to be completed, as it is the most rigid part of the structure; crown walls should be initiated when most breakwater settlements have already occurred. Figure 1.5 shows an image of the construction of a mound breakwater with a voluminous core, a filter layer, a secondary cover layer, a toe berm and a single-layer Cubipod[®] armor.

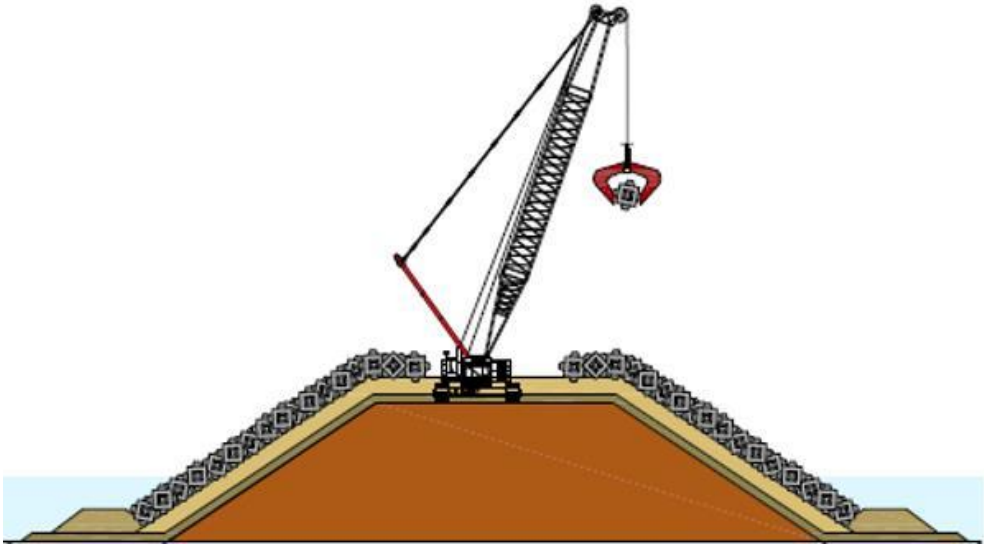


Figure 1.5 Construction of a Cubipod[®] armored mound breakwater.

1.3. Quarry materials supply

Mound breakwaters require relatively large volumes of quarry materials (quarry run, quarry stones of different size ranges, aggregates for concrete, etc.). Obtaining an adequate supply of quarry materials at a reasonable price is usually the greatest logistic challenge and it is essential to keep the overall construction cost low. The feasibility of a specific breakwater design and construction frequently depends on available quarries and equipment as well as transportation systems which can be used to extract and move quarry materials to the construction site.

Quarries located far from the construction site can be exploited to obtain the required stone size or density; however, imported stones are usually very expensive. As a general rule, only small rubble-mound breakwaters, designed to withstand very low intensity wave storms ($H_{sd}[m] < 5$), can be protected using only quarry stones. Larger breakwaters designed to resist intense wave storms usually require precast concrete units for the armor layer and also for the secondary cover layer if the design wave storm is very intense. An exception to this general rule is the statically stable Icelandic-type berm breakwater (see Van der Meer and Sigurdarson, 2014); in this case available quarries are analyzed in detail to define unconventional berm breakwater cross sections to withstand more intense wave storms using a small volume of very large quarry rocks.

The supply of quarry materials is especially relevant when designing large mound breakwaters (volume of materials), for unpopulated areas (equipment and transportation network), environmentally protected islands (available quarries) or large sedimen-

tary areas such as deltas of the largest continental rivers (no rocks available nearby). If suitable quarries are available near the construction site in an unpopulated area (cheap and large rocks but expensive equipment), the Icelandic-type berm breakwater may be a good design alternative. *Cubipod® Manual 2016* refers only to conventional mound breakwaters; berm breakwaters are not analyzed here.

The types of quarries near the construction site always condition the volumes and sizes of stones to be used in the breakwater. If the available quarries are not far from the construction site, the quarry materials supply costs will be low; the larger rock sizes which can be extracted from the quarries (sufficient volume) condition which part of the breakwater can be protected with quarry stones and which part will require concrete armor units. In these conditions, the unit cost (€/m³) of the quarry stones will be much lower than that of concrete units; therefore, the maximum rock size which a quarry can supply will determine the final construction cost.



Figure 1.6 View of a quarry at Punta Langosteira (Spain).

The mass density of quarry materials and aggregates is the first design factor affecting the hydraulic stability of a armor units (rock or concrete). The higher the mass density, the smaller the required armor units and concrete consumption. For a given construction site and wave climate, if the concrete mass density is 4% higher ($\rho_r[t/m^3]=2.40$ rather than 2.30), concrete armor unit mass decreases by 20% and concrete consumption decreases by 7%. Therefore, the mass density of quarry materials and aggregates, as well as the volumes of stones available in the quarries, are usually the two major design factors affecting the logistics and the cost of the breakwater.

In addition to the direct economic cost of the quarry materials, the terrestrial transportation of materials from the quarries to the construction site usually generates a relevant environmental impact (energy consumption, dust, traffic, noise, etc.). For large mound

breakwaters, it is convenient to avoid congestion in the road network by exploiting quarries close to the construction site or those with access to maritime transportation. In these cases, regardless of the location of the quarries, it is essential to take advantage of the high efficiency and low environmental impact of maritime transportation systems (barges) to place most of the submerged part of the breakwater (core, filter layer, etc.), reducing traffic on the breakwater crest when transporting of quarry materials and precast concrete units.

A reasonable design for a mound breakwater requires a previous detailed analysis of the available quarries to adapt the design to the volumes of each class of materials which can be supplied at an acceptable price. One of the secondary objectives of the design will be to minimize the volume of quarry materials to be extracted from the quarry but not used in the breakwater. If only a small part of the quarry materials are used in the breakwater, the economic, logistic and environmental impact will be significant. The best economic and environmental design allows all materials extracted from the quarries to be used.

Quarry availability, wave climate and seafloor at the construction site, are three factors which condition the breakwater design. Wave climate and bathymetry determine the design storm at the toe of the structure (H_{sd}). Sea bottoms (rocky, sandy, etc.) condition the breakwater foundation; a sandy seafloor will require a bedding layer or apron to prevent scour. If the bearing capacity is low, pre-load construction phases and wide bottom berms may be necessary to prevent uncontrolled settlements.

The design storm at the breakwater toe should be calculated first, and the breakwater foundation (bedding layer, berms and scour protection) is designed later. Once the wave climate and the structure foundation are defined, the available quarries determine the volume of stones of different sizes to be used in the breakwater. Core, berms, filter layer and quarry-stone main and secondary cover layers should be designed according to the quarry exploitation plan. Available quarries are relevant for construction logistics and breakwater design. This is especially true for large breakwaters (huge quarry materials volumes to be transported) and breakwaters designed to withstand intense wave storms (it may be necessary to use concrete units for the secondary cover layer if the quarries are not able to provide sufficient stones of the appropriate size).

1.4. Concrete supply

Mound breakwaters designed to withstand moderate or intense wave storms ($H_{sd}[m]>5$) usually require precast concrete units for the breakwater. *Cubipod[®] Manual 2016* refers to the use of Cubipod[®] units in the armor layer.

For any given wave climate and construction site, the volume of concrete required for the armor layer depends on decisions taken during the design process. The concrete consumption (V) is approximately proportional to $L \times H_{sd}^2$, where L is the breakwater length and H_{sd} is the design significant wave height. The volume of concrete used in

the armor layer (V) also depends on the selection of the armor unit (Cubipod[®]), number of layers (single- or double-layer) and packing density (e.g. $\phi=0.59$). The unit placement indirectly affects concrete consumption because placement conditions armor porosity. For slope cot $\alpha=1.5$, single- and double-layer Cubipod[®] armors require an approximate concrete supply given by

$$V_{\text{single-layer}}[\text{m}^3] \approx 0.9 \times L_b[\text{m}] \times H_{sd}^2[\text{m}^2] \text{ and } V_{\text{double-layer}}[\text{m}^3] \approx 1.3 \times L_b[\text{m}] \times H_{sd}^2[\text{m}^2]$$



Figure 1.7 Concrete being poured into the molds to manufacture 25-tonne Cubipod[®] units.

Concrete supply is usually a relevant economic and logistic factor affecting large mound breakwater construction, after the quarry materials supply described previously. Concrete is an artificial material which does not usually have quality or quantity restrictions; however, the unit cost ($\text{€}/\text{m}^3$) may vary significantly depending on the construction site (unit cost differs considerably from country to country), concrete characteristics and volume to be supplied. The characteristic tensile strength (f_{ctk}) is often the critical variable to design unreinforced concrete armor units, although characteristic compressive strength (f_{ck}) is the variable systematically controlled during the manufacturing process.

The compressive strength of unreinforced concrete is much higher than the tensile strength; therefore, unreinforced armor units break when flexures or torsions generate significant tensile stresses exceeding the tensile strength limit. Fragile breakage is likely to occur when the maximum tensile stress is similar to the mean tensile strength (f_{ctm}). The maximum tensile stress created within the armor unit (handling, placement, etc.) depends mainly on size and unit geometry. For a given unit size, tensile stress is higher for a slender armor unit than for a massive one. For a given armor unit and han-

dling and placement procedure, larger units generate higher stress because the static loads are proportional to $D_n^3=(W/\gamma_r)$ and the strength is proportional to D_n^2 ; compressive and tensile strengths are roughly proportional to D_n .

According to EHE-08 (Eurocodes), if $f_{ck}<50$ MPa, the 5% characteristic tensile strength (f_{ctk}) can be estimated by $f_{ctk}=0.21f_{ck}^{2/3}$, where f_{ck} [MPa] and f_{ctk} [MPa] are the characteristic compressive and tensile strengths at 28 days, respectively.

Prototype drop tests carried out by Medina et al. (2011) confirmed that conventional cube block and Cubipod[®] are massive armor units with similar robustness and structural strength. According to Burcharth and Maciñeira (2015), no structural integrity problems were observed during the manufacturing, handling and placement of 150-tonne (D_n [m]=4.00) cubes for the 3.35 km-long main breakwater of the Outer Port at Punta Langosteira (A Coruña, Spain). Taking into account a characteristic compressive strength f_{ck} [MPa]=31 for concrete used in these cubic blocks, the characteristic tensile strength (f_{ctk}) can be estimated by f_{ctk} [MPa]= $0.21f_{ck}^{2/3}=2.1$. Assuming a linear relationship between armor unit size (D_n) and characteristic tensile strength (f_{ctk}) and a concrete unit weight γ_r [t/m³]=2.35, Table 1.1 shows the required minimum characteristic tensile strength as $f_{ctk}(D_n)=2.1(D_n/4.00)$, and the estimated minimum characteristic compressive strength as $f_{ck}(D_n)=(f_{ctk}(D_n)/0.21)^{3/2}$, where D_n is given in meters and f_{ck} and $f_{ct,k}$ in MPa.

Table 1.1 Minimum characteristic compressive and tensile strengths at 28 days for concrete to manufacture cube and Cubipod[®] armor units.

γ_r [t/m ³]=2.35		$f_{ck}(D_n$ [m]=4.00)=31 MPa	
W[t]	D_n [m]	f_{ck} [MPa]	$f_{ct,k}$ [MPa]
150	4.00	31	2.1
130	3.81	29	2.0
110	3.60	27	1.9
90	3.37	24	1.8
80	3.24	23	1.7
70	3.10	21	1.6
60	2.94	20	1.5
50	2.77	18	1.4
40	2.57	16	1.3

Source: Authors' elaboration

In accordance with Table 1.1, cube and Cubipod[®] units with W [t]≤60 can be manufactured using concrete with a characteristic compressive strength f_{ck} [MPa]=20 (f_{ctk} [MPa]=1.5). This design criterion has a considerable safety margin as seen in the case of 70-tonne (D_n [m]=3.1) conventional cubes manufactured, handled and placed in the Southern Extension of the Port of Valencia (1991-1995), using concrete with a

characteristic compressive strength $f_{ck}[\text{MPa}] = 18$ ($f_{ctk}[\text{MPa}] = 1.4$). To date, no significant structural integrity problems during construction or service time (over twenty years) have been observed. Table 1.1 shows the minimum characteristic compressive and tensile strengths at 28 days, required to manufacture cube and Cubipod® armor units; however, national codes may impose more restrictive limits than those given in Table 1.1 (e.g. $f_{ck}[\text{MPa}] \geq 30$ in EHE-08). As a general rule, using concrete with $f_{ck}[\text{MPa}] \geq 20$ is recommended because the technical and scientific knowledge about this concrete is far superior to that for concrete with very low compressive strength ($f_{ck}[\text{MPa}] < 20$).

In order to increase the characteristic compressive and tensile strengths of unreinforced concrete, a significant increase in the unit cement consumption [kg/m^3] and the unit economic cost [$\text{€}/\text{m}^3$] is often necessary. As a rule of thumb, an increase in the characteristic compressive strength $\Delta f_{ck}[\text{MPa}] = 10$ ($\Delta f_{ct,k}[\text{MPa}] \approx 0.5$) will increase the unit cost [$\text{€}/\text{m}^3$] of the concrete supply by 10%.

Vertical formworks for cube and Cubipod® units can be lifted 6 to 8 hours after concrete pouring and vibration. Units are usually moved to the stacking area 24 hours after vibration. In the case of slender armor units, the required minimum characteristic compressive and tensile strengths are much higher than those required for massive armor units. Waiting times for de-molding, handling and transportation to stacking area are much longer for slender armor units; therefore, the number of formworks and the size of the manufacturing areas are much larger for slender units than massive ones.

1.5. Construction. Manufacturing, stacking and placement

The construction of a large mound breakwater requires solving a complex logistical problem. In addition to the quarry materials and concrete supply, an efficient construction demands a robust scheduling of multiple tasks under numerous restrictions in space and time. The overall economic savings depend on the strict scheduling and coordination in time and space of workforce and equipment, and not only on a good design and the use of the best available equipment. Bottlenecks and uncontrolled interruptions must be avoided. Guaranteeing the personal safety of the workforce is usually the best way to avoid personal injuries and to minimize undesired interruptions. The breakwater design and the construction logistics should be guided by economic optimization, simplicity and robustness to withstand environmental conditions (waves, wind, etc.) and unlikely events (accidents, etc.).

When using precast concrete units to construct an armor layer, it is necessary to first solve specific logistic problems associated with the concrete supply, manufacturing, handling, stacking and placement on the slope.

Manufacturing armor units is the first process to be considered when analyzing the construction of the armor layer. In order to calculate the number of formworks to be placed in the production line, it is necessary to take into account the specific armor unit

(e.g. Cubipod[®]), manufacturing cycle, the available space in the block yard and the unit supply requirements for placement in the armor. Cube and Cubipod[®] units can be manufactured at a rate of 2 units/mold/day in 12 hour/day work cycles or 3.5 units/mold/day in 24 hour/day work cycles.

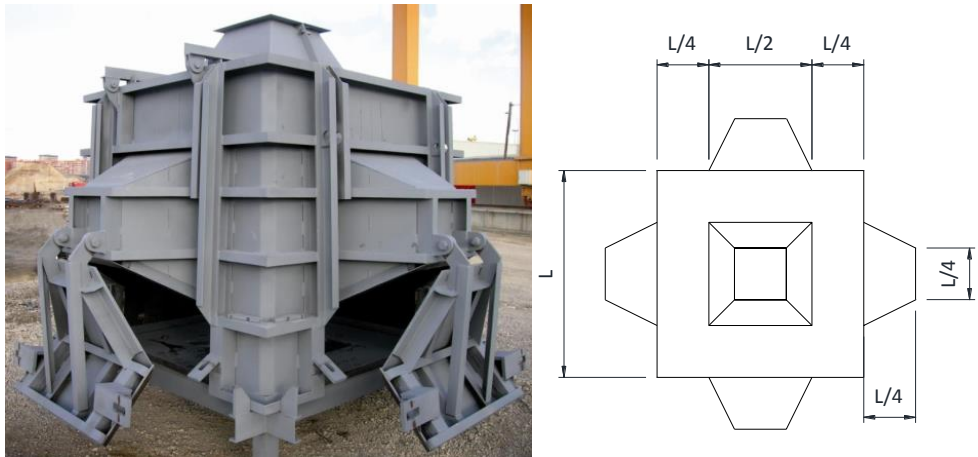


Figure 1.8 SATO-designed formwork to manufacture 7-m³ (16-tonne) Cubipod[®] units.

The optimum manufacturing process depends on work cycles, personnel, available space and equipment, as well as the required daily production rate. The unit cost associated with manufacturing depends on the total volume of armor units ($V[m^3]$) and the manufacturing duration [days]. The formworks designed by SATO allow Cubipod[®] units to be manufactured like conventional cubes with vertical de-molding. The production rate (2 to 3.5 units/mold/day) is much higher than for slender or bulky units (1 unit/mold/day), whose manufacture requires much more complex formworks and horizontal de-molding. Figure 1.8 shows the articulated vertical formwork designed by SATO to manufacture up to 7-m³ (16-tonne) Cubipod[®] units.

Double pressure clamps, similar to those used for cubic blocks, are used to handle Cubipod[®] units in the block yard; pressure clamps are much more efficient and much safer than the slings commonly used to handle slender units. Cubipod[®] units can be stacked vertically in multiple layers using different arrangements (closed, semi-closed, open, etc.) and porosities (between 30% and 50%), depending on the space available in the block yard. A granular bedding layer is first spread to homogenize the ground in the block yard stacking area, and small regular holes or trenches are excavated later to place the first layer of Cubipod[®] units. The number of layers of Cubipods vertically stacked will depend mainly on the available space in the block yard; the scarcer the space, the higher the stacks. Figure 1.9 shows the five-level stacking of Cubipod[®] units in the block yard of the Port of Málaga during the construction of the San Andrés Breakwater.



Figure 1.9 Five-level stacking of Cubipod[®] units (Port of Málaga, Spain).

Finally, once the specified strength (28 days) is reached, armor units can be transported and placed in the breakwater armor. The block yard has to be properly managed to minimize the costs, producing and stacking the right number of units every day to guarantee the output required by the placement team. Cubipod[®] units are placed on the slope using crawler cranes with a 6 to 8 unit/hour ratio, depending on the Cubipod[®] size.

Gantry or wheel cranes use double pressure clamps, to load Cubipod[®] units onto platform trucks in the block yard. These trucks transport the units to the breakwater and the crawler crane takes each Cubipod[®] from the platform using single or double pressure clamps to place the unit on the slope following the prescribed placement grid. Even though Cubipod[®] units re-arrange themselves with random orientation, they must be placed following a specific placement grid (depending on slope, unit size and trunk or roundhead curvature) to obtain the recommended packing density ($p[\%]=41$).

If the secondary cover layer and toe berm are well constructed, divers are not necessary to correctly place Cubipod[®] units because the placement grids have been tested in the laboratory with moderate waves and blind placement (see Pardo et al., 2014). Only horizontal X-Y coordinates are required (crawler crane GPS) to correctly place the Cubipod[®] armor units. As a general rule, attention should focus on proper construction of the toe berm and the placement of the first row of Cubipod[®] units.

1.6. Construction costs of Cubipod[®] armors

Mound breakwater construction naturally involves a number of complex logistic and optimization challenges which may be solved considering the circumstances and restrictions that change in time and space. Tasks must be defined and scheduled in advance, and equipment and work teams must be organized to properly estimate the associated costs. Promoters, contractors and designers usually focus attention on construction cost and duration; nevertheless, social and environmental impact assessments (carbon, energy and ecological footprints) are increasingly relevant in many countries. Given the impact of energy consumption on the economic cost of basic construction components (cement, steel, transportation, etc.), there is usually a high correlation between construction costs and energy and carbon footprints. The economic optimization of the breakwater usually leads to a minimization of the carbon and energy footprints.

In order to estimate the economic cost of single- and double layer Cubipod[®] armors and double-layer conventional cube armors, Corredor et al. (2008) conducted a parametric economic analysis based on the breakwater cross section shown in Figure 1.10. The parametric analysis covered the range of variables $5 \leq h_t[\text{m}] \leq 20$, $400 \leq L_b[\text{m}] \leq 2500$ and $10 \leq W[\text{t}] \leq 150$, where h_t is the water depth at the toe berm, L_b the breakwater length, and W is the armor unit weight.

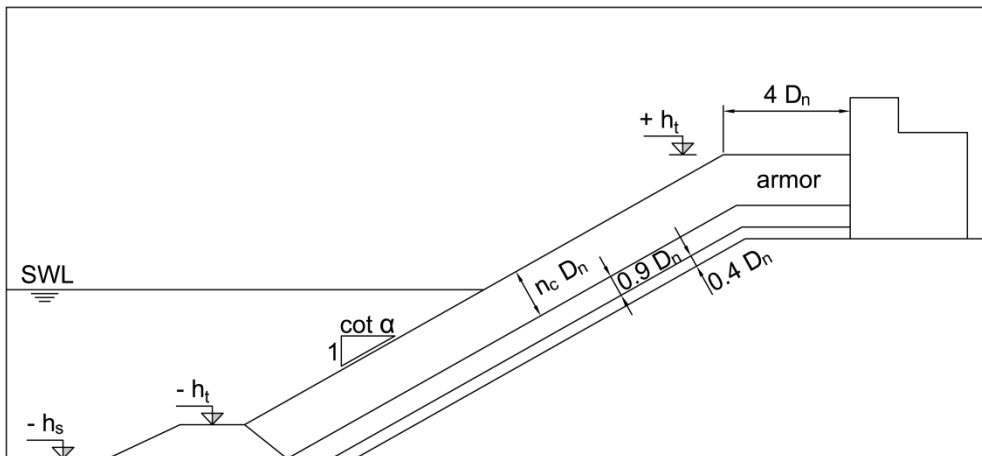


Figure 1.10 Breakwater cross section used in the parametric study of construction costs (Corredor et al., 2008).

Different types of costs were estimated for each case: (1) concrete supply, (2) manufacture, (3) gantry crane and handling, (4) transportation and placement, (5) casting and stacking area, and (6) formworks and pressure clamps. Figure 1.11 shows a classification of armor construction costs corresponding to a double-layer 20-tonne Cubipod[®] armor on a 1-km long breakwater at a water depth $h_t[\text{m}] = 15$ ($h_s[\text{m}] \approx 18$).

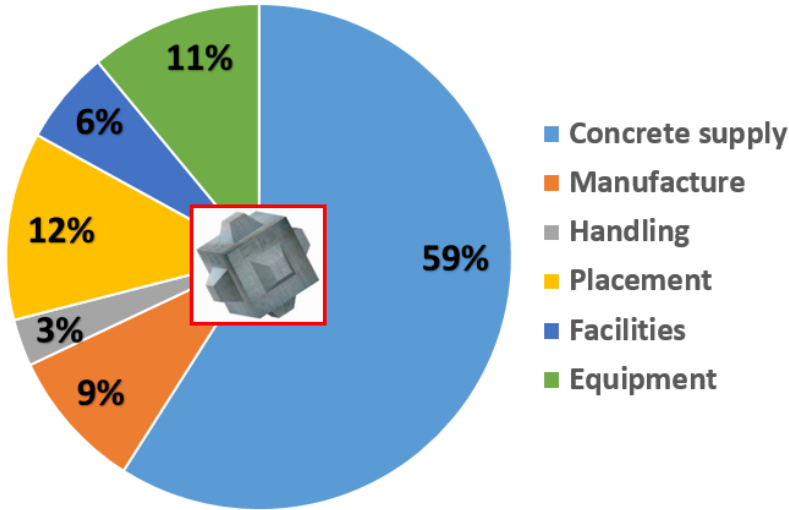


Figure 1.11 Classification of armor construction costs ($L_b[m]=1000$, $h_t[m]=15$, $W[t]=20$).

Considering the results obtained from the 153 different cases analyzed by Corredor et al. (2008) in his parametric analysis, Molines (2009) and Medina et al. (2010) proposed using Equations 1.1 and 1.2 to estimate the unit construction cost [$\text{€}/\text{m}^3$] of conventional cube (C_B) and Cubipod[®] (C_C) armor units.

$$C_B \left[\frac{\text{€}}{\text{m}^3} \right] = (205 + HOR) + 0.75 \left[10^5 \left(\frac{1}{\ln(V_B W_B)} \right)^2 - 10^4 \left(\frac{1}{\ln(V_B W_B)} \right) \right] \quad 1.1$$

$$C_C \left[\frac{\text{€}}{\text{m}^3} \right] = (265 + HOR) + 1.00 \left[10^5 \left(\frac{1}{\ln(V_C W_C)} \right)^2 - 10^4 \left(\frac{1}{\ln(V_C W_C)} \right) \right] \quad 1.2$$

in which $HOR[\text{€}/\text{m}^3]$ is the unit cost of the concrete supplied, $W_B[t]$ and $W_C[t]$ are the weights of cube and Cubipod[®] units and $V_B[\text{m}^3]$ and $V_C[\text{m}^3]$ are the total volumes of concrete used in the armor to manufacture cube and Cubipod[®] units, respectively.

For the same wave climate and environmental conditions ($H_s[m]$, $h_s[m]$ and $L_b[m]$), the construction cost of single- and double-layer Cubipod[®] armors ($V_C C_C$) is usually much less than conventional double-layer cube armors ($V_B C_B$), because the stability coefficient is higher and number of layers is equal or lower. Depending on the wave climate and construction site conditions, costs are normally reduced from 20% to 50%. In some feasible cases, it may be economically beneficial to increase the size of the armor units above the minimum size required for hydraulic stability. According to Equation 1.2, if W_C increases, V_C and $V_C W_C$ increase, C_C decreases and $V_C C_C$ may not increase.

If the armor unit size increases above the minimum size required for safety, the concrete consumption increases (higher concrete supply cost) but fewer units are needed (lower logistic costs); the optimum armor size is not always the smallest.

Equations 1.1 and 1.2 are valid for armors built with one single armor unit size; however, breakwaters may require different sizes of armor units in different sections of the armor (trunk, roundhead, etc.) depending on the design wave conditions at the structure toe. To estimate the construction cost of an armor with different armor unit sizes, the approximations given by Equations 1.3 and 1.4 can be used in Equations 1.1 and 1.2, respectively.

$$V_B = \sum_{m=1}^M [V_m] \text{ and } W_B = \frac{\sum_{m=1}^M [V_m W_m]}{V_B} \quad 1.3$$

$$V_C = \sum_{n=1}^N [V_n] \text{ and } W_C = \frac{\sum_{n=1}^N [V_n W_n]}{V_C} \quad 1.4$$

in which M and N are the number of different cube and Cubipod[®] unit sizes, m and n identify unit sizes for cubes (m=1, 2, ..., M) and Cubipods (n=1, 2, ..., N), $W_m[t]$ and $W_n[t]$ are the different cube and Cubipod[®] unit weights, $V_m[m^3]$ and $V_n[m^3]$ are the volumes of concrete used to manufacture cube and Cubipod[®] units for each size, and $V_B[m^3]$ and $V_C[m^3]$ are the total volumes of concrete for cube and Cubipod[®] units placed in the breakwater.

The cost estimations given by Equations 1.1 to 1.4 are reasonable if the volumes corresponding to each unit size ($V_m[m^3]$ or $V_n[m^3]$) are not very different. The cost will increase if only a few armor units of a specific size are manufactured. As a general rule, mound breakwaters should be designed using as few armor unit sizes as possible, so as to keep logistic costs low. The cost estimations given by Equations 1.1 to 1.4 are reliable only to compare conventional cube and Cubipod[®] armored breakwaters, because costs at a specific construction site may be notably influenced by local material supply cost, local equipment, local personnel cost and concrete supply cost (different for different countries and construction sites). Equations 1.1 and 1.2 were derived from the parametric economic study by Corredor et al. (2008) assuming a unit cost for concrete supply in the construction site $HOR[€/m^3]=60$.

Example 1.1

Given: Two alternative designs for a mound breakwater are considered: (1) double-layer cube armored and (2) single-layer Cubipod[®] armored breakwater. The cube armor has 20-tonne cubes (35,000 m³) and 30-tonne cubes (50,000 m³); the Cubipod[®]

armor has 10-tonne Cubipods (15,000 m³) and 15-tonne Cubipods (20,000 m³). Unit cost for concrete supply to the construction site is 65 €/m³.

Find: (1) Estimated construction costs for the two alternative armors and (2) Cost-sensitivity to an increase in armor unit size.

Solution: Considering Equations 1.3 and 1.4,

$$V_B[\text{m}^3] = V_{m1} + V_{m2} = 35,000 + 50,000 = 85,000$$

$$W_B[t] = ([20 \times 35,000] + [30 \times 50,000]) / 85,000 = 25.9$$

$$V_C[\text{m}^3] = V_{n1} + V_{n2} = 15,000 + 20,000 = 35,000$$

$$W_C[t] = ([10 \times 15,000] + [15 \times 20,000]) / 35,000 = 12.9$$

Unit costs for cubes and Cubipods are given by Equations 1.1 and 1.2

$$C_B \left[\frac{\text{€}}{\text{m}^3} \right] = (205 + 65) + 0.75 \left[10^5 \left(\frac{1}{\ln(85,000 \times 25.9)} \right)^2 - 10^4 \left(\frac{1}{\ln(85,000 \times 25.9)} \right) \right] = 108.1$$

$$C_C \left[\frac{\text{€}}{\text{m}^3} \right] = (265 + 65) + 1.00 \left[10^5 \left(\frac{1}{\ln(35,000 \times 12.9)} \right)^2 - 10^4 \left(\frac{1}{\ln(35,000 \times 12.9)} \right) \right] = 151.8$$

$$\text{Cube armor construction cost (1a)} = V_B C_B = 85,000[\text{m}^3] \times 108.1[\text{€/m}^3] = 9.19 \text{ M€}$$

$$\text{Cubipod}^{\text{®}} \text{ armor construction cost (2a)} = V_C C_C = 35,000[\text{m}^3] \times 151.8[\text{€/m}^3] = 5.31 \text{ M€}$$

If only 30-tonne cubes and 15-tonne Cubipods are used (logistics are simplified), the costs can be estimated in a similar way using Equations 1.1 and 1.2. In this case, armor thickness will increase with the nominal diameter, $D_n = (W/\gamma_r)^{1/3}$

$$V_B[\text{m}^3] = (35,000 \times [30/20]^{1/3}) + 50,000 = 90,060 \text{ and } W_B[t] = 30$$

$$V_C[\text{m}^3] = (15,000 \times [15/10]^{1/3}) + 20,000 = 37,168 \text{ and } W_C[t] = 15$$

$$C_B \left[\frac{\text{€}}{\text{m}^3} \right] = (205 + 65) + 0.75 \left[10^5 \left(\frac{1}{\ln(90,060 \times 30)} \right)^2 - 10^4 \left(\frac{1}{\ln(90,060 \times 30)} \right) \right] = 105.5$$

$$C_C \left[\frac{\text{€}}{\text{m}^3} \right] = (265 + 65) + 1.00 \left[10^5 \left(\frac{1}{\ln(37,168 \times 15)} \right)^2 - 10^4 \left(\frac{1}{\ln(37,168 \times 15)} \right) \right] = 145.5$$

$$\text{Cube armor construction cost (1b)} = V_B C_B = 90,060[\text{m}^3] \times 105.5[\text{€/m}^3] = 9.50 \text{ M€}$$

$$\text{Cubipod}^{\text{®}} \text{ armor construction cost (2b)} = V_C C_C = 37,168[\text{m}^3] \times 145.5[\text{€/m}^3] = 5.39 \text{ M€}$$

Increasing cube size from 20-tonnes to 30-tonnes will simplify the logistics of the breakwater because fewer units are needed and only one cube size would be manufactured, handled, stacked and placed. However, concrete consumption would increase by 6% and construction costs by 3.4%.

Increasing the Cubipod[®] size from 10-tonnes to 15-tonnes will simplify the logistics of the breakwater. However, concrete consumption would increase by 6.2% and construction cost by 1.5%. Construction costs for smaller armors ($V_B W_B$ or $V_C W_C$) are less sensitive to changes in unit size.

Chapter 2

Hydraulic stability of the armor layer

2.1. Introduction

The hydraulic stability of concrete armor units (characterized by unit geometry, number of layers, slope, packing density and placement) is discussed here in terms of the armor's ability to withstand wave attack (H_{sd}) in relation to unit size (D_n) and submerged relative specific weight (Δ). Hudson's formula, based on Iribarren (1938), popularized later by SPM (1975), includes the stability coefficient (K_D) to take into account the different hydraulic stabilities of a variety of armor units.

$$W = \frac{1}{K_D} \frac{H^3}{\left(\frac{\gamma_r}{\gamma_w} - 1\right)^3} \cot \alpha \quad 2.1$$

where W is armor unit weight, γ_r and γ_w are the specific weights of concrete and water, H is the wave height corresponding to Initiation of Damage (IDa) and α is the angle of structure slope. Equation 2.1 may be re-written taking the equivalence $H = H_{sd}$ proposed by SPM (1975), and considering the submerged relative specific weight, $\Delta = (\gamma_r/\gamma_w - 1)$, and the nominal diameter or equivalent cube size, $D_n = (W/\gamma_r)^{1/3}$. The generalized Hudson's formula is given by Equation 2.2.

$$N_{sd} = \frac{H_{sd}}{\Delta D_n} = (K_D \cot \alpha)^{1/3} \quad 2.2$$

where N_{sd} is the design stability number, and H_{sd} is the design significant wave height. Hudson (1959) originally proposed using Equation 2.1 with stability coefficients (K_D) appropriate to design to IDa, assuming a relevant implicit safety factor to Initiation of Destruction (IDe) for the two-layer armors built half a century ago (quarry stones, concrete cubes, etc.). Effects of wave randomness (H in Equation 2.1 corresponds to regular waves) and other sources of uncertainty were assumed to be compensated by the implicit safety factor to IDe.

Equation 2.2 does not explicitly take into account the duration of the wave storm, the wave period or wave steepness, the permeability of core and filter layers, or other relevant factors affecting the hydraulic stability of the armor layer. Nevertheless, Equation 2.2 is still widely used by practitioners for preliminary design and feasibility studies to compare construction costs of different breakwater designs using different armor units. The generalized Hudson formula is so extensively used in practice that K_D is required to commercialize any new armor unit. This formula is reasonable for double-layer armors and non-interlocking units; however, K_D is also given for proprietary single-layer interlocking unit armors which increase hydraulic stability with steeper slope angles (α). According to Hudson's formula, most armor units (randomly placed) increase hydraulic stability if the slope angle is reduced, unlike single-layer interlocking units. Accordingly, $\cot\alpha=4/3$ is usually recommended for most single-layer interlocking unit armoring; if the slope angle is reduced to $\cot\alpha=3/2$, the unit weight should not be reduced as in Equation 2.2 because the hydraulic stability of interlocking units does not affect the slope angle (α) as predicted by Hudson's formula.



Figure 2.1 Units for single-layer armoring.

The Accropode[™] (patented in 1980) was the first precast concrete armor unit for interlocked single-layer armoring (see Figure 2.1). The single-layer armoring with a brittle failure function significantly changed how alternative armor designs to protect breakwaters were compared. Armor design to IDa, popularized by SPM (1975), had to be adapted to a new type of armor with a brittle failure function in which IDa and IDe are very close. In order to maintain a reasonable safety factor to IDe, the patent owners

recommended K_D corresponding to a level of armor damage much lower than IDa. The values of K_D for single- and double-layer armors are based on small-scale physical tests and may change slightly over time, depending on experience, safety factors and the author's criteria.

There is a general agreement in the scientific and engineering community about the use of probabilistic techniques to design large breakwaters. For instance, the Spanish ROM 0.0-01 (2002) recommended Level II and Level III probabilistic techniques to design large mound breakwaters for Spanish coasts. However, due to the complexity of probabilistic techniques, the difficult traceability and the need in practice to simplify a problem with many variables not fully characterized, the Level I design technique (safety factors) is usually preferred during the preliminary design phase (project feasibility analysis). For most mound breakwaters, the key design decisions for the armor layer are usually based on the literature and a subjective selection of the empirical formulas to characterize the main failure modes (hydraulic stability, overtopping, toe berm stability, etc.). A preliminary design is obtained during the feasibility analysis and the design is then validated or optimized later with small-scale 2D or 3D physical tests.

To rationalize the use of stability coefficients (K_D) when characterizing the hydraulic stability of the armor layer, Medina and Gómez-Martín (2012) proposed explicitly specifying the safety factors associated to each K_D . Based on the physical experimental results for each armor unit, the safety factors SF(IDa) and SF(IDE) are the ratio between the stability number to IDa and IDE and the design stability number, $SF(IDa)=N_s(IDa)/N_{sd}$ and $SF(IDE)=N_s(IDE)/N_{sd}$ (N_{sd} is given by Equation 2.2). For a given series of hydraulic stability tests, if a lower K_D were recommended, N_{sd} would decrease and the two safety factors would increase. Therefore, armors with a similar failure function (e.g. single-layer or double-layer) should have similar safety factors, high enough to take into account model effects (differences between prototype and tested model), errors and other variables not considered in Equation 2.2.

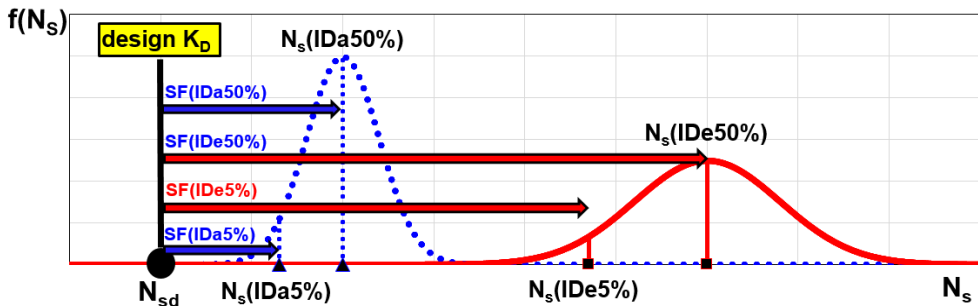


Figure 2.2 Schematic representation of N_{sd} and safety factors.

The stability numbers associated with IDa and IDE are subject to significant experimental variability; it is convenient to describe them using 5% and 50% percentiles

corresponding to low and medium values. For instance, $N_s(\text{IDe}5\%)$ is the stability number corresponding to IDe with only 5% probability of not being surpassed, and $N_s(\text{IDa}50\%)$ is the median value of the stability number to IDa. Figure 2.2 shows a scheme of the probability density functions of the variables $N_s(\text{IDa})$ and $N_s(\text{IDe})$, the design stability number N_{sd} (corresponding to K_D) and four safety factors: $\text{SF}(\text{IDa}5\%)$, $\text{SF}(\text{IDa}50\%)$, $\text{SF}(\text{IDe}5\%)$ and $\text{SF}(\text{IDe}50\%)$. Table 2.1 provides the safety factors calculated by Medina and Gómez-Martín (2012) for different armors and concrete units.

Table 2.1 K_D and safety factors associated with different concrete armor units.

Design K_D and global safety factors					Initiation of Damage (IDa)		Initiation of Destruction (IDe)	
Section	CAU	K_D	# layers	slope	SF(IDa5%)	SF(IDa50%)	SF(IDe5%)	SF(IDe50%)
Trunk	Cube	6.0	2	3/2	0.67	0.86	1.05	1.35
	Cubipod [®]	28.0	2	3/2	0.82	0.99	1.09	1.40
	Cubipod [®]	12.0	1	3/2	1.06	1.27	1.31	1.64
	Accropode [™]	15.0	1	4/3	0.93 a 1.24	1.15 a 1.38	1.05 a 1.40	1.26 a 1.51
	Xbloc [®]	16.0	1	4/3	1.17	1.32	1.17	1.68
Round-head	Cube	5.0	2	3/2	0.88	1.13	1.17	1.40
	Cubipod [®]	7.0	2	3/2	0.99	1.18	1.19	1.36

2.2. Trunk hydraulic stability of double-layer Cubipod[®] armors ($K_D=28$)

The hydraulic stability of double-layer Cubipod[®] armor trunks was tested during the research project CUBIPOD (2007-2009). 2D hydraulic stability tests of similar models (non-breaking, non-overtopping and $\cot\alpha=1.5$ slope) were carried out in the Laboratory of Ports and Coasts at the *Universitat Politècnica de València* (LPC-UPV) and *Instituto de Hidrodinámica Aplicada* (INHA); tests and results are described in Gómez-Martín and Medina (2014) and Gómez-Martín (2015). LPC-UPV tested double-layer randomly-placed cube and Cubipod[®] armors while INHA tested single- and double-layer Cubipod[®] armors. Hydraulic stability results (stability numbers) for double-layer Cubipod[®] armors were similar in the LPC-UPV and INHA tests; this agreement allows for the comparison of the hydraulic stability of double-layer cube and Cubipod armors.

Figure 2.3 shows the stability numbers for double-layer cube and Cubipod armors (trunk) observed as a function of the wave steepness (s_{op}). The stability numbers for Initiation of Damage, $N_s(\text{IDa})$, for cube and Cubipod[®] armors are represented by white squares (cubes) and green triangles and rhombuses (Cubipods). The design stability numbers, N_{sd} , are those corresponding to the recommended stability coefficients given in Table 2.1 ($K_D=6$ for cubes and $K_D=28$ for Cubipods). The stability numbers for Initiation of Destruction, $N_s(\text{IDe})$, are represented by blue squares (cubes) and red trian-

gles and rhombuses (Cubipods). The safety margins are wide, except for cubes in the range $s_{0p} < 0.01$ ($I_{rp} > 7$) and Cubipods in the range $s_{0p} > 0.06$ ($I_{rp} < 2.7$).

The design stability numbers, N_{sd} , corresponding to the recommended stability coefficients ($K_D=6$ for cubes and $K_D=28$ for Cubipods) are higher than average for double-layer cube armors ($SF(IDa50\%)=0.86$) and close to average for double-layer Cubipod armors ($SF(IDa50\%)=0.99$). The safety factors to IDE are $SF(IDE50\%)=1.35$ for cubes and $SF(IDE50\%)=1.40$ for Cubipods (see Table 2.1).

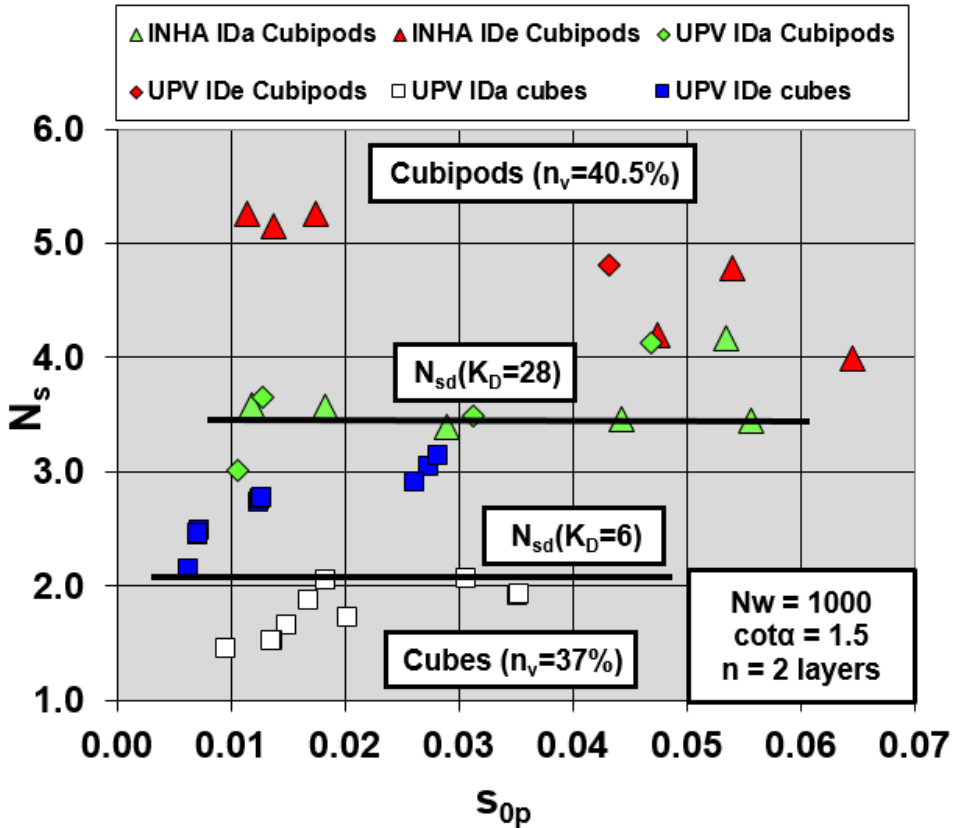


Figure 2.3 Stability numbers corresponding to IDa and IDE (for double-layer cube and Cubipod[®] armors).

Table 2.2 shows 5% and 50% percentiles of safety factors for IDa and IDE corresponding to double-layer randomly-placed cube and Cubipod[®] armors, calculated by Medina and Gómez-Martín (2012) using the results from the aforementioned experiments and others described in the literature. $SF(IDE50\%)=N_s(IDE)/N_{sd}$ is relevant because $N_s(IDE50\%)$ is the stability number corresponding to IDE with only 5% probability of not being surpassed during experimental tests. $SF(IDE50\%)=1.05$ and $SF(IDE50\%)=1.09$

for double-layer cube and Cubipod[®] armors, respectively. Additional small-scale tests of 3D models with a gentler slope ($\cot\alpha=2.0$) confirmed the high hydraulic stability of double-layer Cubipod[®] armors (see Corredor et al., 2012).

The recommended stability coefficient and design stability number for double-layer cube and Cubipod[®] armors are reasonable because the armor porosities measured in the laboratory are close to the recommended values for prototypes, and Pardo et al. (2015) developed feasible placement grids to achieve the prescribed armor porosities. Small-scale cube armors usually have a packing density $\Phi=1.26$, higher than the recommended value ($\Phi=1.18$), and the initial porosities used in practice ($\Phi=1.08$ is not rare). Medina et al. (2015) provided correction factors for the hydraulic stability of the double-layer randomly-placed cube armors if the armor porosity significantly differs from the recommended or tested values.

Table 2.2 Safety factors of double-layer cube and Cubipod[®] armor trunks.

Design K_D and global safety factors					Initiation of Damage (IDa)		Initiation of Destruction (IDe)	
Section	Unit	K_D	# layers	slope	SF(IDa5%)	SF(IDa50%)	SF(IDe5%)	SF(IDe50%)
Trunk	Cube	6.0	2	3/2	0.67	0.86	1.05	1.35
	Cubipod [®]	28.0	2	3/2	0.82	0.99	1.09	1.40

Compared to cube armors, the high homogeneity (uniform porosity) and roughness of Cubipod[®] armors tend to lessen the run-up, reduce the pressures during the run-down, and diminish the corresponding extraction forces. When the wave intensity increases, the IDa limit is reached when the first armor units are extracted. Cubipod[®] units tend to self-repair, covering or blocking the voids generated by extractions. If wave intensity increases far above IDa, Cubipod[®] units are extracted near SWL and units in the upper part of the armor move to cover the armor voids. If the wave intensity continues to rise, this process will continue until a relevant number of units are extracted, and the voids in the upper part of the armor make the filter layer visible and increase the risk of more units being extracted (IDe).

Small-scale tests using double-layer Cubipod[®] armored models of curved trunks subjected to oblique wave attack confirmed the high hydraulic stability given in Table 2.2. In a curved trunk or a trunk under oblique wave attack, the flux of energy is not as high as it is in conventional 2D tests; therefore, it is reasonable to assume that hydraulic stability does not decrease in these cases. Double-layer Cubipod[®] armors may be more stable for curved trunks and oblique waves than for straight trunks under orthogonal wave attack; nevertheless, it is not worth considering a higher hydraulic stability during the preliminary design phase due to the number of variables involved (wave angle, slope, radius, etc.) and the limited number of tested cases.

Example 2.1

Given: Two alternative designs are considered for the trunk of a mound breakwater: (1) double-layer cube armor and (2) double-layer Cubipod[®] armor. The cube armor has 120-tonne cubic concrete units ($V_B[m^3]=150,000$) and the mass densities of concrete and sea water are $\rho_r[t/m^3]=2.350$ and $\rho_w[t/m^3]=1.025$. Water depth at the toe of structure is $h_s[m]=40.0$, armor slope is $\cot\alpha=1.5$ and tidal range is $\Delta h[m]=3.0=HWL-LWL$.

Find: (1) Significant wave height of design storm, (2) Alternative double-layer Cubipod[®] armor and (3) Estimated armor damage levels when design storm is surpassed.

Solution: According to Equation 2.2 and Table 2.2

$$D_n[m] = \left(\frac{120}{2.350} \right)^{1/3} = 3.71$$

$$N_{sd}(cubes_2L) = \frac{H_{sd}}{\Delta D_n} = (K_D \cot \alpha)^{1/3} = (6.0 \times 1.5)^{1/3} = 2.08$$

$$H_{sd}[m] = 2.08 \times (\Delta D_n) = 2.08 \times \left(\frac{2.350}{1.025} - 1 \right) \times 3.71 = 2.08 \times 1.293 \times 3.71 = 9.96$$

$$H_{sd}/h_s = 9.96/40 = 0.25 (<0.39, \text{ non-breaking wave conditions at LWL})$$

(1) The significant wave height of the design storm is $H_{sd}[m] \approx 10.0$

Using the same concrete to manufacture Cubipod[®] units, the design stability number for double-layer Cubipod[®] armors is

$$N_{sd}(Cubipods_2L) = \frac{H_{sd}}{\Delta D_n} = (K_D \cot \alpha)^{1/3} = (28.0 \times 1.5)^{1/3} = 3.47$$

$$D_n[m] = \frac{3.71 \times 2.08}{3.47} = 2.22 \quad \text{and} \quad W[t] = 2.350 \times (2.22)^3 = 25.8$$

Another way to calculate the weight of the Cubipod[®] units involves taking into account Equation 2.1 and the same slope and specific weights:

$$W[t] = \frac{120 \times 6.0}{28.0} = 25.7 \approx 25.8 \quad (\text{the slight difference is due to rounding errors})$$

(2) Alternative design: double-layer 26-tonne Cubipod[®] armor

To estimate damage to the cube and Cubipod[®] armors when the design storm is exceeded, the safety factors listed in Table 2.2 are considered.

(3a) Double-layer cube armor

SF(IDa50%)=0.86, SF(IDe50%)=1.35, SF(IDa5%)=0.67 and SF(IDe5%)=1.05

There is a 50% probability of reaching

Initiation of Damage (IDa) with $H_{si}[m] < 0.86 \times 10.0 = 8.6$

Initiation of Destruction (IDe) with $H_{si}[m] < 1.35 \times 10.0 = 13.5$

There is a 5% probability of reaching

Initiation of Damage (IDa) with $H_{si}[m] < 0.67 \times 10.0 = 6.7$

Initiation of Destruction (IDe) with $H_{si}[m] < 1.05 \times 10.0 = 10.5$

(3b) Double-layer Cubipod[®] armor

SF(IDa50%)=0.99, SF(IDe50%)=1.40, SF(IDa5%)=0.82 and SF(IDe5%)=1.09

There is a 50% probability of reaching

Initiation of Damage (IDa) with $H_{si}[m] < 0.99 \times 10.0 = 9.9$

Initiation of Destruction (IDe) with $H_{si}[m] < 1.35 \times 10.0 = 14.0$

There is a 5% probability of reaching

Initiation of Damage (IDa) with $H_{si}[m] < 0.82 \times 10.0 = 8.2$

Initiation of Destruction (IDe) with $H_{si}[m] < 1.09 \times 10.0 = 10.9$

The estimations given above are based on the generalized Hudson formula, which does not take into account the effect of wave steepness. Figure 2.3 shows the influence of wave steepness on hydraulic stability, where wave steepness is $s_{0p} = 2\pi H_{m0}/gT_p^2$. To assess the sensitivity of armor damage level to wave steepness, three wave steepnesses are considered: $s_{0p} = 0.01$, 0.03 and 0.05.

$s_{0p} = 0.01$ ($T_p[s] \approx 25$):

Experimental IDa (cubes_2L) $H_{si}[m] = (1.5/2.08) \times 10 = 7.2$ (<8.6)

Experimental IDe (cubes_2L) $H_{si}[m] = (2.6/2.08) \times 10 = 12.5$ (<13.5)

Experimental IDa (Cubipods_2L) $H_{si}[m] = (3.0/3.47) \times 10 = 8.6$ (<9.9)

Experimental IDe (Cubipods_2L) $H_{si}[m] = (5.1/3.47) \times 10 = 14.7$ (≈ 14.0)

$s_{0p} = 0.03$ ($T_p[s] \approx 15$):

Experimental IDa (cubes_2L) $H_{si}[m] = (2.1/2.08) \times 10 = 10.1$ (>8.6)

Experimental IDe (cubes_2L) $H_{si}[m] = (3.1/2.08) \times 10 = 14.9$ (>13.5)

Experimental IDa (Cubipods_2L) $H_{si}[m] = (3.5/3.47) \times 10 = 10.1$ (≈ 9.9)

Experimental IDE (Cubipods_2L) $H_{si}[m]=(5.0/3.47) \times 10=14.4 (\approx 14.0)$

$s_{0p}=0.05(T_p[s] \approx 11)$:

Experimental IDa (Cubipods_2L) $H_{si}[m]=(3.5/3.47) \times 10=10.1 (\approx 9.9)$

Experimental IDE (Cubipods_2L) $H_{si}[m]=(4.5/3.47) \times 10=13.0 (<14.0)$

2.3. Trunk hydraulic stability of single-layer Cubipod[®] armors ($K_D=12$)

Studies on the hydraulic stability of Cubipod[®] armored trunks were carried out during the research project CUBIPOD (2007-2009). Two laboratories, LPC-UPV and INHA, conducted 2D tests of similar armor models with slope $\cot\alpha=1.5$, non-overtopping and nonbreaking conditions (see Gómez-Martín and Medina, 2014). Double-layer cube and Cubipod[®] armors were tested at LPC-UPV while single- and double-layer Cubipod[®] armors were tested at INHA. The two laboratories reported similar findings for double-layer Cubipod[®] armors. Specifically, the good coherence of results allows for comparison of the single-layer Cubipod[®] armor (tested at INHA) and the double-layer randomly-placed cube armor (tested at LPC-UPV).

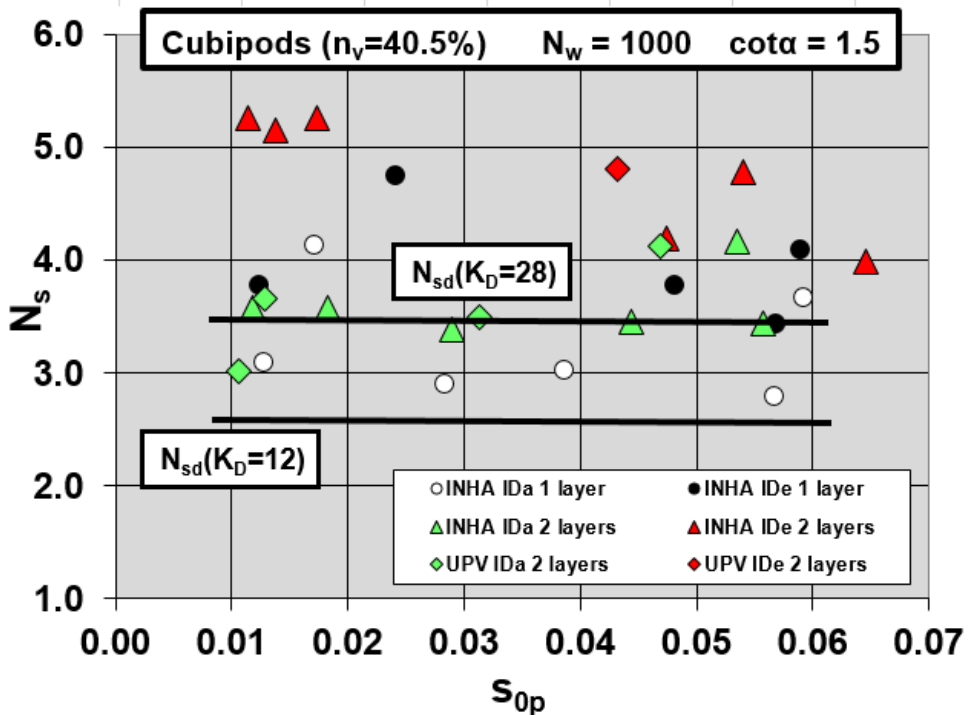


Figure 2.4 Stability numbers to IDa and IDE observed for single- and double-layer Cubipod[®] armor trunks.

Figure 2.4 shows the stability numbers for single- and double-layer Cubipod[®] armors (trunk), as function of the wave steepness (s_{op}). The stability number to Initiation of Damage, $N_s(IDa)$, for these armors are represented with white circles (single-layer) and green triangles and green rhombuses (double-layer). The design stability numbers, N_{sd} , associated with the stability coefficients recommended in Table 2.1 ($K_D=12$ and $K_D=28$ for single- and double-layer Cubipod[®] armors) correspond to values much lower than the median value for single-layer Cubipod[®] armors ($SF(IDa50\%)=1.27$) and close to the median value for double-layer Cubipod[®] armors ($SF(IDa50\%)=0.99$).

The stability numbers to Initiation of Destruction, $N_s(IDe)$, for Cubipod[®] armors are represented with black circles (single-layer) and red triangles and red rhombuses (double-layer). The safety margins are wider for single-layer Cubipod[®] armors given its less homogeneous response and less tenacious failure function. The median value of the safety factors to IDe are $SF(IDe50\%)=1.64$ for single-layer Cubipod[®] armors and $SF(IDe50\%)=1.40$ for double-layer Cubipod[®] armors.

Table 2.3 lists the 5% and 50% percentiles of the safety factors to IDa and IDe for the single- and double-layer Cubipod[®] armors (trunk) as reported by Medina and Gómez-Martín (2012). During the design process, the safety factor $SF(IDe5\%)$ is especially relevant as there is only a 5% probability of observing a lower value during the experimental tests. $SF(IDe5\%)=1.31$ and 1.09 for single- and double-layer Cubipod[®] armors, respectively. This high hydraulic stability was confirmed by additional small-scale tests using models protected with double-layer Cubipod[®] armors and slope $\cot\alpha=2.0$.

Table 2.3 Safety factors to IDa and IDe (percentiles 5% and 50%) for double-layer cube armor and single- and double-layer Cubipod[®] armors (trunk).

Design K_D and global safety factors					Initiation of Damage (IDa)		Initiation of Destruction (IDe)	
Part	Unit	K_D	# layers	slope	$SF(IDa5\%)$	$SF(IDa50\%)$	$SF(IDe5\%)$	$SF(IDe50\%)$
Trunk	Cube	6.0	2	3/2	0.67	0.86	1.05	1.35
	Cubipod [®]	28.0	2	3/2	0.82	0.99	1.09	1.40
	Cubipod [®]	12.0	1	3/2	1.06	1.27	1.31	1.64

The geometric design of the Cubipod[®] unit facilitates a homogeneous random placement on the breakwater slope. Cubipods tend to self-order on the slope with a low uniform porosity and random orientation; this behavior makes HeP insignificant and allows for single-layer armoring. Single-layer Cubipod[®] armors show a low roughness factor ($\gamma_f=0.46$) and homogeneous porosity. When wave action is intense, Cubipod[®] units move slightly adapting to the armor slope. When the start of damage limit (IDa) is reached, the first units are extracted from the armor; however, Cubipods move slightly to cover the voids and the armor self-repairs. While only a few armor units are extracted, the armor withstands the wave action with only minor damage. If the wave action increases, more units are extracted near MWL and other units (from the upper

part of the slope) move downward and cover the voids. This process may continue until a relevant number of units are lost from the same area; large voids are formed in the upper part of the slope, the filter layer becomes visible, and filter erosion (IDe) is an obvious risk.

Small-scale tests focusing on curved trunks and oblique wave attack confirmed the stability coefficients in Table 2.3; no significant reduction in armor hydraulic stability was found. Compared to a 2D frontal wave attack, the flux of energy is reduced for oblique and curved trunks; therefore, it is reasonable to consider the same hydraulic stability for preliminary design purposes. The hydraulic stability of curved and oblique trunks may be higher than that of trunks under perpendicular wave attack; however, it is not reasonable to consider a higher hydraulic stability during preliminary design because of the many parameters involved (wave angle, slope, radius, etc.), and the relatively limited number of tested cases.

Example 2.2

Given: Water depth at the toe of the breakwater is $h_s[m]=40.0$, tidal range is $\Delta h[m]=5.0$ and design storm is $H_{m0}[m]=10$ and $T_p[s]=18$. Armor slope is $\cot\alpha=1.5$ and mass densities of concrete and sea water are $\rho_r[t/m^3]=2.300$ and $\rho_w[t/m^3]=1.025$.

Find: (A) Weights of precast concrete units for (1) double-layer cube armor, (2) single-layer Cubipod[®] armor and (3) double-layer Cubipod[®] armor. (B) Estimated armor damage when design storm is surpassed.

Solution: $H_{sd}/h_s=10/40=0.25$ (LWL) and $H_{sd}/h_s=10/45=0.22$ (HWL); Equation 2.2 and Table 2.3 can be used because the breakwater is subject to non-breaking wave conditions ($H_{sd}/h_s<0.39$). The design stability numbers for double-layer cube armor and single- and double-layer Cubipod armors are:

$$N_{sd}(\text{cubes}_{-2L}) = \frac{H_{sd}}{\Delta D_n} = (K_D \cot \alpha)^{1/3} = (6.0 \times 1.5)^{1/3} = 2.08$$

$$N_{sd}(\text{Cubipods}_{-1L}) = \frac{H_{sd}}{\Delta D_n} = (K_D \cot \alpha)^{1/3} = (12.0 \times 1.5)^{1/3} = 2.62$$

$$N_{sd}(\text{Cubipods}_{-2L}) = \frac{H_{sd}}{\Delta D_n} = (K_D \cot \alpha)^{1/3} = (28.0 \times 1.5)^{1/3} = 3.47$$

Equivalent cube side length or nominal diameters and armor unit weights are

$$\text{cubes}_{-2L}: D_n[m] = \frac{10}{2.08 \times \left(\frac{2.300}{1.025} - 1 \right)} = 3.87 \quad \text{and} \quad W[t] = 2.300 \times (3.87)^3 = 133.3$$

$$\text{Cubipod}^{\text{®}}_{-1L}: D_n[m] = \frac{10}{2.62 \times \Delta} = 3.07 \quad \text{and} \quad W[t] = 2.300 \times (3.07)^3 = 65.5$$

$$\text{Cubipod}^{\text{®}}_{s-2L}: D_n[m] = \frac{10}{3.47 \times \Delta} = 2.32 \quad \text{and} \quad W[t] = 2.300 \times (2.32)^3 = 28.7$$

(A) Weights of precast concrete armor units: (1) W[t]=134, (2) W[t]=66 and (3) W[t]=29. Weights of concrete armor units are very sensitive to the specific weight of concrete, which is slightly different from Example 2.2 ($\gamma_r=2.35 \text{ t/m}^3$) to Example 2.3 ($\gamma_r=2.30 \text{ t/m}^3$).

(B1) and (B3) Damage levels for double-layer cube and Cubipod[®] armor trunks are given in Example 2.1.

To estimate the damage levels for trunks of single-layer Cubipod[®] armors when the design storm is exceeded, the safety factors given in Table 2.3 can be used as an initial approximation (wave steepness is not considered).

(B2) Single-layer Cubipod[®] armor

SF(IDa50%)=1.27, SF(IDe50%)=1.64, SF(IDa5%)=1.06 and SF(IDe5%)=1.31

There is a 50% probability of reaching

Initiation of Damage (IDa) with $H_{si}[m] < 1.27 \times 10.0 = 12.7$

Initiation of Destruction (IDe) with $H_{si}[m] < 1.64 \times 10.0 = 16.4$

There is a 5% probability of reaching

Initiation of Damage (IDa) with $H_{si}[m] < 1.06 \times 10.0 = 10.6$

Initiation of Destruction (IDe) with $H_{si}[m] < 1.31 \times 10.0 = 13.1$

The estimations given above are based on the generalized Hudson formula, which does not take into account the influence of wave steepness. Figures 2.3 and 2.4 plot the influence of wave steepness on hydraulic stability when wave steepness is $s_{0p} = 2\pi H_{m0} / g T_p^2 \approx 0.020$

Experimental IDa (cubes_2L) $H_{si}[m] < (1.8/2.08) \times 10 = 8.7$ (≈ 8.6)

Experimental IDe (cubes_2L) $H_{si}[m] < (2.9/2.08) \times 10 = 13.9$ (≈ 13.5)

Experimental IDa (Cubipods_1L) $H_{si}[m] < (3.2/2.62) \times 10 = 12.2$ (≈ 12.7)

Experimental IDe (Cubipods_1L) $H_{si}[m] < (4.4/2.62) \times 10 = 16.8$ (≈ 16.4)

Experimental IDa (Cubipods_2L) $H_{si}[m] < (3.5/3.47) \times 10 = 10.1$ (≈ 9.9)

Experimental IDe (Cubipods_2L) $H_{si}[m] < (5.1/3.47) \times 10 = 14.7$ (≈ 14.0)

2.4. Roundhead hydraulic stability of double-layer Cubipod[®] armors ($K_D=7$)

A series of physical tests were designed to study the hydraulic stability of roundheads protected with a double-layer Cubipod[®] armor. During the research project CUBIPOD (2007-2009), 3D tests were carried out in the wave basins at IH Cantabria and Aalborg University (AAU). Both laboratories tested similar roundhead models having slope $\cot\alpha=1.5$, in non-breaking and non-overtopping conditions. Long-crested waves were generated in the tests done at IH Cantabria (see Lomónaco et al., 2009). Short- and long-crested waves were generated in the tests conducted at AAU (see Burcharth et al., 2010). A similar hydraulic stability of roundheads (IDa and IDE) was observed in the two laboratories; the directionality of waves (short- or long-crested waves) did not significantly affect roundhead hydraulic stability when protected with double-layer Cubipod[®] armors. Figure 2.5 shows the 3D small-scale models built in IH Cantabria (Fig. 2.5a) and AAU Fig. 2.5b).

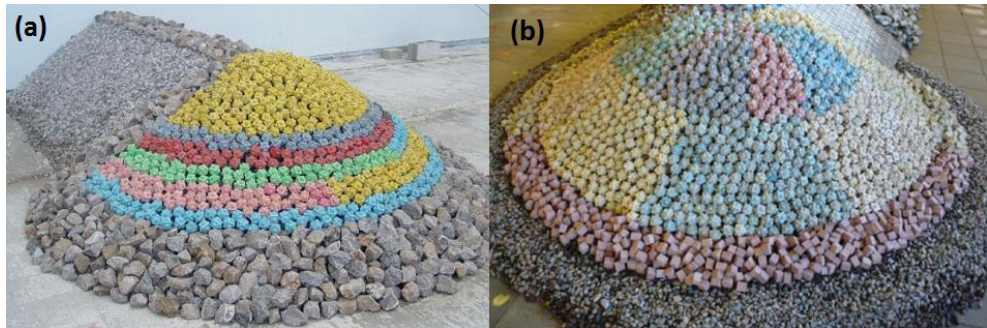


Figure 2.5 3D models of roundheads protected with double-layer Cubipod[®] armors: (a) IH Cantabria, (b) AAU.

After the non-breaking and non-overtopping models protected with double-layer cube and Cubipod[®] armors were tested in these two laboratories, it was possible to reliably compare the hydraulic stability of armors in roundheads with similar characteristics (relative radius, slope angle, wave steepness, etc.). With short- and long-crested waves, double-layer Cubipod[®] armors protecting roundheads were more stable than double-layer cube armors; the stability coefficient of Cubipods ($K_D[\text{Cubipod}]=7.0$) is 40% higher than that of cubes ($K_D[\text{cube}]=5.0$). Compared to the conventional double-layer cube armor, the higher hydraulic stability of Cubipods allows for a significant reduction in the mass of the units in the roundhead.

Building the roundhead is more complex than the trunk; there may be a significant difference between the ideal placement conditions found in the laboratory (construction by hand, dry conditions, perfect views, etc.) and the real conditions usually found at sea (crawler cranes, wind, waves, underwater blind placement, etc.). These differences between small-scale and prototype may be relevant (model effect) in the case of cubic

blocks, which tend to put one face parallel to the slope, face-to-face fitting and HeP, reducing the armor porosity in the lower part of the armor and increasing the porosity in the upper part. For roundheads protected with Cubipods, the tendency of units to random-orientation and self-arrangement on the slope significantly reduces the differences between prototype and small-scale models (smaller model effect).

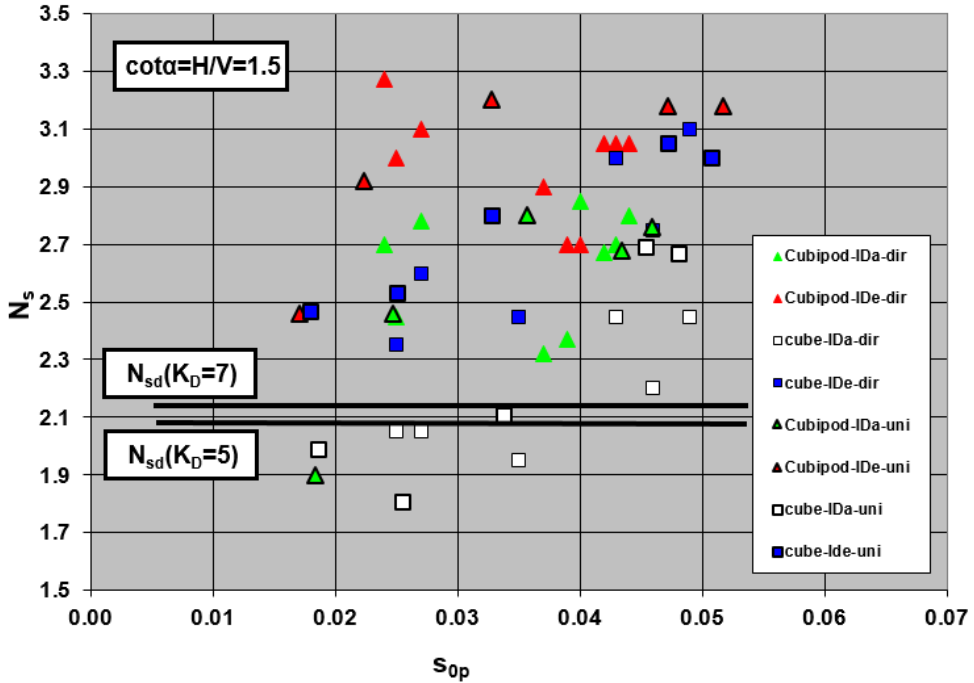


Figure 2.6 N_s (IDa) and N_s (IDe) of double-layer cube and Cubipod[®] armors in roundhead.

Figure 2.6 plots the observed stability numbers corresponding to IDa for double-layer cube and Cubipod[®] armors in roundhead, as a function of wave steepness (s_{0p}). The stability numbers corresponding to IDa are represented with white squares (cubes) and green triangles (Cubipods). Squares and triangles with thick black contours correspond to tests with unidirectional waves (long-crested waves) while those with thin grey contours correspond to tests with directional waves (short-crested waves). The design stability numbers N_{sd} are those associated with the recommended stability coefficients ($K_D=5$ for cubes and $K_D=7$ for Cubipods) which are lower than the average values (see Table 2.4); $SF(IDa50\%)=1.13$ and 1.18 for cubes and Cubipods, respectively (see Medina and Gómez-Martín, 2012).

Figure 2.6 also indicates stability numbers corresponding to IDe for double-layer cube and Cubipod[®] armored roundheads, as a function of the wave steepness (s_{0p}). The stability numbers corresponding to IDe are represented by blue squares (cubes) and red

triangles (Cubipods). The safety margins are wide for both armors, $SF(IDE5\%)=1.17$ and 1.19 for cubes and Cubipods, respectively. It is necessary to point out that wave steepness, roundhead radius and armor porosity may significantly alter the safety margins given in Table 2.4. Specifically, if wave steepness is in the low range ($s_{0p}<0.02$, $Ir_p>5$), the observed safety margins are significantly lower than those indicated in Table 2.4.

Table 2.4 Safety factors for double-layer cube and Cubipod[®] armors in trunk and roundhead.

Design K_D and global safety factors					Initiation of Damage (IDa)		Initiation of Destruction (IDe)	
Part	Unit	K_D	# layers	slope	SF(IDa5%)	SF(IDa50%)	SF(IDE5%)	SF(IDE50%)
Trunk	Cube	6.0	2	3/2	0.67	0.86	1.05	1.35
	Cubipod [®]	28.0	2	3/2	0.82	0.99	1.09	1.40
Round-head	Cube	5.0	2	3/2	0.88	1.13	1.17	1.40
	Cubipod [®]	7.0	2	3/2	0.99	1.18	1.19	1.36

Example 2.3

Given: Water depth at the toe of the structure is $h_s[m]=30.0$; tidal range is $\Delta h[m]=3.0$ and design storm is $H_{m0}[m]=10$ and $T_p[s]=18$. Armor slope is $\cot\alpha=1.5$ and mass densities of concrete and sea water are $\rho_c[t/m^3]=2.400$ and $\rho_w[t/m^3]=1.025$.

Find: (A) Weights of precast concrete units placed on roundhead for (1) double-layer cube armor and (2) double-layer Cubipod[®] armor. (B) Estimated armor damage levels when design storm is surpassed.

Solution: $H_{sd}/h_s=10/30=0.33$ (LWL) and $H_{sd}/h_s=10/35=0.29$ (HWL); Equation 2.2 and Table 2.4 can be used because the breakwater is under non-breaking wave conditions ($H_{sd}/h_s<0.39$).

The roundhead design stability numbers for double-layer cube and Cubipod armors are:

$$N_{sd}(\text{cubes}_{-2L}) = \frac{H_{sd}}{\Delta D_n} = (K_D \cot \alpha)^{1/3} = (5.0 \times 1.5)^{1/3} = 1.96$$

$$N_{sd}(\text{Cubipods}_{-2L}) = \frac{H_{sd}}{\Delta D_n} = (K_D \cot \alpha)^{1/3} = (7.0 \times 1.5)^{1/3} = 2.19$$

Equivalent cube side lengths or nominal diameters and armor unit weights are

$$\text{cubes}_{-2L}: D_n[m] = \frac{10}{1.96 \times \left(\frac{2.400}{1.025} - 1 \right)} = 3.80 \quad \text{and} \quad W[t] = 2.400 \times (3.80)^3 = 131.7$$

$$\text{Cubipods}_{2L}: D_n[m] = \frac{10}{2.19 \times \Delta} = 3.40 \quad \text{and} \quad W[t] = 2.400 \times (3.4)^3 = 94.3$$

(A) Weights of concrete armor units: (1) W[t]=132 and (2) W[t]=95

Weights of concrete armor units are very sensitive to the specific weight of concrete, which is slightly different from Example 2.2 ($\gamma_r=2.35 \text{ t/m}^3$), Example 2.3 ($\gamma_r=2.30 \text{ t/m}^3$) and Example 2.4 ($\gamma_r=2.40 \text{ t/m}^3$).

To estimate the damage to the two roundhead armors when the design storm is exceeded, the safety factors given in Table 2.4 can be used as an initial approximation (wave steepness and roundhead radius are not considered).

(B1) Double-layer cube armor on roundhead

SF(IDa50%)=1.13, SF(IDE50%)=1.40, SF(IDa5%)=0.88 and SF(IDE5%)=1.17

There is a 50% probability of reaching

Initiation of Damage (IDa) with $H_{si}[m] < 1.13 \times 10.0 = 11.3$

Initiation of Destruction (IDE) with $H_{si}[m] < 1.40 \times 10.0 = 14.0$

There is a 5% probability of reaching

Initiation of Damage (IDa) with $H_{si}[m] < 0.88 \times 10.0 = 8.8$

Initiation of Destruction (IDE) with $H_{si}[m] < 1.17 \times 10.0 = 11.7$

(B2) Double-layer Cubipod[®] armor on roundhead

SF(IDa50%)=1.18, SF(IDE50%)=1.36, SF(IDa5%)=0.99 and SF(IDE5%)=1.19

There is a 50% probability of reaching

Initiation of Damage (IDa) with $H_{si}[m] < 1.18 \times 10.0 = 11.8$

Initiation of Destruction (IDE) with $H_{si}[m] < 1.36 \times 10.0 = 13.6$

There is a 5% probability of reaching

Initiation of Damage (IDa) with $H_{si}[m] < 0.99 \times 10.0 = 9.9$

Initiation of Destruction (IDE) with $H_{si}[m] < 1.19 \times 10.0 = 11.9$

2.5. Roundhead hydraulic stability of single-layer Cubipod[®] armors (K_D=5)

The hydraulic stability of roundheads protected with single-layer Cubipod[®] armors was studied in a series of small-scale physical tests. During the research project MMONO-CAPA (2013-2015), systematic 3D tests were carried out in the *Universidade da Coru-*

$\tilde{n}a$ (UDC) wave basin (long-crested waves) and IH Cantabria ocean basin (short- and long-crested waves). Similar double roundhead models protected with single-layer armors were tested in the two laboratories with slope $\cot\alpha=H/V=1.5$ in non-breaking and non-overtopping conditions. Different roundhead radius and wave steepnesses were considered in the corresponding test matrix. Unidirectional (long crested) irregular waves perpendicular to the structure were generated in the UDC wave basin; directional (short- and long-crested) waves were generated in the IH Cantabria facility with angles $\theta=0^\circ$ (perpendicular waves) and $\theta=22^\circ$ (oblique waves). Wave directional spreading was $\sigma=16^\circ$ in the IH Cantabria ocean basin. A similar hydraulic stability of roundheads (IDa and IDe) was found in the two laboratories; therefore, obliquity and directional spreading in the range $0^\circ<\theta<22^\circ$ and $0^\circ<\sigma<16^\circ$ did not significantly alter the hydraulic stability of single-layer Cubipod[®] armored roundheads when subjected to long-crested waves perpendicular to the trunk ($\theta=\sigma=0^\circ$). Figure 2.7a shows the 3D model of the trunk with a double roundhead protected with a single-layer Cubipod[®] armor, tested at UDC. Figure 2.7b shows a plan view of the models tested at UDC and IH Cantabria.

The hydraulic stability of roundheads protected with single-layer Cubipod[®] armors was studied using similar physical models in these two laboratories with different wave generators (short- and long-crested waves). Roundheads with different characteristics (radius, wave steepness, etc.) were tested in non-breaking and non-overtopping conditions. Both laboratories obtained lower hydraulic stability to IDe for single-layer Cubipod[®] armors, compared to double-layer Cubipod[®] armors. A stability coefficient, $K_D=5.0$, is recommended for single-layer Cubipod[®] armors in the roundhead.



Figure 2.7a Double roundhead 3D model with single-layer Cubipod[®] armor tested at UDC.

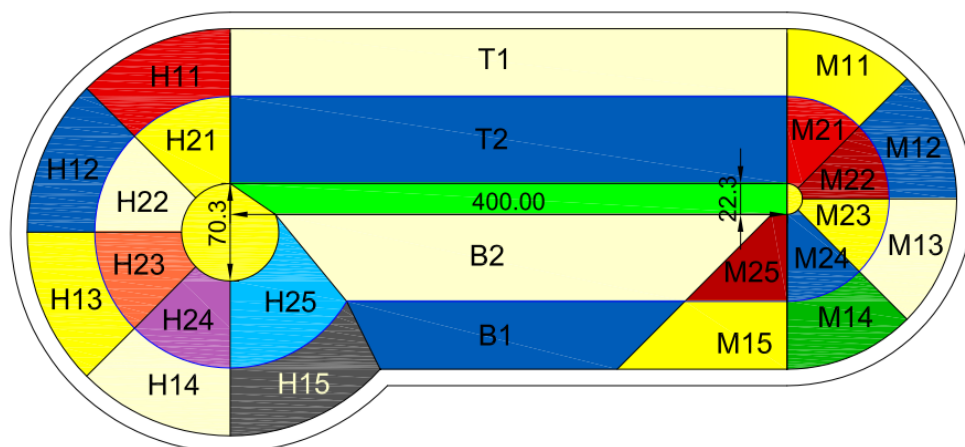


Figure 2.7b Plan view of double roundhead 3D model with single-layer Cubipod[®] armor tested at UDC and IH Cantabria.

The hydraulic stability to IDa for single-layer Cubipod[®] armors in the roundhead is usually higher than that corresponding to double-layer armors; however, the failure function of double-layer Cubipod[®] armors is more flexible. As a rule of thumb, single-layer Cubipod[®] armors have a typical ratio $N_s(\text{IDe})/N_s(\text{IDa})=1.10$, significantly lower than the ratio 1.20 corresponding to double-layer Cubipod[®] armors in the roundhead.

Compared to the conventional double-layer cube armor, the roundhead protected with a single-layer Cubipod[®] armor usually has a higher hydraulic stability to IDa but lower hydraulic stability to IDe. Using $K_D=5.0$ and 7.0 for single- and double-layer Cubipod[®] armors, in preliminary design phases, is recommended; single-layer armors require wider safety margins and several roundhead characteristics (radius, wave steepness, etc.) affect the hydraulic stability of roundhead armors.

It is necessary to emphasize that constructing roundheads is much more complex than trunks. Underwater armor unit placement of prototypes (almost blind placement by crawler crane with waves) is significantly different from that of small-scale models (by hand and perfect viewing), and this is especially true for roundheads. This model effect is particularly relevant for single-layer armors because a serious placement mistake at prototype scale may result in part of the roundhead being left unprotected leading to progressive failure. The tendency of Cubipods to self-arrangement on the slope reduces the differences between prototype and small-scale placement (smaller model effects); however, the Cubipod[®] placement in single-layer armors requires a much stricter quality control procedure than double-layer armors.

Figure 2.8 shows the stability numbers to IDe for single-layer Cubipod[®] armors on roundheads for wave storms with different wave directions and directional spreading. It is necessary to consider that safety margins may be lower for waves storms with low

wave steepnesses ($s_{0p}=H_{m0}/L_{0p}$) and higher for high wave steepnesses. Furthermore, the roundhead radius and real armor porosity may significantly affect armor hydraulic stability.

Finally, several tests were carried out with the breakwater almost perpendicular to the coastline (groin) and wave crests ($\theta=90^\circ$). In these conditions, the armor on the roundhead has a much higher hydraulic stability than armors with waves attacking almost perpendicular to the structure ($0^\circ \leq \theta \leq 22^\circ$). On the one hand, hydraulic stability increases for high obliquity waves in roundheads and trunks; on the other hand, scouring may be more relevant if the breakwater is placed on a sandy sea bottom.

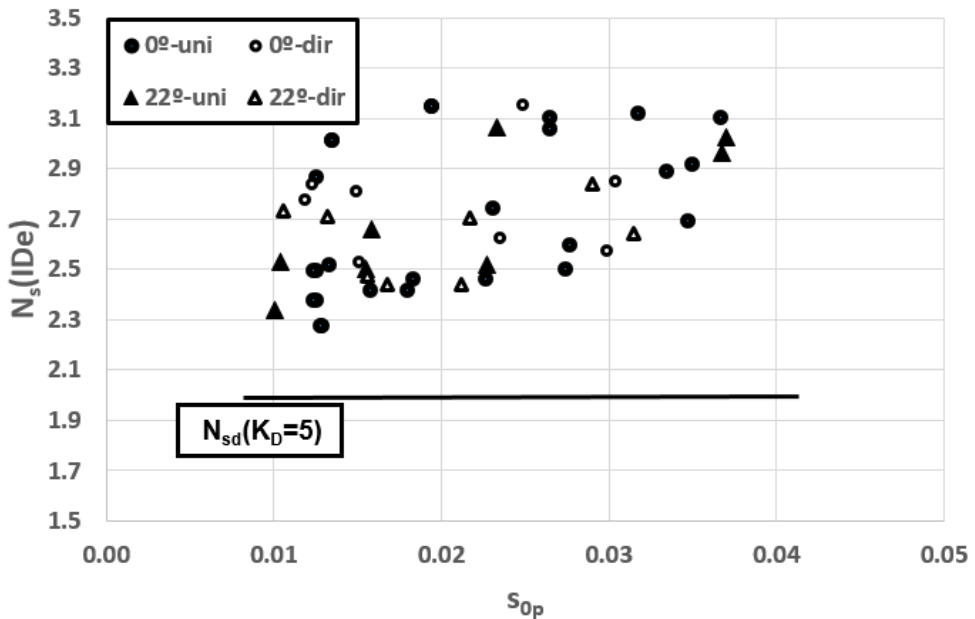


Figure 2.8 Stability numbers to IDe for single-layer Cubipod[®] armored roundheads.

Example 2.4

Given: Water depth at the toe of the structure is $h_s[m]=30.0$; tidal range is $\Delta h[m]=3.0$ and design storm is $H_{m0}[m]=10$ and $T_p[s]=18$. Armor slope is $\cot\alpha=1.5$ and mass densities of concrete and sea water are $\rho_c[t/m^3]=2.400$ and $\rho_w[t/m^3]=1.025$.

Find: (A) Weights of precast concrete units placed on roundhead for (1) double-layer cube armor, (2) single-layer Cubipod[®] armor and (3) double-layer Cubipod[®] armor. (B) Estimated armor damage levels when design storm is surpassed.

Solution: $H_{sd}/h_s=10/30=0.33$ (LWL) and $H_{sd}/h_s=10/35=0.29$ (HWL); Equation 2.2, Table 2.4 and Figure 2.8 can be used because the breakwater is under non-breaking wave conditions ($H_{sd}/h_s < 0.39$).

The roundhead design stability numbers and nominal diameters for double-layer cube and Cubipod armors are given in Example 2.3. The roundhead design stability number, nominal diameter and armor unit weight for single-layer Cubipod armors are:

$$N_{sd}(\text{Cubipods}_{_1L}) = \frac{H_{sd}}{\Delta D_n} = (K_D \cot \alpha)^{1/3} = (5.0 \times 1.5)^{1/3} = 1.96$$

$$\text{Cubipods}_{_1L}: \quad D_n [m] = \frac{10}{1.96 \times \left(\frac{2.400}{1.025} - 1 \right)} = 3.80 \quad \text{and}$$

$$W[t] = 2.400 \times (3.80)^3 = 131.7$$

(A) Weights of concrete armor units: (1) $W[t]=132$, (2) $W[t]=132$ and (3) $W[t]=95$

To estimate the damage levels to the double-layer cube armor and single- and double-layer Cubipod[®] armors on roundheads when the design storm is exceeded, Figures 2.6 and 2.8 can be used as an initial approximation; Figures 2.6 and 2.8 shows the effect of wave steepness on hydraulic stability ($s_{op} = 2\pi H_{m0}/gT_p^2 \approx 0.020$), but roundhead radius and other effects are not considered. Additionally, it was assumed that hydraulic stability to IDa for single-layer Cubipod[®] armors is usually slightly higher than that corresponding to double-layer armors in roundheads.

(B1) Double-layer cube armor on roundhead

Experimental IDa50% (cubes_2L) $H_{si}[m] = (2.0/1.96) \times 10 = 10.2$

Experimental IDe50% (cubes_2L) $H_{si}[m] = (2.45/1.96) \times 10 = 12.5$

(B2) Single-layer Cubipod[®] armor on roundhead

Experimental IDe5% (Cubipods_1L) $H_{si}[m] > (2.4/1.96) \times 10 = 12.2$

Experimental IDe50% (Cubipods_1L) $H_{si}[m] > (2.7/1.96) \times 10 = 13.8$

(B3) Double-layer Cubipod[®] armor on roundhead

Experimental IDa50% (Cubipods_2L) $H_{si}[m] = (2.3/2.19) \times 10 = 10.5$

Experimental IDe50% (Cubipods_2L) $H_{si}[m] = (2.75/2.19) \times 10 = 12.6$

2.6. Cubipod[®] armors in depth-limited breaking wave conditions

The hydraulic stability (trunk) of single- and double-layer Cubipod[®] armors in breaking conditions was studied in a series of physical tests. Although most physical exper-

iments have been carried out in non-breaking conditions, specific 2D hydraulic stability tests in depth-limited breaking wave conditions were conducted at the LPC-UPV (CUBIPOD Project, 2007-2009). Using the same core and filter layers, three models with different armoring protection were tested in breaking and non-overtopping conditions with slope $\cot\alpha=1.5$. Single- and double-layer Cubipod[®] armors with toe berm and double-layer armor without toe berm were tested.

The hydraulic stability tests in depth-limited breaking wave conditions aimed to determine the minimum hydraulic stability of armors on breakwaters placed on horizontal seafloors ($\beta=0\%$) at a given water depth. The reference scale was 1/50 and the objective was to find, for a given water depth, a unit size which made the armor invulnerable regardless of the deep water wave storm conditions. In breaking conditions, the maximum wave height attacking the breakwater depends on the water depth at the toe (h_s), the wave period (T) and the bottom slope ($\beta=0\%$ in this case). The worst test conditions were not those generating irregular waves, but rather those trains of regular waves with a variety of wave periods. For different water depths (h_s [m]=15.0, 17.5, 19.0, etc. at prototype scale), trains of regular waves in the range $6 < T_m$ [s] < 18 (prototype scale) were generated with increasing wave height (H). For a given water depth (h_s) and wave period (T_m), if H is too high, the waves break before reaching the structure and there is no damage; if H is too small, the waves will not cause the maximum damage to the structure. The methodology described above ensured that the most damaging waves will attack the structure in depth-limited breaking wave conditions.

Figure 2.9 shows the cross section of a double-layer Cubipod[®] armor with toe berm and a detail of the toe berm used in these experiments. For 16-tonne Cubipod[®] units (1/25 scale), a different armor damage is observed for each water depth (h_s); the higher the water depth, the greater the armor damage. For each water depth, regular wave trains of 50 waves were generated with a wide range of wave periods ($6 < T_m$ [s] < 18) and increasing wave height (H) up to the armor being severely damaged (IDe). The accumulated armor damage was measured to obtain the maximum armor damage associated with each water depth. The methodology ensured that 50 waves attacked the armor with the most damaging combination of wave height and period for the given water depth. Equivalent dimensionless armor damage (D_e) was measured following the Virtual Net (VN) method described by Gómez-Martín and Medina (2014). It was verified that, for a given water depth, any irregular wave train caused very low armor damage compared to the damage caused by the series of regular waves corresponding to the experimental methodology indicated above. Therefore, the design based on the results of these experiments with regular waves in breaking conditions is on the safe side.

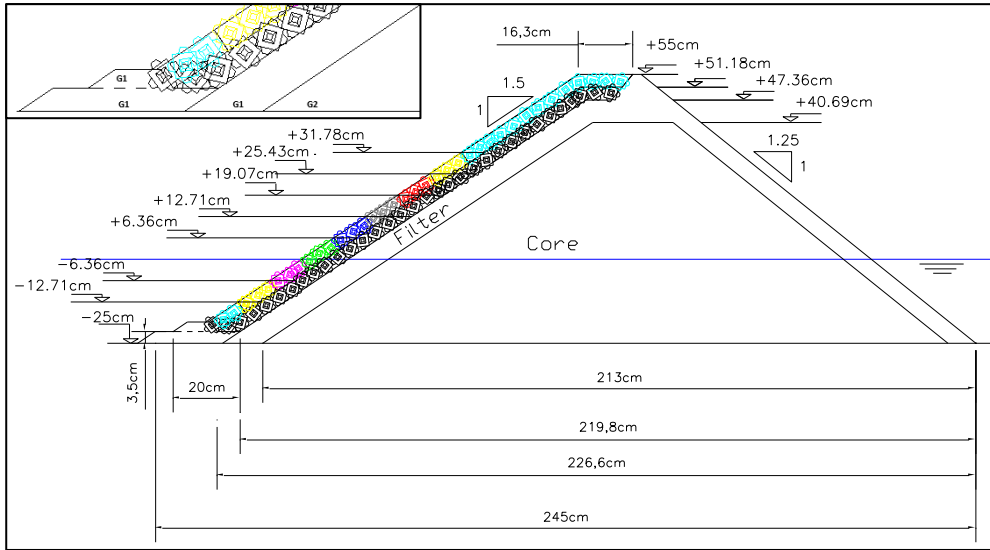


Figure 2.9 Cross section of the 2D model of double-layer Cubipod[®] armor with toe berm in breaking conditions and detail of the toe berm.

Figure 2.10 shows the accumulated armor damage measured at different water depths for three armors: (1) double-layer Cubipod[®] armor without toe berm (C2), (2) double-layer Cubipod[®] armor with toe berm (C2b) and (3) single-layer Cubipod[®] armor with toe berm (C1b). Given the direct relationship between water depth and the normalized design wave height, it is reasonable to define dimensionless failure functions to describe the hydraulic stability of breakwaters in depth-limiting breaking wave conditions. The observed failure function is

$$D_e = 10^{-4} \left(\frac{h}{\Delta D_n} \right)^5 \quad 2.3$$

in which D_e is the equivalent dimensionless armor damage, $h=h_s$ is the water depth ($\beta=0\%$), Δ is the relative submerged mass density and D_n is the equivalent cube side length.

Considering that initiation of damage (IDa) corresponds to equivalent dimensionless damage $1.0 < D_e < 2.0$, say $D_e=1.6$, then $h=h_s < 7.0(\Delta D_n)$ is the water depth which guarantees that both single- and double-layer armors will not exceed IDa. Furthermore, the tests carried out indicate a relevant safety margin to initiation of destruction (IDE). Assuming a safety factor $SF(IDE)=1.15$ for double-layer Cubipod[®] armors and $SF(IDE)=1.30$ for single-layer Cubipod[®] armors, the following design values are obtained for breakwaters placed on a horizontal seafloor ($\beta=0\%$): $h=h_s < 7.0(\Delta D_n)$ and $h=h_s < 6.2(\Delta D_n)$ for double- and single-layer Cubipod[®] armors, respectively.

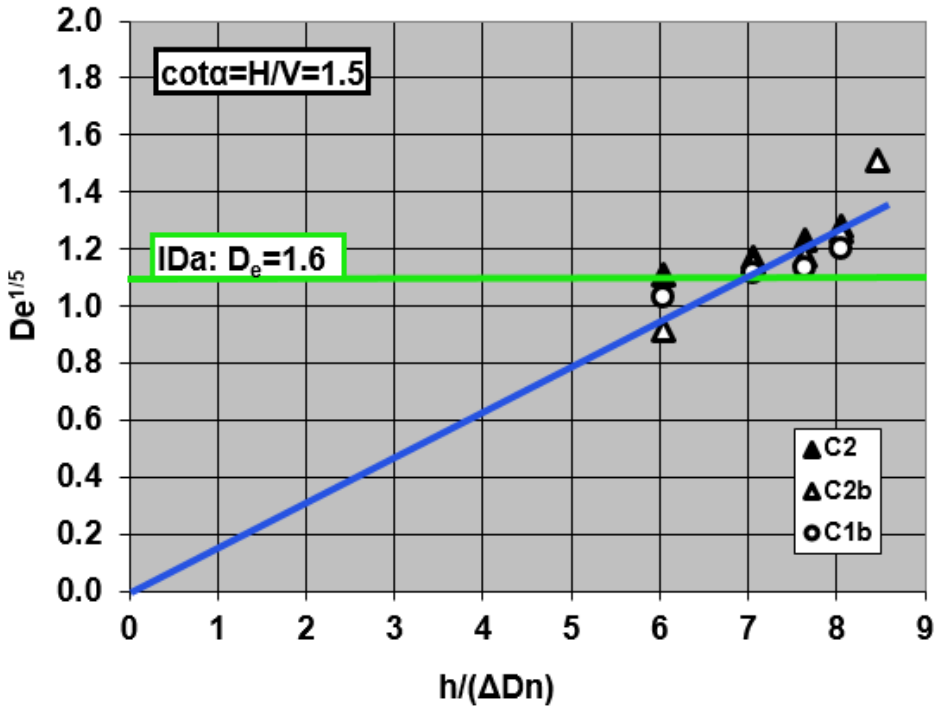


Figure 2.10 Equivalent dimensionless armor damage (De) as a function of relative water depth.

The highest wave heights measured in the model area were approximately 60% of the water depth, $H_{max}/h_s \approx 0.60$ with a horizontal seafloor ($\beta=0\%$). For gentle bottom slopes ($\beta>0$), a criterion similar to that given by Goda (2010) should be used. The design water depth (h) is calculated at a distance three times the water depth at the toe of the structure (h_s), $h=h_s(1+3 \tan\beta)$. This approximation is valid for gentle bottom slopes ($\tan\beta \approx 2\%$); for steep bottom slopes (e.g. $\tan\beta=10\%$), the toe berm design is critical and armor layer and toe berm must be studied simultaneously. Small-scale models are highly recommended when breakwaters are placed on steep sea bottoms in depth-limited breaking wave conditions.

Figure 2.11 shows the water depth at the toe (h_s) and the design water depth for depth-limited wave conditions, $h=h_s(1+3 \tan\beta)$. Once the design water depth (h) is calculated, the size of Cubipod[®] units can be estimated to design invulnerable armors with $cota=1.5$ for any deep water wave climate:

$$\text{Double-layer Cubipod}^{\text{®}} \text{ armors: } D_n > h/7.0\Delta = h_s(1+3 \tan\beta)/(7.0\Delta) \quad 2.4$$

$$\text{Single-layer Cubipod}^{\text{®}} \text{ armors: } D_n > h/6.2\Delta = h_s(1+3 \tan\beta)/(6.2\Delta) \quad 2.5$$

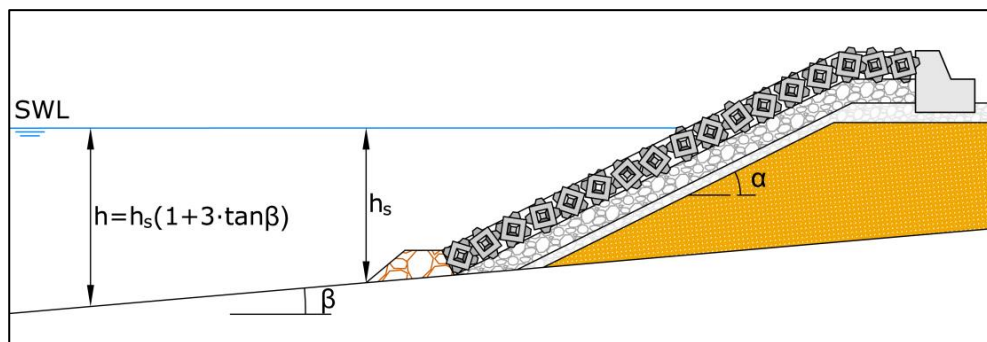


Figure 2.81 Schematic cross section of a breakwater in breaking conditions.

For sandy seafloors, it is convenient to design a breakwater scour protection and to estimate erosion, scour, as well as long-term water depth fluctuations; if necessary, design water depth should be increased to take into account water depth during service lifetime.

Example 2.5

Given: Water depth at the toe of the structure is $h_s[\text{m}]=10.0$ (referred to LWL), tidal range is $\Delta h[\text{m}]=\text{HWL}-\text{LWL}=2.5$ and bottom slope is $\tan\beta=3\%$. Mass densities of concrete and sea water are $\rho_r[\text{t/m}^3]=2.350$ and $\rho_w[\text{t/m}^3]=1.025$.

Find: A preliminary design for a Cubipod[®] armored breakwater (trunk) in wave breaking conditions.

Solution: For double-layer Cubipod[®] armors ($\cot\alpha=1.5$), Eq. 2.4 is applicable. The most damaging wave breaking conditions are given at HWL (larger waves attacking the structure)

$$D_n[\text{m}] > h_s[\text{m}](1+3 \tan\beta)/(7.0\Delta) = (10.0+2.5)(1+0.09)/(7.0 \times ((2.350/1.025)-1)) = 1.51$$

$$W[\text{t}] > 2.35 \times 1.51^3 = 8.1$$

For single-layer Cubipod[®] armors (slope $\cot\alpha=1.5$), Eq. 2.5 is applicable.

$$D_n[\text{m}] > h_s[\text{m}](1+3 \tan\beta)/(6.2\Delta) = (10.0+2.5)(1+0.09)/(6.2 \times ((2.350/1.025)-1)) = 1.71$$

$$W[\text{t}] > 2.35 \times 1.71^3 = 11.7$$

The breakwater can be protected with either a 8-tonne (3.5 m³) double-layer or 12-tonne (5.0 m³) single-layer Cubipod[®] armor. These armors are hydraulically stable (armor damage below IDa) and are able to withstand any wave storm (H_s and T_p) in any tidal level $\Delta h[\text{m}] \leq 2.5$. The safety factors to IDE of these double- and single-layer Cubipod[®] armors are 1.15 and 1.30, respectively.

Chapter 3

Overtopping and forces on crown wall

3.1. Introduction

For a given wave storm, run-up and overtopping on a mound breakwater depend on several armor characteristics (thickness, porosity and unit geometry), permeability of core and filter layers and crown wall geometry, among other factors. Focusing on the armor layer, a higher roughness (lower γ_f) reduces overtopping and allows for designs with a lower crest elevation, reducing construction costs and the forces on the crown wall. To estimate the roughness factors of double-layer cube armors, and single- and double-layer Cubipod[®] armors, a series of 2D overtopping tests were carried out using similar models, with the same core and filter layer, but different crown-wall elevations (pressure on crown wall was also measured). The objective of these physical tests was to estimate the roughness factors of the three different armors.

During the CUBIPOD project (2007-2009), we estimated the overtopping rates corresponding to cube and Cubipod[®] armors, through a series of 2D run-up and overtopping tests carried out at the LPC-UPV wave flume. Conventional double-layer, randomly-placed cube armors as well as single- and double-layer Cubipod[®] armors, with slope $\cot\alpha=1.5$ in non-breaking conditions, were tested using the same core and filter layer. The methodology (see Medina et al., 2002) was similar to that used for CLASH (2002-2005).

Figure 3.1 shows the cross section of the model with a reference scale of 1/100 and 1/50 for large breakwaters on the Atlantic and Mediterranean coasts of Spain, respectively. Both Smolka et al. (2009) and Medina et al. (2010) reported that overtopping

was not significant ($Q < 10^{-7}$) for high values of dimensionless crest elevation, $R_c/H_{m0} > 2.6$. If dimensionless crest elevation $R_c/H_{m0} < 2.6$, Smolka et al. (2009) proposed using Equation 3.1.

$$Q = \frac{q}{\sqrt{gH_{m0}^3}} = 0.2 \exp \left(0.53 Ir_p - 3.27 \frac{A_c}{R_c} - \frac{2.16}{\gamma_f} \frac{R_c}{H_{m0}} \right) \quad 3.1$$

where Q is the dimensionless overtopping rate, R_c/H_{m0} is the dimensionless crest elevation, q [m³/s/m] is the overtopping rate, H_{m0} is the significant wave height, $\cot\alpha=1.5$, $Ir_p = (\tan\alpha)/(2\pi H_{m0}/gT_p^2)Q^{0.5}$ is Iribarren's number using H_{m0} and the peak period ($T_p=1/f_p$), R_c and A_c are crown wall and armor crest freeboard, respectively. The cross section of the model is shown in Figure 3.1. γ_f is the roughness factor corresponding to a given armor unit, number of layers and overtopping formula (see Molines and Medina, 2015). In these experiments, $\gamma_f=0.50$ for double-layer cube armors, and $\gamma_f=0.46$ and 0.44 for single- and double-layer Cubipod® armors, respectively. Equation 3.1 is valid in the range $0.70 < A_c/R_c < 1.00$ (double-layer cube armor), $0.40 < A_c/R_c < 0.65$ (single-layer Cubipod® armor), $0.58 < A_c/R_c < 0.80$ (double-layer Cubipod® armor) and $10^{-6} < Q < 10^{-3}$.

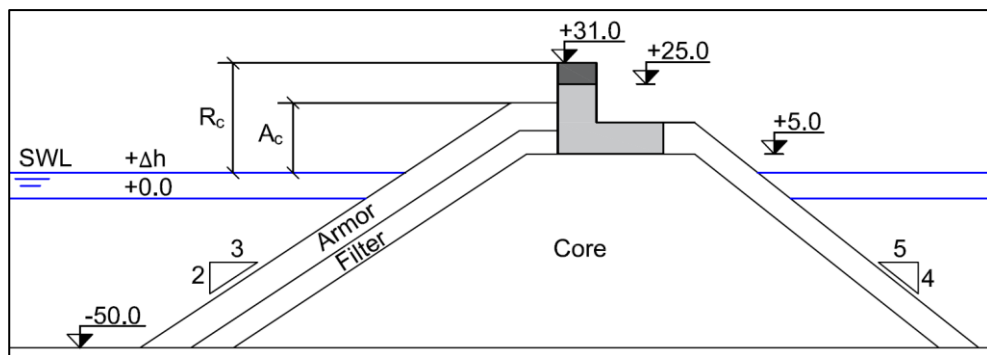


Figure 3.1 Cross section of 2D model used in overtopping tests (dimensions in cm).

It is widely accepted (see Bruce et al., 2009) that the roughness factor γ_f depends on the armor unit (cube, Tetrapod, etc.), placement (random, ordered, etc.) and number of layers (one or two). Recently, Molines and Medina (2015) pointed out that γ_f also depends on the specific formula or overtopping predictor in which γ_f is used. For specific structural characteristics (slope, crest elevation, etc.) and design storms, the higher the γ_f , the higher the overtopping rates. Molines and Medina (2015) provide appropriate roughness factors for different overtopping predictors with different ranges of application.

Compared to conventional randomly-placed double-layer cube armors, Cubipod[®] armors significantly reduce overtopping rates; crest elevation can be lowered, crown wall size reduced, and design overtopping rates maintained.

To assess the crown-wall stability, different crown wall models were tested during the overtopping tests described above; pressures on the crown wall as well as horizontal and uplift forces were analyzed. Molines (2011) considered the maximum horizontal force (F_h) and the maximum uplift force ($F_v(F_h)$) generated by a single wave. Although these peak forces are not usually generated at the same time, they are usually considered to be acting simultaneously (in order to be conservative). The maximum horizontal and uplift forces, F_h and $F_v(F_h)$, were used by Molines (2011) to assess the stability of the crown wall. Sliding is usually the most critical crown wall failure mode. His statistical analysis validated the use of F_h and $F_v(F_h)$ to estimate the safety factor for crown wall sliding. The formulas given by Molines (2011) considered the roughness factor associated with the armor, used to estimate overtopping rates, because the roughness factor is related to the virtual run-up on the slope, which affects the pressure on the crown wall.

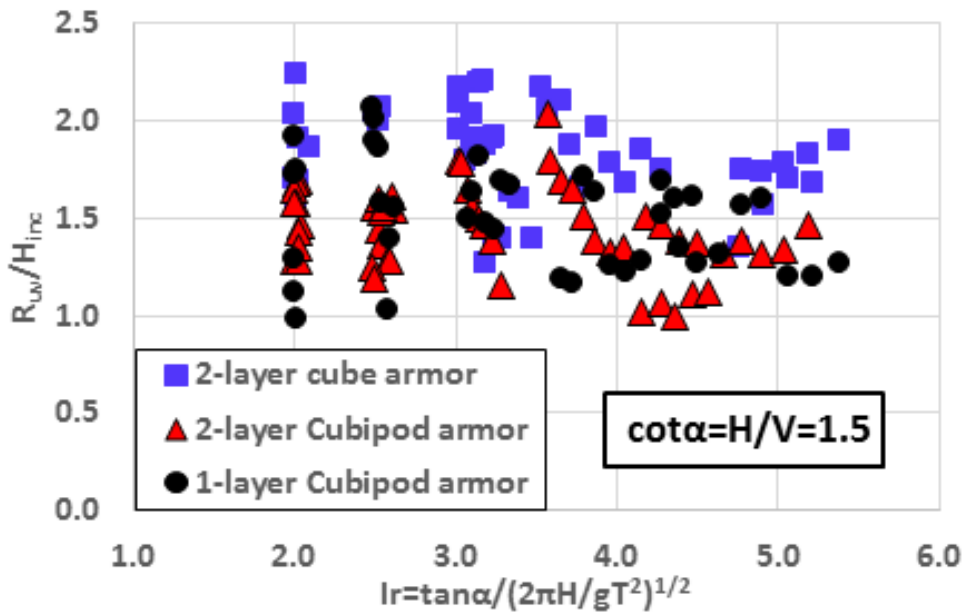


Figure 3.2 Dimensionless visual run-up R_{uv}/H_{inc} corresponding to double-layer cube, single- and double-layer Cubipod[®] armors (regular waves).

Smolka et al. (2009) described physical experiments for run-up tests (no overtopping) using visual observation and step gauge sensors on the slope. Visual observations are easy to take but usually provide significantly higher run-up values than those measured

with instruments. Figure 3.2 shows visual run-up values (R_{uv}) related to incident regular wave height (H_{inc}) corresponding to double-layer cube armors and single- and double-layer Cubipod[®] armors.

Visual run-up is significantly lower for Cubipod[®] armors, which agrees with the lower roughness factors when analyzing overtopping rates. Cubipod[®] armors have significantly lower roughness factors than conventional cube armors; run-up and overtopping rates are lower as are the forces on the crown wall.

3.2. Overtopping on double-layer Cubipod[®] armors ($\gamma_f=0.44$)

Overtopping on mound breakwaters depends on armor unit geometry and placement, number of layers and other structural characteristics (core permeability, etc.), being the armor roughness factor (γ_f) the most common characterization parameter (see EurOtop Manual, 2007). A higher roughness (lower γ_f) reduces the overtopping rates allowing for a lower crest elevation (lower visual impact) and decreased costs and material consumption.

For the CUBIPOD project (2007-2009), 2D small-scale run-up and overtopping tests were conducted in the LPC-UPV wave flume. Conventional double-layer cube armors and single- and double-layer Cubipod[®] armors were tested, with slope $\cot\alpha=H/V=1.5$ in non-breaking conditions. Conventional double-layer randomly-placed cube armors are well-studied in the literature (see Bruce et al., 2009); therefore, comparison to other armors is reliable and model effects are minimized when testing with the same core, filter layer and crown wall. For double-layer cube and Cubipod[®] armors, Smolka et al. (2009) and Medina et al. (2010) proposed Equation 3.1 to estimate overtopping rates.

The roughness factor $\gamma_f=0.44$ reported by Smolka et al. (2009) for double-layer Cubipod[®] armors is 88% of $\gamma_f=0.50$ obtained for conventional double-layer cube armors. If the overtopping predictor or the database is different, roughness factors may change significantly in absolute values, but not so much in relative values (see Molines and Medina, 2015). For instance, considering the CLASH overtopping neural network predictor and the CLASH data for conventional mound breakwaters, Molines and Medina (2015) found $\gamma_f=0.53$ and 0.45 for double-layer cube and Cubipod[®] armors, respectively; roughness factors were higher but the change in the relative roughness factor was minor (from 88% to 85%).

Figure 3.3 shows the observed visual run-up on double-layer cube and Cubipod[®] armors compared to the dimensionless water depth (kh) in the tests with regular waves and no overtopping described by Smolka et al. (2009). The significant differences in dimensionless run-up (R_{uv}/H_{inc}) agree with those in roughness factor; the higher the roughness factor, the higher the run-up and overtopping.

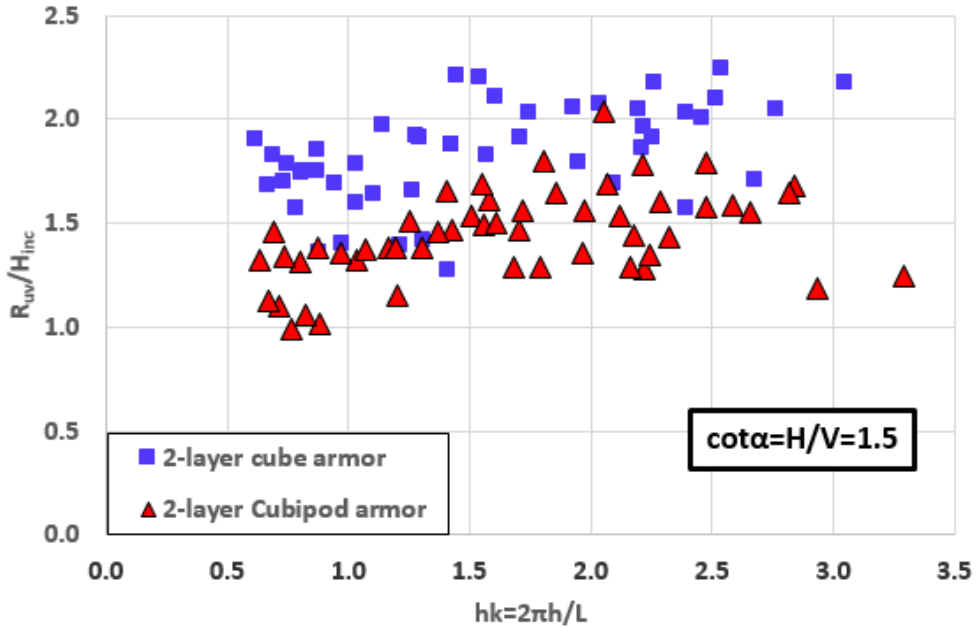


Figure 3.3 Dimensionless visual run-up R_{uv}/H_{inc} observed for double-layer cube and Cubipod[®] armors (regular waves).

Example 3.1

Given: Water depth at the toe of structure is $h_s[m]=40.0$, tidal range is $\Delta h[m]=5.0=HWL-LWL$ and design storm is $H_{m0}[m]=10$ and $T_p[s]=18$. Armor slope is $\cot\alpha=1.5$ and crest elevation of armor and crown wall is around $A_c+\Delta h=R_c+\Delta h=20$ m.

Find: The crest elevation ($R_c+\Delta h$) for double-layer cube and Cubipod[®] armors if the mean overtopping discharge is limited to $q=10.0$ l/s/m for the design storm and HWL.

Solution: $R_c[m]=20-5=15$, $I_{rp}=(2/3)/(2\pi \times 10/[9.8 \times 18^2])^{1/2}=4.7$, $R_c/H_{m0}=15/10=1.5$, $A_c/R_c=1$, $\gamma_f=0.50$ (2-layer cube armor) and $\gamma_f=0.44$ (2-layer Cubipod[®] armor).

Considering Equation 3.1:

$$Q_{cubes} = \frac{q}{\sqrt{gH_{m0}^3}} = 0.2 \exp\left(0.53 \times 4.7 - 3.27 \times \frac{15}{15} - \frac{2.16}{0.50} \times \frac{15}{10}\right)$$

$$Q_{cubes} = \frac{q}{\sqrt{gH_{m0}^3}} = 0.2 \exp(2.49 - 3.27 - 6.48) = 1.40 \times 10^{-4}$$

$$q_{cubes}[m^3/s/m] = (9.8 \times 10^3)^{0.5} Q_{cubes} = 99.0 Q_{cubes}$$

$$q_{\text{cubes}}[\text{m}^3/\text{s}/\text{m}] = 99.0 \times 1.40 \times 10^{-4} = 13.9 \times 10^{-3} \rightarrow q = 13.9 \text{ l/s/m} > 10.0 \text{ l/s/m (failure)}.$$

Increasing the crest elevation by one meter, $R_c/H_{m0} = 16/10 = 1.6$ and $A_c/R_c = 1$

$$Q_{\text{cubes}} = \frac{q}{\sqrt{gH_{m0}^3}} = 0.2 \exp(2.49 - 3.27 - 6.91) = 0.89 \times 10^{-4}$$

$$q_{\text{cubes}}[\text{m}^3/\text{s}/\text{m}] = 99.0 Q_{\text{cubes}} = 8.8 \times 10^{-3} \rightarrow q = 8.8 \text{ l/s/m} < 10.0 \text{ l/s/m}$$

Double-layer cube armor: Crest elevation $(R_c + \Delta h)[\text{m}] = 16 + 5 = 21$

Using a double-layer Cubipod[®] armor, the crest elevation may be reduced to $R_c + \Delta h = 19$ m, because $R_c[\text{m}] \approx 16 \times 0.44 / 0.50 \approx 14$. Lowering the breakwater crest elevation by two meters from the cube armored solution ($R_c/H_{m0} = 14/10 = 1.4$ y $A_c/R_c = 1$), we find

$$Q_{\text{Cubipod}} = \frac{q}{\sqrt{gH_{m0}^3}} = 0.2 \exp\left(0.53 \times 4.7 - 3.27 \times \frac{14}{14} - \frac{2.16}{0.44} \times \frac{14}{10}\right)$$

$$Q_{\text{Cubipod}} = \frac{q}{\sqrt{gH_{m0}^3}} = 0.2 \exp(2.49 - 3.27 - 6.87) = 0.95 \times 10^{-4}$$

$$q_{\text{Cubipods}}[\text{m}^3/\text{s}/\text{m}] = 99.0 Q_{\text{Cubipods}} = 9.4 \times 10^{-3} \rightarrow q = 9.4 \text{ l/s/m} < 10.0 \text{ l/s/m}$$

Double-layer Cubipod[®] armor: Crest elevation $(R_c + \Delta h)[\text{m}] = 14 + 5 = 19$

The double-layer Cubipod[®] armor allows for a two-meter reduction in the breakwater crest elevation, when compared to conventional cube armoring. The crest freeboard is reduced by 13%; thus, construction costs as lower as visual and environmental impacts.

3.3. Overtopping on single-layer Cubipod[®] armors ($\gamma_f = 0.46$)

Overtopping on mound breakwaters depends on roughness factors (see EurOtop Manual, 2007). A higher armor roughness (lower γ_f) reduces the overtopping rates allowing for a lower crest elevation.

2D small-scale run-up and overtopping tests were conducted at the LPC-UPV wave flume during the CUBIPOD project (2007-2009). Conventional double-layer cube armors and single- and double-layer Cubipod[®] armors were tested, with slope $\cot\alpha = H/V = 1.5$ in non-breaking conditions. To estimate overtopping rates of single-layer Cubipod[®] armors, Smolka et al. (2009) and Medina et al. (2010) proposed using Equation 3.1.

The roughness factor $\gamma_f = 0.46$ reported by Smolka et al. (2009) for single-layer Cubipod[®] armors is 92% of $\gamma_f = 0.50$ obtained for conventional double-layer cube armors. If

the overtopping predictor or the database is different, roughness factors may change significantly in absolute values, but not so much in relative values (see Molines and Medina, 2015). For instance, considering the CLASH overtopping neural network predictor and the CLASH data corresponding to conventional mound breakwaters, Molines and Medina (2015) found $\gamma_f=0.53$ and 0.48 for double-layer cube and single-layer Cubipod[®] armors, respectively; roughness factors increased but the change in the relative roughness factor was minor (from 92% to 90%).

Figure 3.4 shows the dimensionless visual run-up observed during the experiments by Smolka et al. (2009) for double-layer cube and single-layer Cubipod[®] armors, depending on relative water depth (kh). Run-up measurements correspond to regular waves in non-breaking and non-overtopping conditions with crown wall. The differences observed in run-up for cube and Cubipod[®] armors agree with those in the roughness factors as noted above ($\gamma_f=0.46$ for single-layer Cubipod[®] and $\gamma_f=0.50$ for double-layer cube armors).

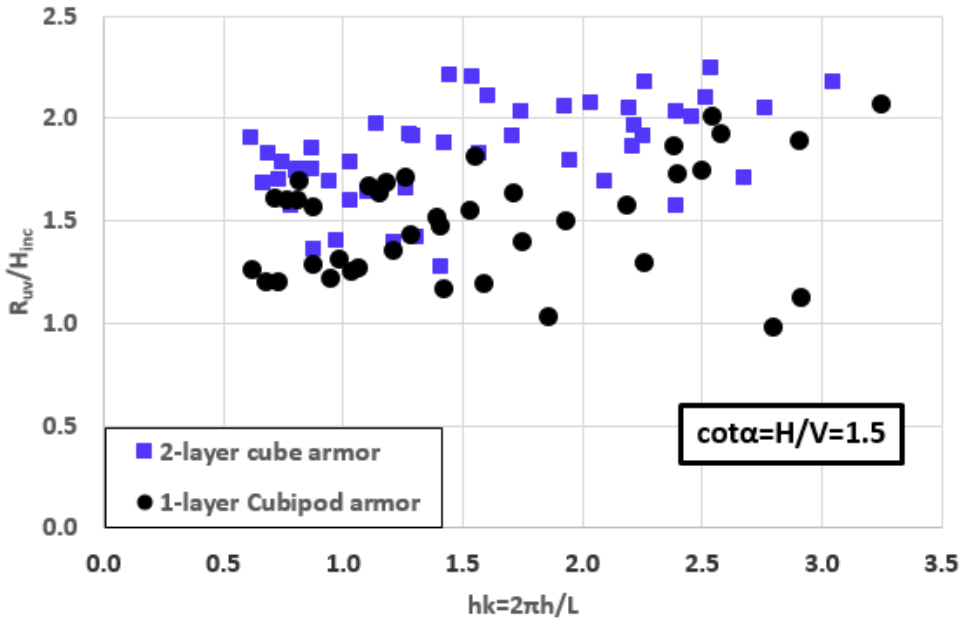


Figure 3.4 Dimensionless visual run-up R_{uv}/H_{inc} corresponding to double-layer cube and single-layer Cubipod[®] armors (regular waves).

Example 3.2

Given: A conventional mound breakwater is designed with a water depth $h_s[m]=40.0$, tidal range $\Delta h[m]=5.0$, design storm $H_{m0}[m]=10.0$ ($T_p[s]=18$), slope $\cot\alpha=1.5$,

$R_c[m]=A_c+5$ and $R_c+\Delta h \approx 20$ m. $q=20$ l/s/m is the maximum admissible overtopping rate for the design storm.

Find: The crest elevation for double-layer cube and single-layer Cubipod® armored breakwaters.

Solution: $R_c[m]=20-5=15$, $A_c[m]=15-5=10$, $I_{rp}=(2/3)/(2\pi \times 10/[9.8 \times 18^2])^{1/2}=4.7$, $A_c/R_c=0.67$, $R_c/H_{m0}=15/10=1.5$, double-layer cubes ($\gamma_f=0.50$) and single-layer Cubipods ($\gamma_f=0.46$).

Considering Equation 3.1:

$$Q_{cubes} = \frac{q}{\sqrt{gH_{m0}^3}} = 0.2 \exp\left(0.53 \times 4.7 - 3.27 \times \frac{10}{15} - \frac{2.16}{0.50} \times \frac{15}{10}\right)$$

$$Q_{cubes} = \frac{q}{\sqrt{gH_{m0}^3}} = 0.2 \exp(2.49 - 2.18 - 6.48) = 4.18 \times 10^{-4}$$

$$q_{cubes}[m^3/s/m] = (9.8 \times 10^3)^{0.5} Q_{cubes} = 99.0 Q_{cubes} = 41.4 \times 10^{-3} \rightarrow q = 41 \text{ l/s/m} > 20 \text{ l/s/m, (failure)}$$

With a two-meter higher crest elevation ($R_c/H_{m0}=17/10=1.7$ and $A_c/R_c=12/17=0.70$)

$$Q_{cubes} = \frac{q}{\sqrt{gH_{m0}^3}} = 0.2 \exp(2.49 - 2.29 - 7.34) = 1.6 \times 10^{-4}$$

$$q_{cubes}(m^3/s/m) = 99.0 Q_{cubes} = 15.8 \times 10^{-3} \rightarrow q = 16 \text{ l/s/m} < 20 \text{ l/s/m}$$

Double-layer cube armor: Crest elevation ($R_c+\Delta h$)[m]=22

Using single-layer Cubipod® armoring, a 0.5-meter rise in crest elevation should be enough to obtain similar results, because $R_c[m] \approx 17 \times 0.46/0.50 = 15.5$. With $R_c[m]=15.5$, $R_c/H_{m0}=15.5/10=1.55$ and $A_c/R_c=10.5/15.5=0.65$

$$Q_{Cubipods} = \frac{q}{\sqrt{gH_{m0}^3}} = 0.2 \exp\left(0.53 \times 4.7 - 3.27 \times \frac{10.5}{15.5} - \frac{2.16}{0.46} \times \frac{15.5}{10}\right)$$

$$Q_{Cubipods} = \frac{q}{\sqrt{gH_{m0}^3}} = 0.2 \exp(2.49 - 2.21 - 7.28) = 1.82 \times 10^{-4}$$

$$q_{Cubipods}(m^3/s/m) = 99.0 Q_{Cubipods} = 18.0 \times 10^{-3} \rightarrow q = 18 \text{ l/s/m} < 20 \text{ l/s/m}$$

Single-layer Cubipod® armor: Crest elevation ($R_c+\Delta h$)[m]=20.5

Compared to conventional double-layer cube armoring, single-layer Cubipod® armoring allows for a 1.5-meter decrease in the breakwater crest elevation, which results in cost-savings and a reduced visual and environmental impact.

3.4. Forces on the crown wall. Single- and double-layer armors

The formulas given by Molines (2011) can be used to estimate the maximum horizontal force (Fh) and the up-lift vertical force corresponding to the wave generating the maximum horizontal force (Fv(Fh)). Fh and Fv(Fh) are not simultaneous; however, on the safe side, they are considered simultaneous to estimate forces on the crown wall. Figure 3.5 depicts a typical example of the horizontal forces (green) and vertical up-lift forces (orange) measured on the crown wall model, corresponding to double-layer cube armoring with $H_s[\text{cm}]=17$, $I_{r_p}=4$, $R_c[\text{cm}]=20$ and $h_s[\text{cm}]=55$. Figure 3.6 shows a scheme of the horizontal (Fh) and vertical up-lift (Fv(Fh)) forces used by Molines (2011) to calculate the crown wall hydraulic stability (sliding is the main failure mode).

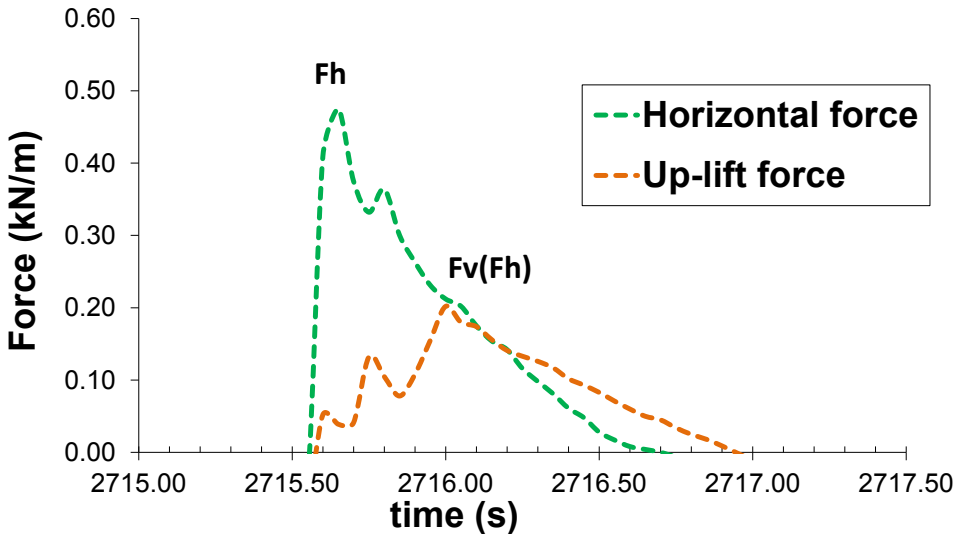


Figure 3.5 Example of measured Fh and Fv(Fh) on a double-layer cube armor model.

In order to verify the assumption associated with the use of Fh and Fv(Fh), Molines (2011) carried out a statistical analysis of the crown-wall sliding performance using the estimators Fh and Fv(Fh). The continuous recording ($\Delta t[\text{s}]=0.05$) of the horizontal force (Fh[t]) and vertical up-lift force (Fv(t)) was available for each test. The sliding safety margin failure function is: $S(n\Delta t)=(W_e-Fv(n\Delta t))\mu-Fh(n\Delta t)$, where $W_e[\text{kN/m}]$ is the crown-wall unit weight and μ is the friction coefficient between the crown wall and rocky bedding layer. For each test, the values $S(n\Delta t)$ were ordered to obtain the minimum value, S_d . On the other hand, the experimental values Fh and Fv(Fh) were used to estimate the safety margin for each test $S_1=(W_e-Fv(Fh))\mu-Fh$.

$S_d=\min[S(n\Delta t)]$ is the desired value, but it requires analyzing the full register. S_1 (associated to $Fh=\max[Fh(n\Delta t)]$) is much easier to calculate. Due to the influence of the friction factor (μ) on the sliding safety margin, Molines (2011) compared S_d and S_1 for

$0.50 \leq \mu \leq 0.70$; Goda (1985) proposed $\mu=0.60$ while ROM 0.5-05 (2008) recommended $\mu=0.70$. Recently, Molines (2016) re-analyzed these data. Estimator S_1 is reasonable because it is on the safety side for more than 92% of the cases. The breakwater cross section for the calculations used by Molines (2016) is that given in Figure 3.6, which illustrates variables, pressures and up-lift forces acting on the crown wall.

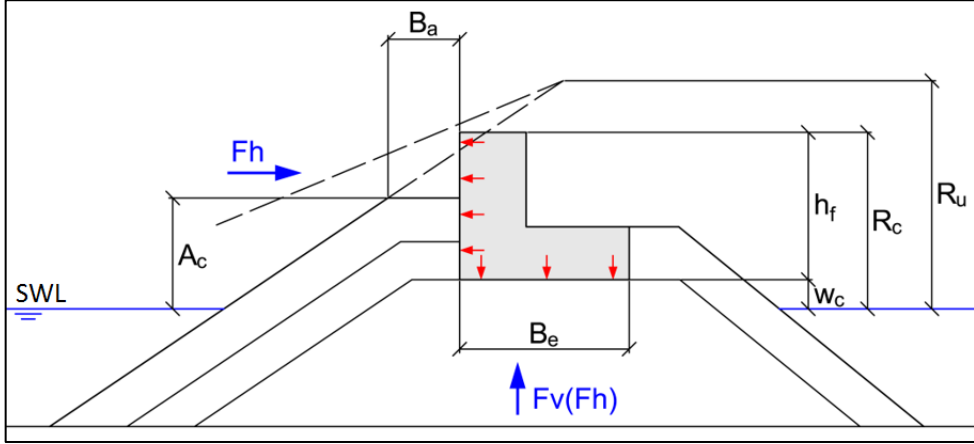


Figure 3.6 Scheme of horizontal and vertical up-lift forces acting on the crown wall.

Molines (2016) proposed Equations 3.3 and 3.4 to estimate F_h and $F_v(F_h)$:

$$\frac{F_h}{0.5\rho_w g h_f^2} = \left(-1.29 + 1.80 \frac{\gamma_f R_u}{R_c} + 0.93 \left(\frac{R_c - A_c}{h_f} \right) + 0.16 \sqrt{\frac{L_m}{B_a}} \right)^2 \quad 3.2$$

$$\frac{F_v(F_h)}{0.5\rho_w g h_f B_e} = \left(-0.86 + 0.75 \frac{\gamma_f \times R_u}{R_c} + 0.41 \left(\frac{R_c - A_c}{h_f} \right) + 0.17 \sqrt{\frac{L_m}{B_a}} - 0.9 \frac{w_c}{h_f} \right)^2 \quad 3.3$$

$$2.58H_s > R_u = R_{u0.1\%} = \begin{cases} 1.12H_s Ir_m & Ir_m \leq 1.5 \\ 1.34H_s Ir_m^{0.55} & Ir_m > 1.5 \end{cases} \quad \text{with } Ir_m = \tan \alpha / \sqrt{2\pi H_s / (gT_{01}^2)}$$

where R_c =crest freeboard, A_c =armor crest berm freeboard, γ_f =roughness factor ($\gamma_f=0.50$ for 2-layer cubes, $\gamma_f=0.46$ for single-layer Cubipods and $\gamma_f=0.44$ for double-layer Cubipods), B_a =armor crest berm width, H_s =significant wave height at the toe, α =slope angle, w_c =crown wall base elevation, B_e =crown wall base width, h_f =crown wall height, F_h =maximum horizontal force, $F_v(F_h)$ =vertical up-lift force associated with F_h , ρ_w =water mass density (kg/m^3), g =gravity acceleration and L_m is the local mean wavelength (using T_{01}) given by Equation 3.4.

$$L_m = \frac{gT_{01}^2}{2\pi} \tanh\left(\frac{2\pi h_s}{L_m}\right) \quad 3.4$$

The range of the variables used in Equations 3.2 and 3.3 are valid for:

$$0.31 < \gamma_f(R_u/R_c) < 0.94, 0.07 < (R_c - A_c)/h_f < 0.59, 0.01 < w_c/h_f < 0.27 \text{ and } 3.13 < \sqrt{\frac{L_m}{B_a}} < 6.54$$

The goodness-of-fit index $rMSE = MSE/Var$, which estimates the proportion of variance not explained by Equations 3.2 and 3.3, was $rMSE = 20.4\%$ for F_h and $rMSE = 7.3\%$ for $F_v(F_h)$. With these formulas, the safety margin $S_1 = (W - F_v(F_h))\mu - F_h$ can be estimated to calculate the safety factors for crown-wall sliding and overturning of conventional mound breakwaters protected with double-layer cube and Cubipod[®] armors and single-layer Cubipod[®] armors. Overturning moment due to F_h and $F_v(F_h)$ can be obtained using Equations 3.5 and 3.6, proposed by Molines (2016). Equation 3.6 is based on the triangular up-lift pressure distribution.

$$M(F_h) = 0.55h_f F_h \quad 3.5$$

$$M(F_v(F_h)) = \frac{2}{3}(B_e)F_v(F_h) \quad 3.6$$

Example 3.3

Given: Water depth at the toe of the structure is $h_s[m] = 40.0$, tidal range is $\Delta h[m] = 5.0 = HWL - LWL$, design storm is $H_{m0}[m] = 10$ ($T_p[s] = 18$) and $\cot\alpha = 1.5$. Mass densities of concrete and sea water are $\rho_r[t/m^3] = 2.30$ and $\rho_w[t/m^3] = 1.025$, respectively, crest berm width is $B_a[m] = 7$ and foundation elevation is $w_c + \Delta h = 8$ m. The crown wall is rectangular in shape with crest elevation of armor and crown wall being $A_c + \Delta h = R_c + \Delta h = 20$ m.

Find: (1) Crown wall base width (B_e) for double-layer cube and Cubipod[®] armors to prevent crown-wall sliding and overturning for the design storm at HWL. (2) Safety factors for sliding and overturning.

Solution: The crown wall geometry is rectangular with a cross section area $h_f \times B_e$ and weight given by $W_e[kN/m] = 2.30 \times 9.81 \times h_f \times B_e$.

The height of the crown wall is $h_f[m] = (R_c + \Delta h) - (w_c + \Delta h) = 20 - 8 = 12.0$

The crown-wall sliding safety factor is $(\mu[W_e - F_v(F_h)])/F_h$

where μ is the friction factor between crown wall and bedding layer (e.g., $\mu = 0.6$)

The crown wall overturning safety factor is $[W_e \times 0.5 \times B_e]/[M(F_h) + M(F_v(F_h))]$

The safety factors are minimum at HWL ($\Delta h[m] = 5.0 = HWL - LWL$)

$$A_c[m]=R_c[m]=20-5=15 \text{ and } w_c[m]=8-5=3$$

$$L_m[m]=273 \text{ (considering } T_p=1.20T_{01}, \text{ local wavelength is } L_m = \frac{g15^2}{2\pi} \tanh\left(\frac{2\pi 45}{L_m}\right))$$

$$I_{r_m} = (1/1.5) / (2\pi 10 / [9.81 \times 15^2])^{1/2} = 4.0 > 1.5$$

$$R_u[m] = \min(2.58H_s; 1.34H_s I_{r_m}^{0.55}) = 25.8$$

$$R_u/R_c = 25.8/15 = 1.72, (R_c - A_c)/h_f = 0, (L_m/B_a)^{0.5} = (273/7)^{0.5} = 6.2, w_c/h_f = 3/12 = 0.25$$

$$\gamma_f = 0.50 \text{ (double-layer cube armor)}$$

$$\gamma_f = 0.44 \text{ (double-layer Cubipod[®] armor).}$$

(1) Crown wall base width (B_e)

* If B_e[m]=7.5 (first trial)

$$Fh_{cubes} [kN / m] = 1.025 \times 9.81 \times 12^2 \times 0.5 \times \\ \times (-1.29 + 1.80 \times 0.5 \times 1.72 + 0.93 \times 0 + 0.16 \times 6.2)^2 = 1131$$

$$Fv(Fh_{cubes}) [kN / m] = 1.025 \times 9.81 \times 7.5 \times 12 \times 0.5 \times \\ \times (-0.86 + 0.75 \times 0.5 \times 1.72 + 0.41 \times 0 + 0.17 \times 6.2 - 0.9 \times 0.25)^2 = 171$$

$$M(Fh_{cubes}) [mkN / m] = 0.55 \times 12 \times 1131 = 7465$$

$$M(Fv(Fh_{cubes})) [kN / m] = 2/3 \times 7.5 \times 171 = 855$$

$$W_e [kN/m] = 2.30 \times 9.81 \times 12 \times 7.5 = 2031$$

(2) The safety factors are:

Neglecting armor earth pressure forces on the crown wall

$$\text{Sliding Safety Factor}_{cubes} = (2031 - 171) \times 0.6 / 1131 = 0.98 < 1.0 \text{ (failure)}$$

$$\text{Overturning Safety Factor}_{cubes} = (2031 \times 0.5 \times 7.5) / (7465 + 855) = 0.91 < 1.0 \text{ (failure)}$$

* Increasing the width of crown-wall base by one meter, B_e[m]=8.5 (second trial)

$$Fh_{cubes} [kN / m] = 1.025 \times 9.81 \times 12^2 \times 0.5 \times \\ \times (-1.29 + 1.80 \times 0.5 \times 1.72 + 0.93 \times 0 + 0.16 \times 6.2)^2 = 1131$$

$$Fv(Fh_{cubes}) [kN / m] = 1.025 \times 9.81 \times 8.5 \times 12 \times 0.5 \times \\ \times (-0.86 + 0.75 \times 0.5 \times 1.72 + 0.41 \times 0 + 0.17 \times 6.2 - 0.9 \times 0.25)^2 = 194$$

$$M(Fh_{cubes}) [mkN / m] = 0.55 \times 12 \times 1131 = 7465$$

$$M(Fv(Fh_{cubes})) [kN / m] = 2 / 3 \times 8.5 \times 194 = 1099$$

$$W_e [kN/m] = 2.30 \times 9.81 \times 12 \times 8.5 = 2301$$

The safety factors are:

$$\text{Sliding Safety Factor}_{cubes} = (2301 - 194) \times 0.6 / 1131 = 1.1 > 1.0$$

$$\text{Overturning Safety Factor}_{cubes} = (2301 \times 0.5 \times 8.5) / (7465 + 1099) = 1.1 > 1.0$$

For design purposes, ROM 0.5-05 (2008) recommended safety factors SF=1.2 for sliding and overturning.

* Using a double-layer Cubipod[®] armor, the crown-wall base width can be reduced to $B_e [m] = 7$.

$$Fh_{Cubipod} [kN / m] = 1.025 \times 9.81 \times 12^2 \times 0.5 \times \\ \times (-1.29 + 1.80 \times 0.44 \times 1.72 + 0.93 \times 0 + 0.16 \times 6.2)^2 = 820$$

$$Fv(Fh_{Cubipod}) [kN / m] = 1.025 \times 9.81 \times 7 \times 12 \times 0.5 \times \\ \times (-0.86 + 0.75 \times 0.44 \times 1.72 + 0.41 \times 0 + 0.17 \times 6.2 - 0.9 \times 0.25)^2 = 122$$

$$M(Fh_{Cubipod}) [mkN / m] = 0.55 \times 12 \times 820 = 5412$$

$$M(Fv(Fh_{Cubipod})) [kN / m] = 2 / 3 \times 7 \times 122 = 569$$

$$W_e [kN/m] = 2.30 \times 9.81 \times 12 \times 7 = 1895$$

The safety factors are:

$$\text{Sliding Safety Factor}_{Cubipods} = (1895 - 122) \times 0.6 / 820 = 1.3 > 1.0$$

$$\text{Overturning Safety Factor}_{Cubipods} = (1895 \times 0.5 \times 7) / (5412 + 569) = 1.1 > 1.0$$

The double-layer Cubipod[®] armor allows for a relevant reduction in the crown-wall size when compared to conventional cube armors. In this case, the rectangular-shape crown-wall volume is reduced by 18%.

The crown wall is usually L-shaped which increases the overturning safety margin while maintaining the sliding safety factor. Crown-wall sliding is usually the critical failure mode for the crown-wall design.

The double-layer Cubipod[®] armor not only allows for a relevant reduction in the crown-wall size but also in the overtopping rate. In this case, considering Equation 3.1 and Example 3.1, the overtopping rates are:

$$R_c [m] = 20 - 5 = 15, \quad I_{rp} = (2/3) / (2\pi \times 10 / [9.8 \times 18^2])^{1/2} = 4.7, \quad R_c / H_{m0} = 15 / 10 = 1.5, \quad A_c / R_c = 1, \\ \gamma_f = 0.50 \text{ (2-layer cube armor) and } \gamma_f = 0.44 \text{ (2-layer Cubipod}^{\text{®}} \text{ armor).}$$

$$Q_{cubes} = \frac{q}{\sqrt{gH_{m0}^3}} = 0.2 \times \exp\left(0.53 \times 4.7 - 3.27 \times \frac{15}{15} - \frac{2.16}{0.50} \times \frac{15}{10}\right) = 1.40 \times 10^{-4}$$

$$q_{cubes}[\text{m}^3/\text{s/m}] = (9.8 \times 10^3)^{0.5} Q_{cubes} = 99.0 \times 1.40 \times 10^{-4} = 13.9 \times 10^{-3} \rightarrow q = 13.9 \text{ l/s/m}$$

$$Q_{Cubipods} = \frac{q}{\sqrt{gH_{m0}^3}} = 0.2 \times \exp\left(0.53 \times 4.7 - 3.27 \times \frac{15}{15} - \frac{2.16}{0.44} \times \frac{15}{10}\right) = 5.8 \times 10^{-5}$$

$$q_{Cubipods}[\text{m}^3/\text{s/m}] = (9.8 \times 10^3)^{0.5} Q_{Cubipods} = 99.0 \times 5.8 \times 10^{-5} = 5.7 \times 10^{-3} \rightarrow q = 5.7 \text{ l/s/m} < 13.9 \text{ l/s/m}$$

3.5. Wave reflection. Single- and double-layer armors

Incident and reflected waves are normally measured in physical tests. The measurement of incident and reflected waves is reliable in 2D tests and very reliable if regular waves are used. Wave reflection is usually characterized by the coefficient of reflection, which is the ratio between reflected and incident wave height ($C_R = H_R/H_I$ or $C_R = H_{sr}/H_{si}$). Wave power is proportional to the squared wave height (H or H_s); therefore, the proportion of wave energy which is reflected by a given structure is proportional to C_R^2 . For instance, if the coefficient of reflection of a mound breakwater is $C_R = 20\%$, the breakwater reflects 4% of the energy of the incident waves (96% is dissipated or transmitted). The reflected waves will be added to the incident field increasing the wave energy; if significant incident wave height is $H_{si}[\text{m}] = 6$ and $C_R = 20\%$, the reflected significant wave height is $H_{sr}[\text{m}] = 1.2$ and the total significant wave height is $H_s[\text{m}] = (6^2 + 1.2^2)^{1/2} = 6.12$.

Wave reflection is usually quite relevant when designing vertical breakwaters (high C_R), but it is not so important for mound breakwaters (low C_R). Nevertheless, wave reflection is frequently an issue to be taken into consideration (wave agitation in basins and port areas). In the following, experimental results are given to assess the reflectivity of single- and double-layer Cubipod[®] armored breakwaters.

Figure 3.7 shows the coefficient of reflection ($C_R = H_R/H_I$) measured in the 2D tests by Smolka et al. (2009) for double-layer cube and Cubipod[®] armors and single-layer Cubipod[®] armors. Conventional mound breakwater models with crown wall were tested in non-breaking and non-overtopping conditions, using regular waves and slope $\cot\alpha = 1.5$. Relative water depth (kh) is a dimensionless parameter which explains the reflectivity of all the tested armors very well. The relative water depth (kh) is clearly a key explicative parameter, while armor unit (cube and Cubipod[®]) and number of layers (1-layer and 2-layer) only have a minor influence on wave reflectivity. Figure 3.7 refers only to slope $\cot\alpha = 1.5$; therefore, armor slope may also significantly influence breakwater reflectivity.

It is necessary to point out that reflection coefficients lower than 20% correspond to very low fluxes of reflected energy which may be sensitive to small errors in the separation of incident and reflected waves. Figure 3.8 shows the proportion of energy which is reflected from the breakwater (C_R^2) corresponding to Figure 3.7.

A simple empirical approximation for the coefficient of reflection of cube and Cubipod[®] armors for slope $\cot\alpha=H/V=1.5$ in non-breaking conditions, represented in Figures 3.7 and 3.8, is

$$C_R \approx \sqrt{\frac{1}{20(kh - 0.5)}} \pm 0.05 \quad ; \quad 0.50 < kh < 3.5 \quad 3.7$$

in which $kh=2\pi L/h$ is the dimensionless local water depth.

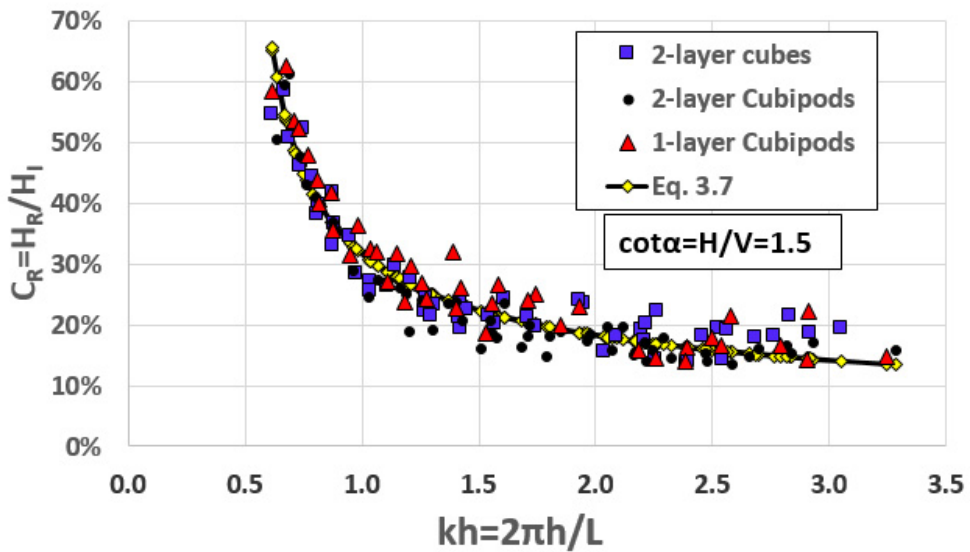


Figure 3.7 Measured coefficient of reflection $C_R(kh)=H_R/H_I$ (regular waves).

The coefficient of reflection ($C_R=H_R/H_I$ or $C_R=H_{st}/H_{si}$) can also be related to the surf similarity parameter or Iribarren's number, $Ir=\tan\alpha/(H_I/L_0)^{0.5}$. Figure 3.9 shows the same information as in Figure 3.7 but using Iribarren's number as an explicative variable (x-axis); the larger dispersion of results in Figure 3.9 (compared to Figure 3.7) indicates that dimensionless water depth (kh) explains the reflectivity observations better than the incident wave steepness (Iribarren's number with constant armor slope).

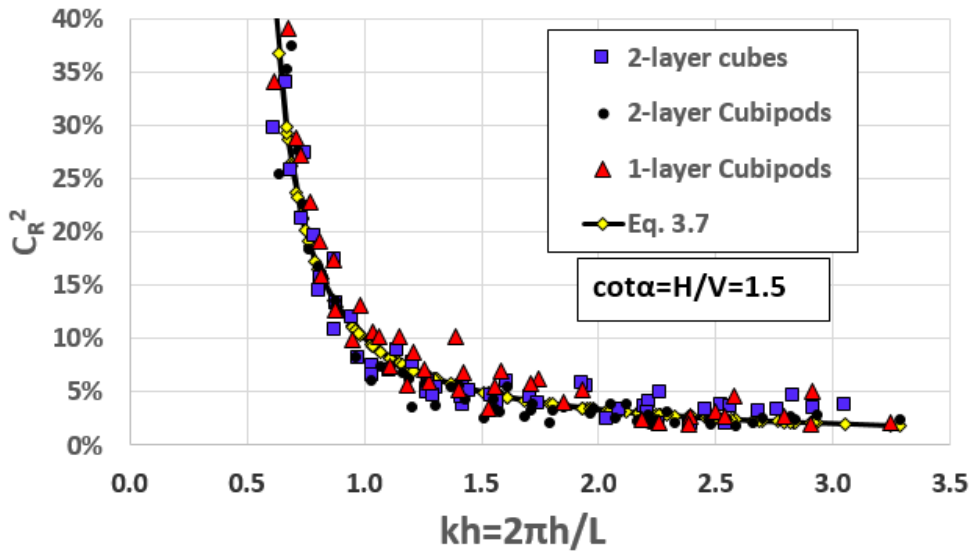


Figure 3.8 Proportion of measured reflected energy $C_R^2(kh)=(H_R/H_I)^2$ (regular waves).

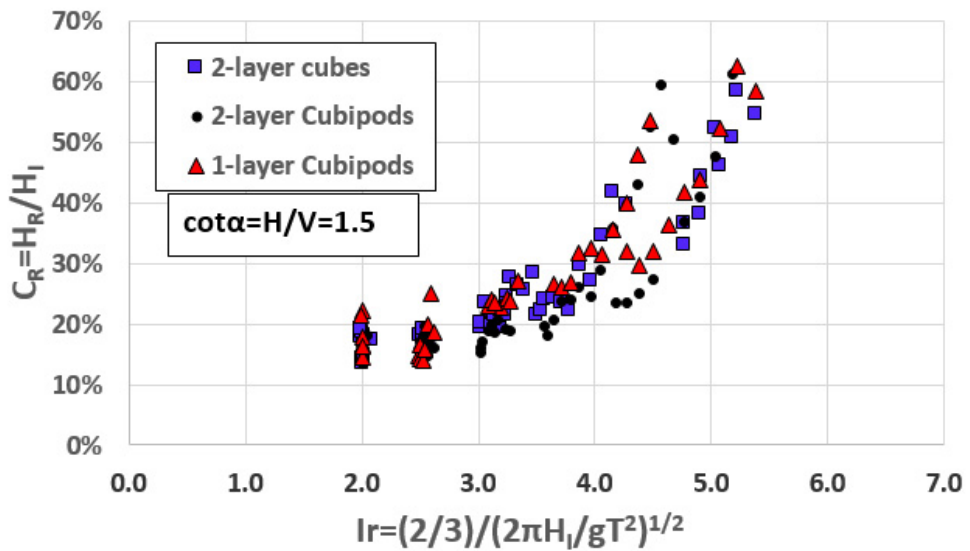


Figure 3.9 Measured coefficient of reflection $C_R(kh)=H_R/H_I$ (regular waves).

Example 3.4

Given: Armor slope is $\cot\alpha=1.5$, water depth at the toe of the structure is $h_s[m]=30.0$, tidal range is $\Delta h[m]=\text{HWL}-\text{LWL}=3.0$ and the design storm is $H_{m0}[m]=10$ and $T_p[s]=18$ ($T_{01}[s]=15$).

Find: (1) Coefficient of reflection for (A) double-layer cube armor, (B) single-layer Cubipod[®] armor and (C) double-layer Cubipod[®] armor. (2) Reflected energy (%).

Solution: $H_{sd}/h_s=10/30=0.33$ (LWL) and $H_{sd}/h_s=10/33=0.30$ (HWL); Figures 3.9 and 3.10 can be used because the breakwater is subject to non-breaking wave conditions ($H_{sd}/h_s<0.39$).

$$L = gT_{01}^2 \tanh(2\pi h/L)/2\pi \rightarrow L[m]=9.81 \times 15^2 \times \tanh(2\pi 30/L[m])/2\pi \rightarrow L[m]=234.2$$

$$kh=2\pi h/L=2\pi 30/234.2=0.805, C_R \approx (1/[20(0.802-0.5)])^{0.5}=40\%$$

(1) $C_R(\text{cubes_2L, Cubipod_2L and Cubipod_1L}) \approx 40\% \pm 5\%$

(2) Reflected energy $\approx 16\% \pm 4\%$

Chapter 4

Structural integrity of Cubipod[®] armor units

4.1. Introduction

The structural strength of units used in the armor layer is a key characteristic when designing large mound breakwaters. Some of the most spectacular failures (Port of Sines, Port of San Ciprián, etc.) were caused by armor units breaking without reaching the design storm. Given a specific geometric shape and handling and placement procedures, the larger units generate higher tensile strengths because static loads rise with D_n^3 while resistance increases only with D_n^2 ($D_n=[W/\gamma_r]^{1/3}$); structural tensile strength is approximately proportional to nominal diameter, D_n . Unreinforced concrete shows a low tensile resistance; therefore, small slender concrete armor units may be robust enough to be used, but not large slender units with higher tensile strengths, which may show a brittle behavior and cause many armor units to break. Numerous breakwaters were successfully protected with small Dolos armor units during the 1960s and 1970s; however, when Dolos units were manufactured above 30 tonnes (e.g. Port of Sines and Port of San Ciprián), many units broke and progressive failure was observed.

Slender concrete armor units (Dolos, tetrapods, etc.) are likely to generate flexions and torsions with high tensile stresses, which can lead to unit breakage and a progressive failure of the armor. Depending on the unit geometry, above a certain unit size, it may be mandatory to use high quality concrete or steel-reinforced concrete to guarantee the structural integrity of the armor unit (see Hanzawa et al., 2006). The unit slenderness will condition the type of concrete to be used for each unit size and also the maximum

unit size; the concrete required may be too expensive or the steel-reinforcement too costly.

The hydraulic stability of armor units is measured in laboratories using Froude's similarity. However, armor unit robustness is higher at small-scale than at prototype scale, because tensile stress caused by static and dynamic loads increases with the size of the unit. Therefore, the hydraulic stability and structural integrity are two key characteristics of armor units which must be examined separately; hydraulic stability may be studied at small-scale, but structural integrity must be studied at prototype scale.

The maximum tensile stress to be considered for the concrete of a given armor unit (manufacturing, handling, placement and service time) mostly depends on two variables: geometric shape and size. Given an armor unit size, the slender geometries generate higher tensile stresses than massive armor units. Cubipod[®] is a massive armor unit which generates relatively low tensile stress, allowing for easy manufacturing, handling and placement of large units like conventional cubes.

The massive armor units belonging to the cube family (cube, parallelepiped block, Antifer cube, Cubipod[®], etc.) may be manufactured as very large units (≥ 150 tonnes) with cheap unreinforced concrete, based on successful experience using very large cube and parallelepiped units in many of the world largest breakwaters. Massive concrete armor units may suffer small edge erosions, but it is not easy to generate internal tensile stress high enough to break the core of the unit, which would lead to a relevant change in unit morphology. Whatever the unit geometry, large concrete units require a strict control of the curing process and especially the heat and thermal stresses which may be generated during concrete hardening; air temperature and wind may significantly influence the curing process and the concrete thermal stresses.

Armor unit breakage is a critical issue which must be prevented from the very beginning of the design process; uncontrolled unit breakage affects safety and logistic efficiency of unit handling and placement. For interlocked armor units, unit breakage may generate serious long-term progressive damage due to the lack of interlocking in some areas. For massive armor units such as conventional cubes or Cubipod[®] units, it is relatively easy to manufacture robust armor units which guarantee the structural integrity in the short term during construction and long term during service time.

In order to ensure the structural integrity of armor units, prototype free-fall tests are the most reliable tests because scale effects are minimized. To assess the structural strength of the Cubipod[®], a series of prototype fall tests were designed to quantitatively measure the resistance of Cubipods and conventional cubes of similar sizes (16- and 15-tonne prototypes), manufactured with the same concrete. The methodology of the prototype fall tests for cubes and Cubipods (see Medina et al., 2011) were similar to that used for other slender units (see Muttray et al., 2005), but the design involved more robust and thicker steel-reinforced concrete bases and much higher drops given the greater robustness of massive armor units.

Figure 4.1 shows the steel-reinforced concrete base used for the Cubipod[®] and cube overturning tests; the platform (10.0x7.5x0.9 m) was placed on a heavily compacted soil in the cube block yard of SATO in the Port of Alicante (Spain). 15-tonne cube prototypes and 16-tonne Cubipod[®] prototypes were overturned in different ways to estimate the loss of mass after 8, 16 and 24 overturns (cubes) and 20, 40 and 80 overturns (Cubipods). Multiple overturns correspond to falls of a few decimeters, which did not cause any relevant damage to cubes (loss of mass < 2%) or Cubipods (loss of mass < 0.2%). Both conventional cubes and Cubipods maintained the geometrical shape with only small edge erosions, which did not affect the morphology or structural integrity of the units.



Figure 4.1 Steel-reinforced concrete overturning platform (10.0x7.5x0.9 m).

During overturning tests, cubes and Cubipods were highly resistant to small repetitive knocks; therefore, it is reasonable to assume that massive armor units will not show fatigue problems during service time; no fatigue-related damage (unit breakage during service time) has been observed in the numerous cube armored breakwaters in service during many decades. The prototype free-fall tests, described later, confirm the high resistance of cubes and Cubipods, which can withstand hundreds of drops of a few decimeters on rigid platforms; only drops from heights on the order of one meter are significant enough to break the massive armor units.

4.2. Prototype fall tests: Free-fall and extreme free-fall tests

The prototype overturning tests provide data to objectively assess the structural integrity of a specific armor unit type during service time (decades). A number of intense storms during service time may generate hundreds of small low-intensity knocks in some units (depending on placement); fatigue-induced armor unit breakage may occur if the units are subject to relevant damage during overturning tests. Nevertheless, the highest risk associated with structural integrity is that corresponding to accidental knocks during handling and placement, and unit-to-unit forces during service time. These loads may generate tensile stress which may exceed the maximum tensile strength of concrete, causing a brittle unit breakage. Once the unit is broken, both shape and weight are altered, suddenly reducing hydraulic stability; if the armor is interlocked, interlocking is lost locally and small broken parts may be transformed into projectiles moved by waves which may cause impact breaking and progressive failure. Massive armor units are not sensitive to these kinds of structural integrity-related problems.

As a rule of thumb (see Burcharth et al., 1991), gravity-related internal stresses not derived from impacts increase directly proportional to the unit size (D_n), while stresses derived from impacts rise proportionally to the square root of the unit size ($D_n^{1/2}$). In the case of prototype free-fall tests with cubes and Cubipods described by Medina et al. (2011), 15-tonne (6.5 m^3) cube prototypes and 16-tonne (7.1 m^3) Cubipod[®] prototypes were used, both bigger than any other slender unit prototype tested before (see Muttray et al., 2005). The concrete platform used for the free-fall tests was also much more resistant than any other platform used before. Prototype units were dropped on a steel-reinforced concrete platform ($5.0 \times 5.0 \times 1.15 \text{ m}$), protected with a 20 mm-thick steel plate, placed on a heavily compacted soil of the cube block yard of SATO in the Port of Alicante (Spain).

Three types of drops (AD=anvil drop, ED=edge drop and RD=random drop) were tested, from different elevations (cubes: 0.5, 1.0, 1.5 and 2.0 meters, and only 2.0 meters for Cubipods). The accumulated relative loss of mass (RLM) was measured after each drop to assess the robustness of each prototype; because Cubipod[®] units (7.1 m^3) were slightly larger than cubes (6.5 m^3) and RLM was significantly lower, it was clear that Cubipod[®] units were much more resistant to impacts than conventional cubes. Figure 4.2 shows the moment just before the fifth drop onto the rigid platform of the Cubipod[®] prototype P05, anvil drop (AD), from a two meter elevation ($h_c[\text{m}]=2.0$); the RLM in the previous four drops reached RLM=0.7%, with slight edge damage.



Figure 4.2 Cubipods dropped on the rigid free-fall platform (5.0x5.0x1.15 m).

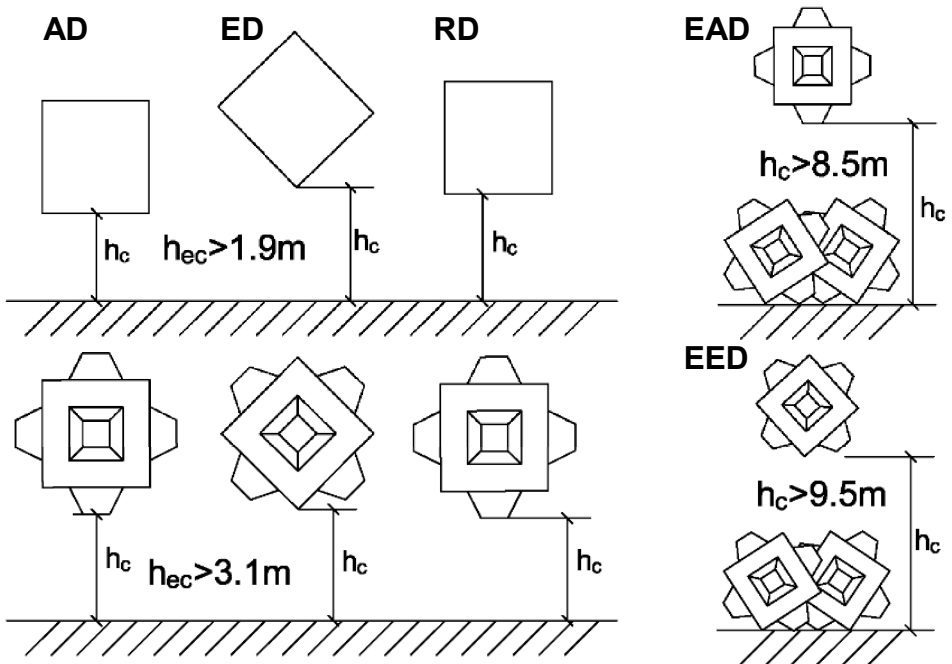


Figure 4.3 Free-fall tests (AD, ED and RD) and extreme free-fall tests (EAD and EED).

Figure 4.3 shows the results of different prototype drop tests (cubes and Cubipods) and extreme free-fall tests (only Cubipods) as pictured in Figure 4.4. The free-fall height (h_c) is defined by the elevation of the lowest point of the unit to be dropped onto the rigid platform. After analyzing the RLM and unit breakage depending on drop height and number of drops, Medina et al. (2011) proposed using the equivalent drop height (h_e) to take simultaneously into account both drop height (h_c) and number of drop repetitions (n_r) for each tested unit. If an armor unit prototype is dropped three times ($n_r=3$) from an elevation of $h_c[m]=1.5$, those drops are equivalent to a single free-fall from $h_e[m]=2.0$ meters because $h_e[m]=h_c[m]n_r^{1/4}=1.5\cdot 3^{1/4}=2.0$. The RLM corresponding to a single drop from $h_c[m]=2.0$ is similar to the accumulated RLM corresponding to three drops from $h_c[m]=1.5$.



Figure 4.4 Sixteen-tonne Cubipod[®] unit being dropped onto four Cubipods in an extreme free-fall test, $h_c[m]=9.5$ (EED).

Figure 4.5 describes the prototype drop test results; cubes and Cubipods did not show significant loss of mass if $h_c[m]<0.5$ (cubes) and $h_c[m]<2.0$ (Cubipods). Above those minimum equivalent drop heights, the loss of mass is small but significant ($RLM<4\%$); if the critical equivalent drop height ($h_{ec}[m]=1.9$ for cubes and $h_{ec}[m]=3.1$ for Cubipods) is exceeded, the core of the unit is broken. Finally, two Cubipod[®] units were dropped from an extreme height emulating a failure of the pressure clamps during the placement process (extreme free-fall tests). Each Cubipod[®] prototype was dropped onto four other Cubipod[®] units placed on the overturning platform (see Figures 4.1 and 4.4), from the maximum height of the available gantry crane, $h_c[m]=8.5$

(EAD=extreme anvil drop) and $h_c[m]=9.5$ (EED=extreme edge drop). Only minor damage (RLM<2%) was observed during the two extreme free-fall tests; Cubipods were able to resist higher drop impacts than cubes.

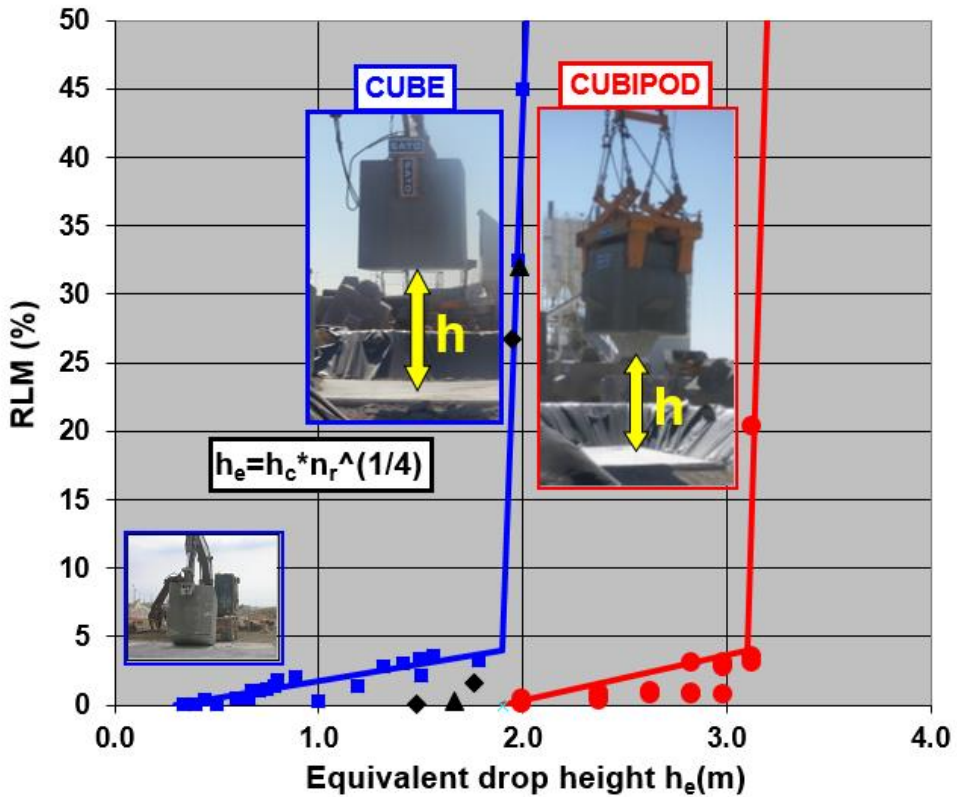


Figure 4.5 Relative loss of mass (RLM) for armor units dropped onto a rigid platform.

4.3. Concrete to manufacture Cubipods. Tensile strength

The results described in the previous section indicate that conventional cube and Cubipod[®] units have similar structural strength. The manufacturing process (vertical formworks and demolding time), handling (pressure clamps) and stacking (multiple levels) are very similar for Cubipods and conventional cubes. Therefore, one should expect Cubipods to have a resistance to unit breakage similar to conventional cubes which have been successfully manufactured, handled and placed during decades in large breakwaters.

Due to the fact that unreinforced concrete has a much higher resistance to compression stress than tensile stress, the breakage of concrete armor units is associated with the

tensile stresses within the concrete which surpass a given tensile strength. Furthermore, the unit breakage is always brittle because local tensile stresses suddenly increase when core fracture starts. The tensile strength to be considered for a given concrete armor unit depends on its geometry and size (given manufacturing, stacking, handling and placement processes). Given a unit size, a slender unit geometry generates larger tensile stresses. Given a unit geometry, the larger units generate higher tensile stresses because static loads increase with the volume (D_n^3) and resistance only increases with the section (D_n^2).

Larger concrete armor units must be manufactured using concrete with a tensile strength higher than that of smaller units. The required tensile strength will condition the required compressive strength as they are related characteristics of concrete. Because concrete tensile strength is considered a random variable, it is reasonable to characterize it with a 5% percentile, named characteristic tensile strength ($f_{ct,k}$), which is usually associated with the characteristic compressive strength (f_{ck}) using the relationship proposed by EHE-08 (Eurocodes): $f_{ct,k}[\text{MPa}] = 0.21 f_{ck}[\text{MPa}]^{2/3}$, valid for concrete with $20 \leq f_{ck}[\text{MPa}] \leq 50$. Taking into consideration that 150-tonne ($D_n[\text{m}] = 4.00$) cubic blocks were manufactured for Punta Langosteira main breakwater (see Burcharth et al., 2015) using unreinforced concrete with $f_{ck}[\text{MPa}] = 31$ ($f_{ct,k}[\text{MPa}] = 2.1$), the required minimum characteristic tensile strength for massive armor units can be estimated as proportional to the unit size, $f_{ct,k}[\text{MPa}] = 2.1 D_n[\text{m}] / 4.00$. Characteristic compressive strength for conventional cubes and Cubipods can be estimated by $f_{ck}[\text{MPa}] = 10.4 f_{ct,k}[\text{MPa}]^{1.5} = 3.9 D_n[\text{m}]^{1.5}$.

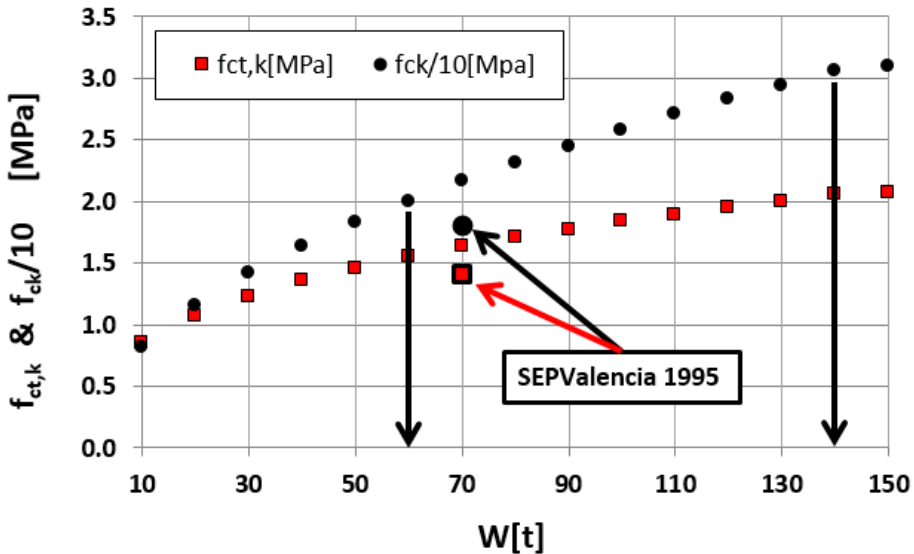


Figure 4.6 Minimum characteristic tensile and compressive strengths for massive armor units.

Figure 4.6 shows the minimum characteristic tensile strength and corresponding compressive strength to maintain the safety margin to unit breakage for the 150-tonne cubic blocks ($D_n[m]=4.00$ and $f_{ck}[MPa]=31$ corresponding to $f_{ct,k}[MPa]=0.21f_{ck}^{2/3}=2.1$) placed in the main breakwater of the Punta Langosteira harbor (Spain). With this simple linear model relating unit size and tensile stress, cubes and Cubipods smaller than 140-tonnes ($D_n[m]=3.8$ m) can be manufactured using unreinforced concrete with $f_{ck}[MPa]=30$; concrete with $f_{ck}[MPa]=20$ can be used to manufacture cubes and Cubipods smaller than 60-tonnes ($D_n[m]=2.94$ m).

Current Spanish regulation applicable to all concrete structures (EHA-08) imposes a minimum amount of cement which usually entails the use of higher than required f_{ck} for massive armor units. In order to analyze the required concrete quality for armor units, earlier cases of conventional cube armors can be studied (without any minimum quantity of cement to manufacture armor units). During the construction of the armor layer of the Southern enlargement of the Port of Valencia (Spain, 1991-1995), 70-tonne ($D_n[m]=3.1$) cubic blocks were manufactured with characteristic compressive strength $f_{ck}[MPa]=18$ ($f_{ct,k}[MPa]=0.21f_{ck}^{2/3}=1.4$). Thousands of conventional cube units were satisfactorily manufactured, stacked, handled and placed during construction, and they have not shown any problem over the last two decades. Thus, this example in the Mediterranean coast places the criterion given above on the safe side ($f_{ct,k}[MPa]=1.4 < 1.6$ MPa). This case confirms the suitability of using concrete with $f_{ck}[MPa]=20$ to manufacture cubes and Cubipods smaller than 25 m^3 (60-tonne). For massive armor units larger than $W[t]=60$ (25 m^3), the rule of thumb is:

$$f_{ck}[MPa] > 3.9 D_n[m]^{1.5} \approx 2.6 W[t]^{0.5}$$

Table 4.1 shows the minimum characteristic tensile and compressive strengths to manufacture cube and Cubipod[®] units with the same safety margin as the 150-tonne cubes of the main breakwater of the Punta Langosteira harbor (Spanish Atlantic coast) completed in 2011, and a higher safety margin than the 70-tonne cubes used for the main breakwater of the Southern enlargement of the Port of Valencia (Spanish Mediterranean coast) completed in 1995. For large cube and Cubipod[®] units ($>25 \text{ m}^3$), it is not recommended to arbitrarily increase the characteristic compressive strength of concrete (by increasing the cement quantity) not only for economic reasons, but also considering the thermal stresses which can be generated during the curing process.

Table 4.1 Minimum characteristic compressive and tensile strengths at 28 days to manufacture cube and Cubipod[®] concrete armor units.

$\rho_r[t/m^3]=2.35$		$f_{ck}(D_n[m]=4.00)=31\text{ MPa}$	
W[t]	$D_n[m]$	$f_{ck}[MPa]$	$f_{ctk}[MPa]$
200	4.40	36	2.3
180	4.25	34	2.2
160	4.08	32	2.1
150	4.00	31	2.1
130	3.81	29	2.0
110	3.60	27	1.9
90	3.37	24	1.8
80	3.24	23	1.7
70	3.10	21	1.6
60	2.94	20	1.5
50	2.77	18	1.4
40	2.57	16	1.3

Source: Authors' elaboration

Example 4.1

Given: Cubipod[®] armor units weighing $W[t]= 20, 40, 80$ and 160 must be manufactured for a large breakwater.

Find: Characteristic compressive strengths of concrete to be used for each unit size.

Solution: Values in Table 4.1 can be used to estimate the characteristics of the concrete to be supplied.

$f_{ck}[MPa]>20$ for 20- and 40-tonne Cubipods.

$f_{ck}[MPa]>23$ for 80-tonne Cubipods

$f_{ck}[MPa]>32$ for 160-tonne Cubipods.

Chapter 5

Manufacture, handling and stacking of Cubipods

5.1. Introduction

The processes related to manufacturing, handling and stacking concrete armor units in the block yard have a direct affection to the final economic cost and logistics of the mound breakwater. If these processes are efficient and safe, personnel injuries, logistic bottlenecks and wasted resources can be avoided.

In order to reduce costs and logistic restrictions, SATO's engineers designed a variety of articulated molds, depending on unit size, for vertical lifting of Cubipods. With these molds, the handling and production rates are similar to those of conventional cubes (2 to 3.5 units/day in 12- and 24-hour working cycles). Figure 5.1 shows vertical molds and bases to manufacture 45-tonne (19 m^3) Cubipod[®] units for the Western Breakwater at Punta Langosteira (A Coruña, Spain).

The usual manufacturing procedure is described as follows. First, the vertical mold is placed on a base and the upper articulated elements are opened; then, more than 95% of the concrete is poured into the mold (from a truck on an elevated track) and the concrete is vibrated. Second, the upper vertical elements are closed and the rest of the concrete is poured and manually vibrated. After 6 hours, the vertical mold is lifted and moved to another base to repeat the cycle. After 24 hours, Cubipod[®] units are ready to be moved (using pressure clamps) to the stacking zone; once the unit is in the stacking zone, the base is free for another use. With this procedure, 3.5 45-tonne Cubipod[®] units/vertical mold/day were manufactured in 24-hour working cycles, for the Western

breakwater of the Outer Port of A Coruña at Punta Langosteira (Spain); to obtain this production rate, 3.5 bases are required for each vertical mold.



Figure 5.1 Vertical molds and bases to manufacture 45-tonne (19 m³) Cubipod® units (Port of Punta Langosteira, Spain).

Armor units can always be handled using slings; however, it is highly recommended to use pressure clamps because they allow personnel to be at safe distances from risky tasks associated with slinging or releasing the concrete armor units. Pressure clamps significantly increase the rates and levels of safety in handling and placement. Figure 5.2 shows double pressure clamps, being used to handle Cubipods in the block yard.



Figure 5.2 Double pressure clamps handling Cubipod® units in the block yard.

The double pressure clamps adapted to handle Cubipod® units have a design and functioning similar to the clamps usually employed to handle conventional cubes; this dou-

ble pressure clamp can be considered two single pressure clamps in a common framework. This framework has the size of the frustro-pyramidal protrusion of the Cubipod[®] to attach to the core of this unit with the same vertical axis. The Spanish engineering community considers mandatory the use of pressure clamps to efficiently and safely handle large concrete armor units.

Less than 24 hours after pouring the concrete, Cubipods are strong enough to be safely handled with double pressure clamps and moved to the stacking zone. In the stacking zone, the Cubipods will be piled in multiple levels and left to reach the required compressive and tensile strengths (usually 28 days). The required surface to manufacture and stack the prefabricated units depends on the breakwater size, the wave climate (winter break), the working cycle (12 or 24 hours) and maximum construction time. Once the manufacturing (molds) and placement equipment (crawler crane) are defined, a block yard has to be designed to manufacture and stack the required units to ensure the unit placement is independent from the manufacturing of units; any logistic bottleneck would significantly increase costs.



Figure 5.3 Five-level stacked Cubipod[®] units in the block yard (Port of Málaga, Spain).



Figure 5.4 Cubipod[®] block yard with gantry cranes (Port of Punta Langosteira, Spain).

Figures 5.3 and 5.4 show Cubipod® block yards with wheeled and crawler cranes (Port of Málaga, Spain) and gantry cranes (Outer Port of A Coruña at Punta Langosteira, Spain).

When Cubipod units are smaller than 3 m³, they can be easily handled using forklifts or boom trucks. Figure 5.5 shows the Cubipod® block yard with a forklift (Marina Bay D'Alger, Algeria) and Figure 5.6 shows a block yard with Cubipods handled with a boom truck (Port of Las Palmas, Spain).



Figure 5.5 Block yard of 3-tonne Cubipod® units handled with a forklift (Marina Bay D'Alger, Algeria).



Figure 5.6 Block yard of 6-tonne Cubipod® units handled by a boom truck (Port of Las Palmas, Spain).

5.2. Molds and manufacturing of Cubipods in the block yard

The molding system designed by SATO to manufacture Cubipod[®] units has three components (1) a fixed base placed on the ground, (2) a vertical mold with two upper articulated elements and (3) four lateral elements which may be articulated to the base or to the vertical mold. This molding system allows for concrete to be poured and vibrated in two phases and vertical demolding after six hours. Figure 5.7 shows a line of molds to manufacture 25-tonne (10.6 m³) Cubipods.



Figure 5.7 Molds and production line of 25-tonne (10.6 m³) Cubipods (Port of Punta Langosteira, Spain).

Using the molds described previously (see Corredor et al., 2013), three 25-tonne (10.6 m³) Cubipod[®] units/mold/day were manufactured in autumn 2012 at Punta Langosteira (Spain) for the Southern breakwater working in 24 hour cycles; three bases per vertical mold were required. During the spring and summer of 2015, 3.5 Cubipod[®] units/mold/day were manufactured at Punta Langosteira (Spain) for the Western breakwater working in 24 hour cycles; 3.5 bases per vertical mold were used in the production line. Figure 5.8 shows a smaller mold (2.6 m³) with all articulated elements connected to the vertical mold, used to produce 6-tonne Cubipods for the Closing Breakwater at Las Palmas (Spain); the molding and demolding procedure and the manufacturing rates were similar to those for larger units.

Manufacturing concrete armor units with vertical lifting molds and not horizontal displacement molds (commonly used for slender units) is recommended, because the production line requires less space, and the manufacturing process is less sensitive to uncontrolled waste and ground irregularities. Slender armor units are not so robust as

massive armor units and require a higher tensile strength in all the phases (demolding, handling, moving to stacking area, etc.), usually requiring 24 hours before horizontal demolding instead of 6 hours for the vertical demolding of massive armor units. Cubes and Cubipods need only 24 hours to be handled with pressure clamps and moved safely to the stacking zone, avoiding the use of slings and the associated risk to sling operators.



Figure 5.8 Vertical molds and bases to manufacture 6-tonne (2.6 m³) Cubipod[®] units (Port of Las Palmas, Spain).

Vertical lifting molds and massive armor units allow for higher manufacturing rates (2 to 3.5 units/mold/day for cubes and Cubipods compared to 1 unit/mold/day for slender units) reducing economic costs and space requirements in the block yard. For a given production target (units/day), vertical demolding (cubes and Cubipods) requires fewer molds and less space than slender units with horizontal demolding. The reduction in the space required in the block yard and stacking in multiple levels allow for an increase in manufacturing and handling efficiency; sometimes this favors the use of gantry cranes in the block yard, reducing economic costs and saving time and energy (shorter and faster displacements in the block yard). Usually, the concrete is poured into the molds from concrete mixer trucks on an elevated track along the production line; molds are aligned in a row beside the elevated track (see Figures 5.7, 5.9 and 5.11). Figure 5.9 shows the block yard and production line of 6-tonne (2.6 m³) Cubipod[®] units for the Closing Breakwater at Port of Las Palmas (Spain).



Figure 5.9 Block yard and production line of 6-tonne (2.6 m^3) Cubipods (Port of Las Palmas, Spain).

The number of vertical molds and bases required to manufacture the prescribed daily production of Cubipods has to be optimized to reduce costs, but there should be enough to manufacture the prescribed daily production of concrete armor units. This optimum number of molds depends on the production rate of the mold (e.g., 3.5 units/mold/day) in the working cycle (e.g., 24 hours) and the required daily production of concrete armor units. Once the number of vertical molds and bases for each size of Cubipod[®] unit used in the breakwater is calculated, the space and location beside an elevated track (single- or double-row of molds) is designed for efficient concrete pouring. Finally, considering the total number of units to be manufactured and the available space and equipment, wheeled cranes (extensive block yard) or gantry cranes (intensive block yard) will be used to handle molds and to handle and stack Cubipods in multiple levels.

To manufacture Cubipods with the same efficiency as conventional cube units, the vertical mold must be designed with not exactly vertical planes for easy demolding, similar to the way conventional cube molds are designed. Figure 5.10 shows the main dimensions of Cubipod[®] units.

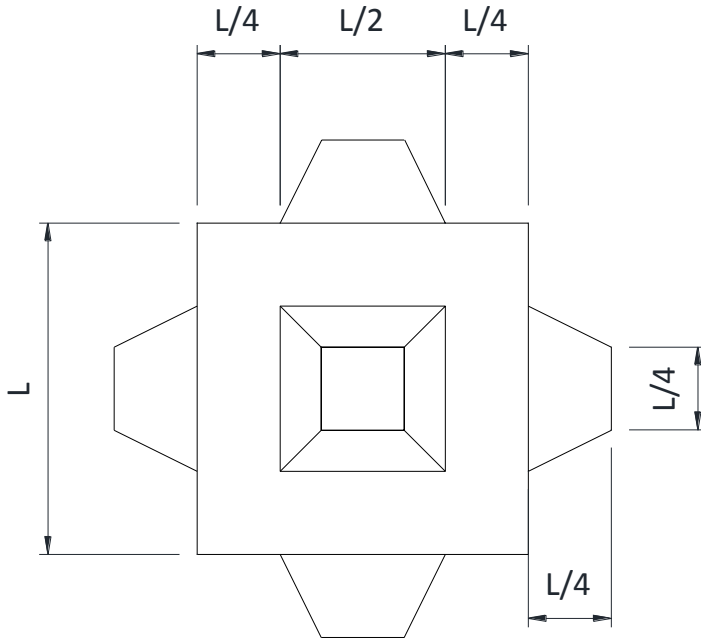


Figure 5.10 Main dimensions of Cubipod[®] units (front/side/top view).

5.3. Stacking Cubipods. Block yard design

After demolding, Cubipods must be stacked during weeks or months (usually 28 days) so the concrete can reach the required strength to be placed in the breakwater armor. Figure 5.11 shows the block yard used for the San Andrés breakwater (Port of Málaga, Spain). Space restrictions meant the block yard had to be located within a given rectangular block in the Málaga urban port area. The elevated track to pour the concrete was located along the perimeter; concrete mixer trucks moved along the perimeter to pour the concrete in the molds aligned beside the elevated track. Molds were placed in the interior row of the perimeter, at a greater distance from the city streets. Wheeled cranes moved the vertical molds between bases and handled and stacked Cubipods in five levels and, once required for placement, moved the Cubipods to the truck platforms to transport them to the placement site.



Figure 5.11 Extensive Cubipod[®] block yard with wheeled cranes at the Port of Málaga (Spain).

Depending on the unit size, space restrictions and available equipment, there are different procedures and layouts to efficiently stack the Cubipod[®] units. Cubipods can be stacked in multiple levels using ordered arrangements with different porosities; Figure 5.12 shows the lower and higher porosity arrangements, named by Corredor et al. (2008) as “open arrangement” (50% porosity) and “close arrangement” (30% porosity). To stack the Cubipods, a thick layer of permeable granular material is spread first on the ground of the block yard; later, regular holes or trenches are dug in the granular layer to place the first layer of Cubipods. Once the first layer of Cubipods are correctly placed (protrusions in the holes or trenches) on the ground, it is easy to stack multiple layers of Cubipods following the arrangement guided by the first layer of Cubipods.

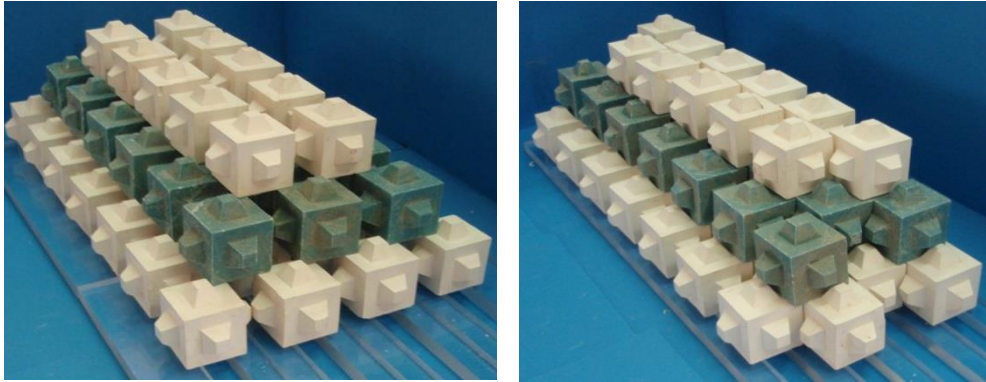


Figure 5.12 Stacking Cubipods in “open” and “closed” arrangements.

When the unit production is high, an intensive block yard served with gantry cranes is recommended so as to guarantee high efficiency and safety in handling operations. Figure 5.13 shows the plan view of a typical intensive block yard with a production row and lateral elevated track to pour the concrete (from concrete mixing truck) and a gantry crane covering all the production and stacking area.

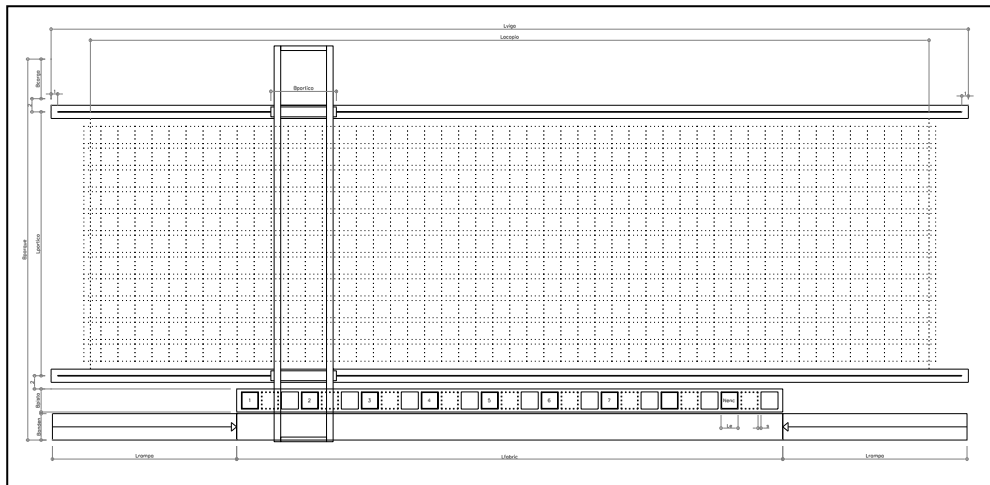


Figure 5.13 Schematic plan view of an intensive block yard with gantry crane.

Finally, the last handling operation in the block yard is to move the cured units onto platforms to be transported to the placement site. Figure 5.14 shows wheeled cranes loading Cubipods onto platforms in the extensive block yard of the Port of Málaga (Figure 5.11).



Figure 5.14 Loading Cubipods onto a platform to be transported to the placement site.

Chapter 6

Cubipod[®] placement in the armor

6.1. Introduction

The placement of units in the armor (random, ordered, patterned, interlocked, etc.) is a key factor conditioning long-term settlements and hydraulic performance of the armor when exposed to wave attack (see Medina et al., 2014). Massive concrete units (cubes and parallelepiped blocks) have been used for more than a century as large artificial stones placed randomly in two layers. Strictly controlled procedures are required when armor units are to be placed orderly (mosaic), interlocked or patterned, because hydraulic stability depends on the whole armor more than the individual units resisting by gravity. Massive armor units resisting by gravity and lateral friction are usually randomly placed, and armor units resisting by interlocking are placed carefully following a specific placement pattern to guarantee construction reliability (model-to-prototype relationship). Single-layer armors require a better placement control than double-layer armors, because a placement mistake in single-layer armors may lead to the filter layer becoming visible.

Hydraulic stability, run-up, overtopping and forces on crown wall are affected by the placement procedure. As a general rule, a lower armor porosity not only increases hydraulic stability, but also the cost, overtopping rates and forces on the crown wall. Therefore, in order to reduce model effect, it is essential to control the armor porosity and placement in prototype and small-scale models. This is easier when using Cubipods, because the random placement and the self-arranging tendency of Cubipod[®] units maintain initial armor porosity with few variations.

The Cubipod® is not an interlocking unit; it is a massive randomly-placed armor unit for single- or double-layer armors. Wave action, differential settlements and small changes in porosity over time tend to generate random changes in orientation and small relative movements among the units. Cubipod® geometry significantly reduces the heterogeneous packing observed in other massive concrete armor units (cube, Antifer cube, etc.), maintaining an almost constant porosity during lifetime. Figure 6.1 shows an aerial view of the 25-tonne single-layer Cubipod® armor which protected the round-head of the Southern Breakwater at Punta Langosteira (first phase of the 1.35 km-long secondary breakwater in December 2012).



Figure 6.1 Twenty-five-tonne single-layer Cubipod® armor protecting the Southern Breakwater at Punta Langosteira (A Coruña, Spain).

The placement of concrete armor units is a critical task when constructing large mound breakwaters. On the one hand, the unit size and equipment available for handling, transportation and placement impose strict safety requirements, easier to fulfill when using pressure clamps for handling. On the other hand, around half the armor units are placed underwater, with a poor visibility and waves and wind affecting units, cables and crawler cranes placing the units.

Before placing Cubipods in the armor, an adequate diamond-type placement grid must be first defined to use with the differential GPS installed in the crawler crane. Each unit must be placed in specific X-Y coordinates following a prescribed order of placement

(see Pardo et al., 2014). The initial armor porosity will depend on the placement grid and the climatic conditions during placement. The random orientation of units is easy to obtain as Cubipod[®] units tend to self-arrange on the slope, covering the slope with uniform placing density. Figure 6.2 shows a crawler crane, equipped with pressure clamps, placing 6-tonne Cubipods in the San Andrés Breakwater (Port of Málaga, Spain).



Figure 6.2 Placing Cubipods in San Andrés Breakwater (Port of Málaga, Spain).

Usually, Cubipod[®] units are transported on a platform lorry from the stacking area of the block yard to the breakwater placement site. The platform lorry remains in place so that it can be reached by the crawler crane which picks up the Cubipods with pressure clamps, lifting them from the lorry for placement on the breakwater. The crane moves the concrete units to place them in the specified X-Y coordinates following the prescribed placement grid and placement order; once the crane puts the unit in the right X-Y coordinates, the unit is slowly lowered until it touches the slope. When the unit is placed on the slope, the cables loosen (the tension) and the pressure clamps are opened and free to move and repeat the working cycle. In addition to the crane driver, one other worker is necessary to slightly adjust the open pressure clamp on the unit before lifting it. The placement cycle takes between 4 and 8 minutes, depending on the Cubipod[®] size, the logistics and climatic conditions.

6.2. Toe berm and scour protection

When using concrete armor units, the armor has to be placed on a toe berm. The toe berm is especially important to support single-layer armors and it is usually made of large quarry rocks. The construction of the toe berm significantly influences the proper placement of the first row of concrete armor units, which affects the upper rows of units, because armor units in a row are placed on units of the row below. Figure 6.3 shows the cross section of a mound breakwater with an armor supported by a toe berm placed on scour protection apron.

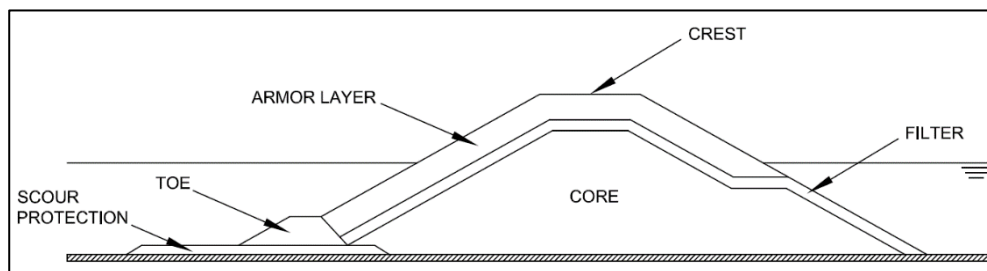


Figure 6.3 Mound breakwater cross section with toe berm and scour protection apron.

The scour protection is necessary when the breakwater is placed on a sandy sea floor, because the sea bottom surface is in dynamic equilibrium with wave and ocean currents (without breakwater); the construction of the breakwater significantly changes the current pattern around the structure modifying the movement of sand and producing scour around the toe of the structure. The new breakwater usually increases the longitudinal currents along the toe eroding the sandy bottom near the breakwater. The riprap apron itself does not significantly change the current pattern on the sea floor; when the mound breakwater is placed on the apron, the new strongest currents along the breakwater find an apron on the sea floor hard to erode. The scour is significantly reduced because the stones of the apron require much stronger currents than the sand to be eroded; the apron protects the toe berm from scour and the toe berm provides a reliable support for the armor.

As a general rule, the toe berm is a trapezoidal-shape structure as indicated in Figure 6.4 and the weight of the rocks in the toe berm is usually between 10% and 20% of the weight of the armor units, depending on the water depth and toe berm depth. The berm width (B) at the toe berm crest is normally about $B=3$ to $4 D_{n50}$. The toe berm thickness is $2 D_{n50}$ and $3 D_{n50}$ for single- and double-layer armors, respectively, in which D_{n50} is the nominal diameter of the rocks in the toe berm.

The toe berm is usually placed on a bedding layer (sandy sea bottom) or directly on the rocky sea bottoms. When the mound breakwater is to be placed in deep water areas, according to the criterion given by Grau (2008), the toe berm supporting the armor can be placed in an elevated position, much above the sea floor; the lower part of the

breakwater slope ($h > 1.5H_{sd}$) is protected with a much lighter armor, similar to the underlayer of the armor of the upper part on the breakwater slope ($h < 1.5H_{sd}$). The wave action on the armor units is significantly attenuated below depth $h = 1.5H_{sd}$. Figure 6.5 shows the cross section of a typical breakwater placed in deep water.

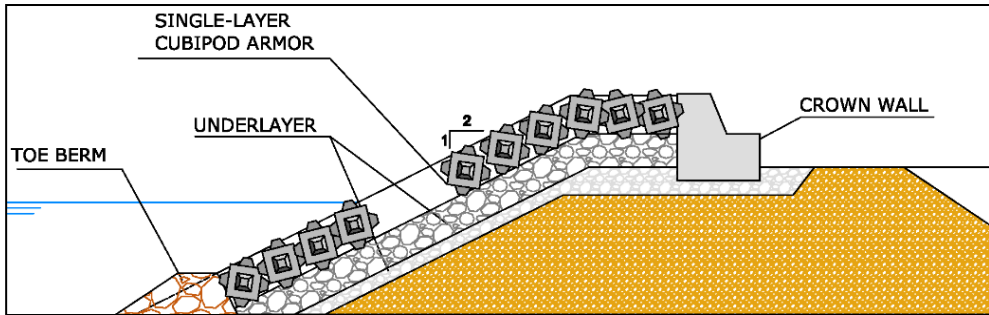


Figure 6.4 Single-layer Cubipod[®] armored breakwater with toe berm and crown wall.

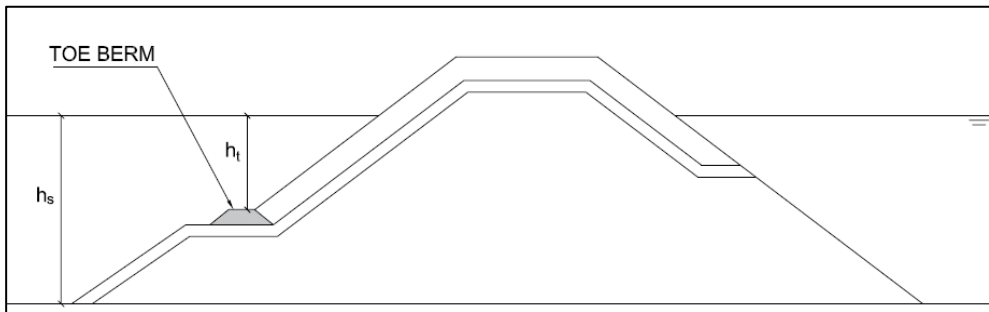


Figure 6.5 Sketch of breakwater in deep water.

The toe berm is a relatively small part of the breakwater and it requires a small volume of materials and cost; therefore, the toe berm is usually designed with a high safety margin. To estimate damage to a given toe berm, it is convenient to use the formula given by Van der Meer (1998), proposed by CIRIA et al. (2007). Figure 6.6 shows the cross section to apply Equation 6.1, tested in the range $0.4 < h_t/h_s < 0.9$.

$$\frac{H_s}{\Delta D_{n50}} = \left(2 + 6.2 \left(\frac{h_t}{h_s} \right)^{2.7} \right) N_{od}^{0.15} \quad 6.1$$

in which h_s = water depth at the breakwater toe, h_t = water depth at the toe berm crest and N_{od} is the toe berm damage (number of units lost in a D_{n50} width). The criterion given by CIRIA et al. (2007) is $N_{od} = 0.5$ (start of damage), 2.0 (moderate damage) and 4.0 (destruction).

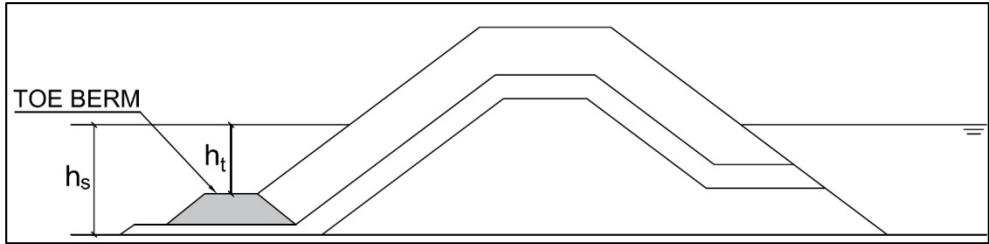


Figure 6.6 Sketch of breakwater cross section with toe berm.

For mound breakwaters in non-breaking conditions, toe berms may be designed for $N_{od}=0.5$ (start of damage) corresponding to a design storm. This criterion will give an additional safety factor of $(4/0.5)^{0.15}=1.37$ against toe berm destruction. If larger than available rocks are required, a wider toe berm can be considered ($B/D_{n50} \gg 3$), and the formula given by Van Gent et al. (2015) may be used to estimate the erosion of this wider berm. In this case, the wider toe berm can withstand much higher values of N_{od} than those recommended by CIRIA et al. (2007) because many toe berm rocks have to be lost before the armor is affected.

For mound breakwaters in breaking conditions, the toe berm must be placed on the sea bottom (on a scour protection apron in the case of a sandy sea floor). In the cases of shallow water depths and steep (rocky) sea bottoms, toe berms may have very low stability numbers, and toe berm rocks may be larger than armor units; in these conditions, the formula given by Herrera and Medina (2015) can be used to estimate the rock size of the toe berm.

Example 6.1

Given: Water depth at the toe of the structure is $h_s[m]=20.0$, tidal range is $\Delta h[m]=3.0$, armor slope is $\cot\alpha=1.5$ and design storm is $H_{m0}[m]=8$ (HWL and LWL). Mass densities of rock and sea water are $\rho_r[t/m^3]=2.700$ and 1.025 , respectively. Maximum available rock size at the quarry is $W_{50}[t]=6.0$.

Find: (A) Toe berm design for single- and double-layer Cubipod[®] armoring. (B) Estimated damage to the toe berm when design storm is exceeded.

Solution: Water depth (h_t) at the toe berm crest is normally about $h_t[m]=1.5H_{sd}=12$. Toe berm stability is the lowest at LWL because $h_t/h_s[LWL]=12/20=0.60 < h_t/h_s[HWL]=15/23=0.65$. Equation 6.1 can be used because $0.4 < h_t/h_s < 0.9$. Using 6-tonne rocks for the toe berm, the nominal diameter is

$$D_{n50}[m] = \left(\frac{6.0}{2.700} \right)^{1/3} = 1.30$$

$$\frac{H_s}{\Delta D_{n50}} = \left(2 + 6.2 \left(\frac{h_t}{h_s} \right)^{2.7} \right) N_{od}^{0.15} \Rightarrow \frac{8.0}{1.30 \times \left(\frac{2.700}{1.025} - 1 \right)} = \left(2 + 6.2 \left(\frac{12}{20} \right)^{2.7} \right) N_{od}^{0.15}$$

$$N_{od} = \left(\frac{3.76}{3.56} \right)^{1/0.15} = 1.4 \quad B[m] > 3.0 \times D_{n50} = 3.9$$

The design storm will cause moderate damage to the toe berm ($N_{od} \approx 2.0$). This design ($h_t = 12\text{m}$) would give a safety factor of $(4/1.4)^{0.15} = 1.17$ against toe berm failure. The safety factor of the toe berm should be higher since the construction cost of toe berm is low.

Increasing one meter the water depth at the toe berm crest, $h_t/h_s[\text{LWL}] = 13/20 = 0.65$

$$\frac{H_s}{\Delta D_{n50}} = 3.76 = \left(2 + 6.2 \left(\frac{13}{20} \right)^{2.7} \right) N_{od}^{0.15} = (2 + 1.94) N_{od}^{0.15}$$

$$N_{od} = \left(\frac{3.76}{3.94} \right)^{1/0.15} = 0.7$$

The design storm will cause start of damage to toe berm ($N_{od} \approx 0.5$). This design would give the toe berm a safety factor of $(2.0/0.7)^{0.15} = 1.17$ for moderate damage ($N_{od} \approx 2.0$) and a safety factor of $(4/0.7)^{0.15} = 1.30$ against toe berm failure ($N_{od} \approx 4.0$).

(A) conventional trapezoidal-shape 6-tonne rock toe berm; water depth and berm width at the toe berm crest are $h_t[\text{m}] = 13$ and $B[\text{m}] = 4D_{n50} = 5.2$, respectively; toe berm thickness is 2.6 meters and 3.9 meters for single- and double-layer armors, respectively. (B) Moderate damage ($N_{od} \approx 2.0$) when $H_s[\text{m}] = 9.4 > 8.0$ and failure ($N_{od} \approx 4.0$) when $H_s[\text{m}] = 10.4 \gg 8.0$.

6.3. Placing Cubipod[®] units in the trunk armor

Cubipods should be placed in the trunk armor following a given diamond-type placement grid. The placement grid determines the X-Y coordinates of each unit in the horizontal plane; first the lowest row is placed on the toe berm, and later the upper rows are placed on the lower rows. Each unit in a row is placed between two units of the row underneath (diamond scheme). Figure 6.7 shows a conventional placement grid and a progressive placement grid to take into account the small downward movement of units due to compaction. The “a” parameter is the distance between the center of gravity of adjacent units (same row) and the “b” parameter is the horizontal distance between consecutive rows. Both “a” and “b” are measured on a horizontal plane.

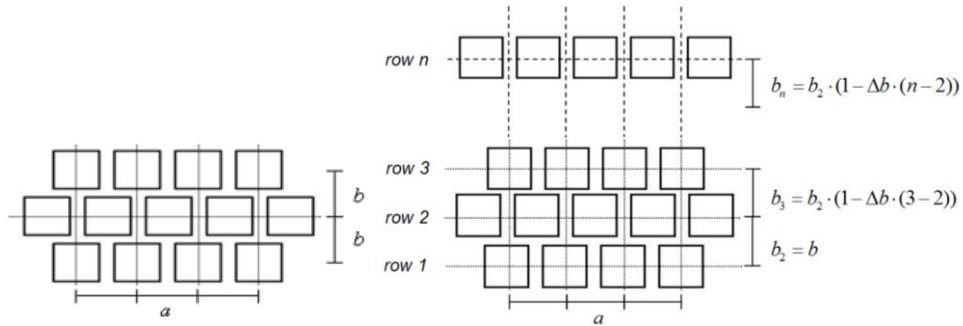


Figure 6.7 Fixed and progressive placement grids.

Based on results from realistic placement tests, Pardo et al. (2014) and Pardo (2015) described the optimum placement grids for cube and Cubipod[®] armor units in trunks and roundheads. Realistic placement tests used small-scale crawler cranes, waves and pressure clamps to place units only with the X-Y coordinate information. Figure 6.8 shows the blind placement of Cubipod[®] units during these realistic placement tests (with small-scale pressure clamps) following a prescribed grid with X-Y coordinates assigned to each unit (E: 1/50).



Figure 6.8 Realistic armor placement. Straight trunk.

With all types of armor units and placement, armor porosity is a key variable directly affecting concrete consumption (higher armor porosity means lower concrete consump-

tion), logistics (number of concrete armor units) and hydraulic performance (higher porosity leads to lower hydraulic stability). The control of armor porosity in small-scale tests and prototype is directly related to the uncertainty about the model effects on the hydraulic performance of the armor. The geometry of Cubipod[®] minimizes the possible change in armor porosity, but an adequate placement grid leads to an optimum placement with a minimum number of units lost during the placement process. If the product “a” by “b” in the fixed placement grid is reduced (see Figure 6.8), the porosity tends to be reduced (higher placing density); however, if the placing density is too high, some units are placed incorrectly, out of the prescribed layer. Thus, there is an optimum combination of “a” and “b” to obtain the minimum armor porosity (highest placing density) without losing units during placement.

For straight trunks protected with Cubipods, the recommended values of the placement grid ($a/D_n=1.58-1.61$ and $b/D_n=1.02-1.05$) depend on the armor slope. The armor porosity of Cubipod[®] armors obtained with these placement grids and moderate waves is $40\% < p < 43\%$ ($0.60 > \Phi > 0.57$ for single-layer armors). The first layer of Cubipods (single-layer on quarry-stone underlayer) has a lower porosity than the upper layer of Cubipods, because the smaller size of the stones of the underlayer favors self-arranging movements.

For curved trunks, the optimum placement grid design depends on the curvature. The bottom row of Cubipods must be placed on the toe berm while the units of the upper rows are placed on top of the lower rows; however, in curved trunks, the curvature increases (smaller radius) in the upper rows and the distance between adjacent units is reduced. If the curvature is high, the distance between adjacent units in the upper rows is significantly reduced and not all units can be placed between two units on the lower row; units may be lost and the conventional diamond-type placement grid must be re-designed. To correctly place units in roundheads or curved trunks, it is necessary to adapt the placement grid to the slope and curvature to minimize the number of irregular points in the grid. For low or moderate curvatures ($R/D_n > 110$), it is sufficient to slightly increase (say 2%) the horizontal distance “a” between units in the bottom row while maintaining the horizontal distance between rows “b”.

Recommendations:

1. It is necessary to carefully construct and profile the toe berm, because the first row of Cubipods is placed on the toe berm, and this row is the one which has the most influence on the overall armor placement.
2. Crawler cranes must be equipped with differential GPS and software to guide the crane operator in identifying the units placed and those to be placed following a placement order previously defined. Before starting the armor unit placement process, a controlled test in dry conditions (blind for the crane operator) will show the errors when placing units in prescribed X-Y coordinates.

3. A correct profiling of filter layer is convenient, because armor layer is placed on the underlayer. Tolerances of $\pm 0.5 D_{n50}$ in under-layer profile is acceptable for the design profile.
4. Progressive placement grids are considered to take into account self-packing during placement; however, the fixed placement grids shown above give good results and are easier to apply.
5. When breakwater curvature increases, it is more difficult to place units with a fixed placement grid. If the curvature is high (roundheads), a conventional diamond type placement grid is not a feasible solution. Roundheads usually require changing the methodology and using coupled grids (see Section 6.4).
6. Cubipod[®] units tend to arrange themselves on the slope with homogeneous armor porosity $40\% < p < 43\%$, but the unit placement in special areas (root, roundhead, changes in alignment, etc.) should be studied carefully.

6.4. Placing Cubipod[®] units in the roundhead

Cubipod[®] units are placed on a roundhead in the same way as they are on the trunk; however, the conventional diamond placement grid shown in Figure 6.7 can not be extended indefinitely to the upper rows because the radius is reduced significantly. Toe berm and Cubipods follow concentric circular rows. The horizontal distance between units (“a”) along the circles may be constant in the same row, but must be reduced in upper rows (smaller radius). For the most usual high curvature roundheads (small radius), there will be a row in which the distances “a” between units will be too small to place the units correctly, and some units will be lost during placement.

In order to optimize the placement of Cubipods on the roundhead, realistic placement tests on roundheads were conducted (see Pardo et al., 2014), with different radius and slopes $\cot\alpha=1.5$ and 2.0 . The best solution involves using coupled grids such as those shown in Figure 6.9; “a” is the distance between consecutive units in the first row and the number of rows of units given by Equation 6.2 are then placed following the one-between-two rule in each unit placement.

$$n_{mi} = \frac{R_{mi}}{b} \left(1 - \frac{(a_{\min}/D_n)_{mi}}{a/D_n} \right) + 1 \quad 6.2$$

in which “mi” is the grid number ($mi=1,2,3,\dots$), “ n_{mi} ” is the number of rows which can be completed within the grid “mi”, and “ $(a_{\min}/D_n)_{mi}$ ” is the minimum relative distance of grid “mi”. The initial radius is $R_{mi}=R_{th}-bn_f$, where “ R_{mi} ” is the radius of the first row of the grid “mi”, “ R_{th} ” is the roundhead initial radius, “b” is the horizontal distance between rows and n_f is the total number of rows placed before the grid “mi”.

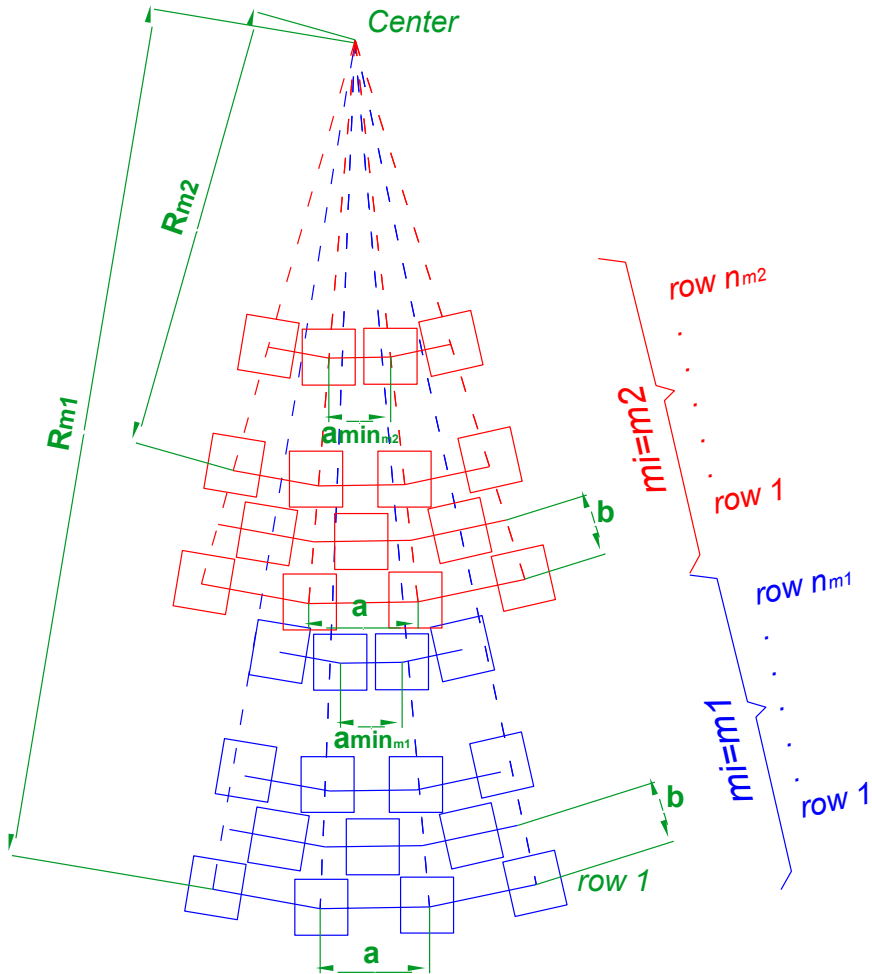


Figure 6.9 Coupled grids to place Cubipods on roundheads.

The recommended values of b/D_n are similar to those for straight trunks, $b/D_n=1.02-1.05$ depending on the armor slope. The initial values “ a/D_n ” are superior to those recommended for straight trunks, because the distance between adjacent units in a row is reduced in the upper rows depending on the roundhead curvature. For $15 < R_{m1}/D_n < 20$, a reasonable relative distance between adjacent units is $1.68 < a/D_n < 1.76$ to obtain armor porosities $41\% < p < 43\%$ ($0.59 > \Phi > 0.57$).



Figure 6.10 Small-scale realistic placement of Cubipods in trunk and roundhead.



Figure 6.11 Reference area to measure the armor porosity in the roundhead.

Figures 6.10 and 6.11 show views of the realistic placement tests. Using small-scale crawler cranes and pressure clamps, different placement grids are tested, the armor

porosities measured and lost units counted. The optimum placement grids are those which minimize the final armor porosity and number of units lost.

6.5. Transitions for changes in armor thickness

The guidelines to place concrete armor units in trunks and roundheads, described above, solve the most common placement problems. Nevertheless, there are two special problems, affecting some units in the armor, which may have to be addressed separately: (1) changes in armor unit size and (2) changes in the number of layers. These special cases require appropriate transitions for a significant change in armor thickness.

Because unit size depends on wave climate and bathymetry, it is often the case that breakwaters are designed with different unit sizes; for instance, a small size for the breakwater root, a medium size for the main trunk and a large size for the roundhead. As general rule, it is not economically optimum to design the breakwater armor with many different unit sizes, because the diversity of sizes increases the logistic costs and restrictions. The economically optimum armor design usually leads to the use, initially, of as much quarry stone as possible, and later as few as possible concrete armor unit sizes. A certain overdesign is usually economically better than designing with multiple unit sizes.

If the concrete unit size required is very small, it is preferable to use quarry-rock (lower supply cost) of a larger size, which is able to withstand the same design storm. Thus, it is common to change from double-layer quarry-stone armor to single- or double-layer small Cubipod[®] armor and, in another area, change to a single- or double-layer large Cubipod[®] armor. Although the unit size is not modified, sometimes it is necessary to change from single- to double-layer (e.g. Western Breakwater of the Outer Port of A Coruña at Punta Langosteira, Spain). In this case, the armor thickness significantly changes, especially when changing from single- to double-layer armor, and a transition must be designed.

In order to design an appropriate transition, it is convenient to take into consideration several hydraulic and construction factors, regardless of the concrete armor unit. Firstly, it is preferable to avoid creating steep steps in the external armor profile, because currents and waves may generate relevant additional forces on the units of the transition. Secondly, an efficient construction requires placing stones in layers with a given frontal slope (e.g. $H/V=1.5$) and a lateral moving slope in which armor units are placed on the slope in a 45° wedge shape (see Figures 6.8 and 6.12), with internal layers advancing first (core first, first under-layer behind, etc.). Larger stones or concrete units are always placed on smaller stones or units. Finally, if the armor unit size is larger, the underlayer will probably be larger as well (W/10 to W/20 rule).

Transition single-to-double layer Cubipod[®] armors. The change in armor thickness is relevant in this transition; it is recommended to progressively increase the thickness of the underlayer to compensate for the change in armor thickness. Because interior

layers are advanced during construction and armor units are placed on the underlayer, the armor advances approximately in a 45° wedge shape. To place the smaller rocks or units on the larger ones (quarry-rocks on Cubipod[®] units), not only must the single-layer Cubipod[®] armor (with thicker underlayer) advance with a 45° wedge shape, but the double-layer Cubipod[®] armor also has to advance in the opposite direction with a 45° wedge shape. When the thicker underlayer touches the interior bottom row of double-layer Cubipod[®] armor, under-layer rocks are placed on the first layer of Cubipods, and the single-layer Cubipod[®] armor is placed on the transition to obtain a plane and homogeneous external armor surface. Figure 6.12 shows the transition from single-to-double Cubipod[®] armor in the 1/51 scale model of the Western Breakwater at Punta Langosteira.



Figure 6.12 Transition single-to-double Cubipod[®] armor.

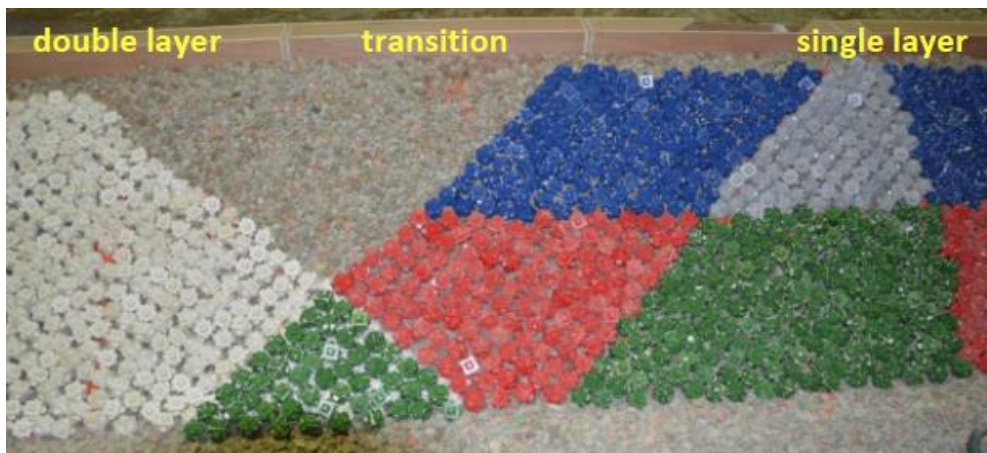


Figure 6.13 Single-layer Cubipod[®] armor advancing on the first layer of Cubipods.

Figure 6.13 shows single-layer armor advancing on the first layer of the previously-placed double-layer Cubipod[®] armor. The exterior armor surface of the single-layer Cubipod[®] armor is quite homogeneous and planar, covering the first layer of the double-layer Cubipod[®] armor to complete the double-layer armor. If the external Cubipod[®] armor layer were removed, either a double-layer quarry-stone armor or a single-layer Cubipod[®] armor would be seen.

The transition described above fulfils all the required restrictions: (1) quarry stones are placed advancing in a 45° wedge shape, (2) Cubipod[®] units are placed on rows below, advancing in a 45° wedge shape, (3) the external armor envelope is homogeneous and plane and (4) rocks are placed on Cubipods and not the other way around.

Transition double-layer quarry-stone to single-layer Cubipod[®] armor. This transition can be designed by increasing the underlayer of the Cubipod[®] armor and placing the quarry stones on the Cubipods. This requires placing the Cubipods in an opposite 45° wedge shape and filling the contact upper wedge with quarry stones (placed on Cubipods).

Transitions for changes in armor unit size. If the number of layers in the armor is the same but the unit size is different, it will be necessary to increase the thickness of the underlayer of the smaller unit armor to obtain a homogeneous external armor surface. If the smaller unit armor is placed first, it is necessary to place the larger units in an opposite 45° wedge shape to finally place the smaller units on top of the large units.

It may be necessary to design other kinds of transition. Whatever the case, it is convenient to keep the external armor envelope plane and homogeneous, and place the smaller units on the larger ones.

Chapter 7

Example

7.1. Introduction

This chapter offers an example to design typical mound breakwaters using cubes and Cubipods according to the *Cubipod[®] Manual 2016*; the objective is to provide a guide to solve certain problems which may arise in the design process. Breakwater design requires optimizing a complex problem with multiple constraints associated to harbor planning, wave climate conditions, sources of materials, available equipment, and logistic, economic, social and environmental restrictions. This chapter focuses attention on solving a schematic problem which involves only some of these restrictions, using design rules and methods described in the *Cubipod[®] Manual 2016*.

In this example, the breakwater layout is defined, as well as the bathymetry and storm conditions at the toe of the structure along the breakwater. The quarry is assumed to be close to the construction site (inexpensive quarry stones) and conventional manufacturing and handling equipment (crawler cranes, trucks, molds, etc.) are available. No special restrictions are assumed in regards to personnel, social or environmental aspects. The objective is to provide preliminary safe and feasible breakwater designs which can lead to a final optimum design, minimizing economic costs and environmental impact (energy and carbon footprints).

2D and 3D small-scale tests are usually quite valuable to validate and optimize preliminary designs. Empirical formulas (based on standard 2D and 3D small-scale tests as those described in previous chapters) are known to be useful in the preliminary design, to estimate the economic costs, and to describe the main logistic aspects of the new

breakwater. Before initiating the detailed design phase, specific 2D or 3D tests are recommended to validate and optimize the preliminary design; different alternatives are usually tested to find the best solution to the design problem.

7.2. Design conditions

A 3.5 km-long mound breakwater on a rocky seabed must withstand the following design storms at water depth $h_s[m]=30$ (toe of the main trunk and roundhead):

Wave direction at toe of the structure: N13°W

No damage ($T_R[\text{year}]=2$): $H_s[m]=7.0$ and $T_p[s]=16$

Initiation of Damage (IDa, $T_R[\text{year}]=100$): $H_s[m]=9.5$ and $T_p[s]=18$

Initiation of Destruction (IDe, $T_R[\text{year}]=1000$): $H_s[m]=11.0$ and $T_p[s]=19$

Tidal range $\Delta h[m]=4.5=HWL-LWL$

The coast is orientated toward the North and has straight bathymetric lines with the following bottom slopes (LWL): $\tan\beta=4\%$ ($h_s[m]<12$), $\tan\beta=2\%$ ($12<h_s[m]<24$), and $\tan\beta=1\%$ ($24<h_s[m]$). The breakwater has two alignments SSW-NNE and W-E (main trunk and roundhead) with a low-curvature curved trunk between the two alignments. Figure 7.1 shows the breakwater plan view.

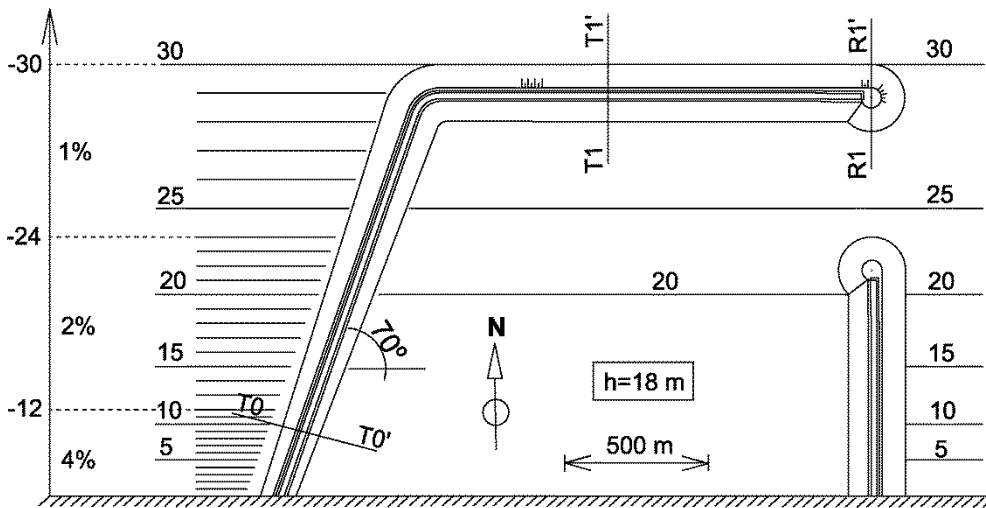


Figure 7.1 Breakwater plan view.

Rock size distribution obtained from the quarry depends on natural rock fragmentation and bench blasting. The materials obtained from the quarry are distributed as follows:

2% $W_{50}[t]=6.0$ ($4.5 < W[t] < 7.5$)

4% $W_{50}[t]=3.5$ ($2.5 < W[t] < 4.5$)

6% $W_{50}[t]=2.0$ ($1.5 < W[t] < 2.5$)

10% $W_{50}[t]=1.0$ ($0.5 < W[t] < 1.5$)

10% $W_{50}[t]=0.3$ ($0.1 < W[t] < 0.5$)

38% $0.005 < W[t] < 0.1$

30% $W[t] < 0.005$

Mass densities of rock, concrete and sea water are $\rho_r[t/m^3]=2.700$, $\rho_c[t/m^3]=2.400$ and $\rho_w[t/m^3]=1.025$, respectively. Unit costs at the construction site for concrete supply $f_{ck}[MPa]=20$ and 35 are $60\text{€}/m^3$ and $65\text{€}/m^3$, respectively.

7.3. Preliminary design and calculations using *Cubipod*[®] *Manual 2016*

The objective of this example is to define several descriptive elements of the best of three alternative solutions to the design conditions given above. The three alternatives are breakwaters protected with: (A) double-layer cube armor, (B) single-layer *Cubipod*[®] armor, and (C) double-layer *Cubipod*[®] armor. The alternative solutions must be defined with trunk and roundhead cross sections and, if necessary, transitions in a plan view.

To select the best alternative, the alternative solutions are compared from the technical and economic points of view. The performance of the proposed designs should be estimated from operational and safety points of view. The experimental design of the corresponding 2D and 3D tests, to validate the breakwater preliminary designs, must be subject to further validation and optimization.

Armor failure (extraction, sliding or heterogeneous packing) is considered the main failure mode for breakwaters armored with massive concrete armor units. The other failure modes (overtopping, toe berm failure, etc.) are not critical during preliminary design. Thus, from the safety point of view, similar alternative solutions must be compared with the same safety factors to Initiation of damage (IDa) and Initiation of Destruction (IDe) of armors. Safety factors are required to take into account model and scale effects as well as multiple sources of risk and uncertainties affecting the hydraulic stability of armors (environmental data, construction methods, materials, neglected or unknown variables, etc.).

Considering the global safety factors given in Table 7.1, IDa can be associated to the Service Limit State (SLS) and may be characterized by $SF(IDa50\%)$. When SLS (IDa)

is surpassed, small or moderate armor damage may occur, but the breakwater has not failed and the armor could be repaired. IDe can be associated to the Ultimate Limit State (ULS) and may be characterized by SF(IDe5%). Once ULS is exceeded, the breakwater fails and breakwater functionality is completely lost; that is why safety factors are higher for IDe than IDa, and IDe5% (percentile 5%) is considered for design. Designing with SF(IDe5%)=1.25 means 95% of small-scale tests showed safety factors higher than 1.25 to IDe ($T_R=1000$ years).

Table 7.1 Safety factors for single- and double-layer trunk and roundhead armors.

Global safety factors		IDa	IDe
Part	# layers	SF(IDa50%)	SF(IDe5%)
Trunk	double-layer	0.90	1.10
	single-layer	1.20	1.30
Roundhead	double-layer	1.10	1.25
	single-layer	1.15	1.30

7.4. Hydraulic stability of armored trunks

Three armoring alternatives are considered: A (double-layer cube armor), B (single-layer Cubipod® armor) and C (double-layer Cubipod® armor). If the structure slope $\cot\alpha=1.5$, Equation 2.2 and Tables 2.3 and 7.1 can be used to estimate the weight of the armor units.

Table 2.3 Safety factors to IDa and IDe (percentiles 5% and 50%) for double- layer cube armor and single- and double- layer Cubipod armors (trunk).

Design K_D and global safety factors					Initiation of Damage (IDa)		Initiation of Destruction (IDe)	
Part	Unit	K_D	# layers	slope	SF(IDa5%)	SF(IDa50%)	SF(IDe5%)	SF(IDe50%)
Trunk	Cube	6.0	2	3/2	0.67	0.86	1.05	1.35
	Cubipod®	28.0	2	3/2	0.82	0.99	1.09	1.40
	Cubipod®	12.0	1	3/2	1.06	1.27	1.31	1.64

$$N_{sd}(A) = \frac{H_{sd}}{\Delta D_n} = (K_D \cot \alpha)^{1/3} = (6.0 \times 1.5)^{1/3} = 2.08$$

$$N_{sd}(B) = \frac{H_{sd}}{\Delta D_n} = (K_D \cot \alpha)^{1/3} = (12.0 \times 1.5)^{1/3} = 2.62$$

$$N_{sd}(C) = \frac{H_{sd}}{\Delta D_n} = (K_D \cot \alpha)^{1/3} = (28.0 \times 1.5)^{1/3} = 3.47$$

Initiation of Damage (IDa):

$$(A): H_{sd}[m] = 2.08(\Delta D_n) = 2.08 \times \left(\frac{2.400}{1.025} - 1 \right) \times D_n = 2.08 \times 1.34 \times D_n = 2.79 \times D_n = 9.5$$

$$D_n(A_IDa) = \frac{9.5}{2.79} \times \frac{0.90}{0.86} = 3.60m$$

$$(B): H_{sd}[m] = 2.62(\Delta D_n) = 2.62 \times \left(\frac{2.400}{1.025} - 1 \right) \times D_n = 2.62 \times 1.34 \times D_n = 3.51 \times D_n = 9.5$$

$$D_n(B_IDa) = \frac{9.5}{3.51} \times \frac{1.20}{1.27} = 2.56m$$

$$(C): H_{sd}[m] = 3.47(\Delta D_n) = 3.47 \times \left(\frac{2.400}{1.025} - 1 \right) \times D_n = 3.47 \times 1.34 \times D_n = 4.65 \times D_n = 9.5$$

$$D_n(C_IDa) = \frac{9.5}{4.65} \times \frac{0.90}{0.99} = 1.86m$$

Initiation of Destruction (IDe):

$$(A): H_{sd}[m] = 2.08(\Delta D_n) = 2.08 \times \left(\frac{2.400}{1.025} - 1 \right) \times D_n = 2.79 \times D_n = 11.0$$

$$D_n(A_IDe) = \frac{11.0}{2.79} \times \frac{1.10}{1.05} = 4.13m > 3.60m \quad W[t] = 2.400 \times (4.13)^3 = 169$$

$$SF(A_IDa50\%) = 0.90 \times \frac{4.13}{3.60} = 1.03$$

A double-layer 169-tonne cube armor in trunk has SF(IDe5%)=1.10 and SF(IDa50%)=1.03, in agreement with the minimum safety factors prescribed in Table 7.1.

$H_{sd}/h_s = 11.0/(30.0+4.5) = 0.32 < 0.39$ (HWL) and $H_{sd}/h_s = 11.0/30.0 = 0.37 < 0.39$. The breakwater is in non-breaking wave conditions at HWL and near the non-breaking wave conditions at LWL (slightly on the safe side because some large waves may break before reaching the structure at LWL).

$$(B): H_{sd}[m] = 2.62(\Delta D_n) = 2.62 \times \left(\frac{2.400}{1.025} - 1 \right) \times D_n = 3.51 \times D_n = 11.0$$

$$D_n(B_IDe) = \frac{11.0}{3.51} \times \frac{1.30}{1.31} = 3.11m > 2.56m \quad W[t] = 2.400 \times (3.11)^3 = 72$$

$$SF(B_IDa50\%) = 1.20 \times \frac{3.11}{2.56} = 1.41$$

A single-layer 72-tonne Cubipod[®] armor in trunk has SF(IDe5%)=1.30 and SF(IDa50%)=1.41, in agreement with the minimum safety factors prescribed in Table 7.1.

$$(C): H_{sd}[m] = 3.47(\Delta D_n) = 3.47 \times \left(\frac{2.400}{1.025} - 1 \right) \times D_n = 4.65 \times D_n = 11.0$$

$$D_n(C_IDe) = \frac{11.0}{4.65} \times \frac{1.10}{1.09} = 2.39m > 1.86m \qquad W[t] = 2.400 \times (2.39)^3 = 33$$

$$SF(C_IDa50\%) = 0.90 \times \frac{2.39}{1.86} = 1.16$$

A double-layer 33-tonne Cubipod[®] armor in trunk has SF(IDe5%)=1.10 and SF(IDa50%)=1.16, in agreement with the minimum safety factors prescribed in Table 7.1.

7.5. Overtopping and breakwater crest design

Crest elevation is conditioned by the permissible overtopping rates at HWL. Taking into account the limits for overtopping listed in the EurOtop Manual (2007), the following limits for the mean discharge can be considered in this case:

$T_R[\text{year}] = 2, q[l/s/m] < 1$ (hazard for pedestrians and equipment)

$T_R[\text{year}] = 100, q[l/s/m] < 7$ (hazard for trained staff, vehicles, small boats and buildings)

$T_R[\text{year}] = 1000, q[l/s/m] < 40$ (hazard for large yachts and unprotected rear slope)

During breakwater service time, to avoid personal injuries due to overtopping, access to the breakwater crest will have to be mandatorily limited during maximum yearly storms. Severe damage to small boats, buildings, equipment, vehicles and personnel (if not evacuated in time) may occur with a probability of 50% (50/100) during service time (50 years). Finally, there is a 5% probability (50/1000) during service time (50 years) of having 40 l/s/m threatening the rear slope if not well protected.

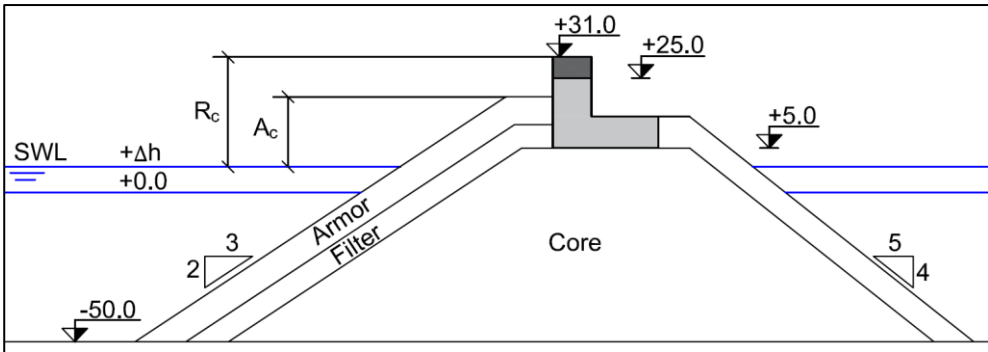


Figure 3.1 Cross section of 2D model used in overtopping tests (dimensions in cm).

According to Equation 3.1 and Figure 3.1, overtopping rates for $H_{sd}[T_R=1000 \text{ years}]=11.0 \text{ m}$ and $T_p[s]=19$ can be estimated for alternatives A, B and C as follows:

(A) Considering upper armor and crest freeboard $A_c[m]=R_c[m]=20.0-4.5=15.5$, $A_c/R_c=1$, $I_{rp}=(2/3)/(2\pi \times 11/[9.8 \times 19^2])^{1/2}=4.8$, $R_c/H_{m0}=(20.0-4.5)/11.0=1.41$ and $\gamma_f=0.50$ (double-layer cube armor).

$$Q_A = \frac{q}{\sqrt{gH_{m0}^3}} = 0.2 \times \exp\left(0.53 \times 4.8 - 3.27 \times \frac{15.5}{15.5} - \frac{2.16}{0.50} \times \frac{15.5}{11}\right)$$

$$Q_A = \frac{q}{\sqrt{gH_{m0}^3}} = 0.2 \times \exp(2.54 - 3.27 - 6.09) = 2.19 \times 10^{-4}$$

$$q_A[m^3/s/m] = (9.8 \times 11^3)^{0.5} Q_A = 114.2 Q_A = 114.2 \times 2.19 \times 10^{-4} = 25.0 \times 10^{-3} \rightarrow 25 \text{ l/s/m} < 40 \text{ l/s/m}$$

(B) Considering upper armor and crest freeboard $A_c[m]=R_c[m]=19.0-4.5=14.5$, $A_c/R_c=1$, $I_{rp}=(2/3)/(2\pi \times 11/[9.8 \times 19^2])^{1/2}=4.8$, $R_c/H_{m0}=(19.0-4.5)/11.0=1.32$ and $\gamma_f=0.46$ (single-layer Cubipod[®] armor).

$$Q_B = \frac{q}{\sqrt{gH_{m0}^3}} = 0.2 \times \exp\left(0.53 \times 4.8 - 3.27 \times \frac{14.5}{14.5} - \frac{2.16}{0.46} \times \frac{14.5}{11}\right) = 1.97 \times 10^{-4}$$

$$q_B[m^3/s/m] = (9.8 \times 11^3)^{0.5} Q_B = 114.2 Q_B = 114.2 \times 1.97 \times 10^{-4} = 22.5 \times 10^{-3} \rightarrow 22.5 \text{ l/s/m} < 40 \text{ l/s/m}$$

(C) Considering upper armor and crest freeboard $A_c[m]=R_c[m]=18.0-4.5=13.5$, $A_c/R_c=1$, $I_{rp}=(2/3)/(2\pi \times 11/[9.8 \times 19^2])^{1/2}=4.8$, $R_c/H_{m0}=(18.0-4.5)/11.0=1.23$ and $\gamma_f=0.44$ (double-layer Cubipod[®] armor).

$$Q_C = \frac{q}{\sqrt{gH_{m0}^3}} = 0.2 \times \exp\left(0.53 \times 4.8 - 3.27 \times \frac{13.5}{13.5} - \frac{2.16}{0.44} \times \frac{13.5}{11}\right) = 2.33 \times 10^{-4}$$

$$q_C[m^3/s/m] = (9.8 \times 11^3)^{0.5} Q_C = 114.2 Q_C = 114.2 \times 2.33 \times 10^{-4} = 26.6 \times 10^{-3} \rightarrow 26.6 \text{ l/s/m} < 40 \text{ l/s/m}$$

The crest elevations (R_c referring to LWL) $R_c[m]=20$ (A), 19 (B) and 18 (C) generate mean overtopping discharges $q[l/s/m]=25.0$ (A), 22.5 (B) and 26.6 (C), below the maximum limit 40 l/m/s corresponding to $T_R=1000$ years.

Similarly, overtopping rates for $H_{sd}[T_R=100 \text{ years}]=9.5 \text{ m}$ and $T_p[s]=18$ can be estimated for alternatives A, B and C as follows:

(A) Considering upper armor and crest freeboard $A_c[m]=R_c[m]=20.0-4.5=15.5$, $A_c/R_c=1$, $I_{rp}=(2/3)/(2\pi \times 9.5/[9.8 \times 18^2])^{1/2}=4.9$, $R_c/H_{m0}=(20.0-4.5)/9.5=1.63$ and $\gamma_f=0.50$.

$$Q_A = \frac{q}{\sqrt{gH_{m0}^3}} = 0.2 \times \exp\left(0.53 \times 4.9 - 3.27 \times \frac{15.5}{15.5} - \frac{2.16}{0.50} \times \frac{15.5}{9.5}\right)$$

$$Q_A = \frac{q}{\sqrt{gH_{m0}^3}} = 0.2 \times \exp(2.60 - 3.27 - 7.05) = 0.89 \times 10^{-4}$$

$$q_A[\text{m}^3/\text{s}/\text{m}] = (9.8 \times 9.5^3)^{0.5} Q_A = 91.7 Q_A = 91.7 \times 0.89 \times 10^{-4} = 8.13 \times 10^{-3} \rightarrow 8.1 \text{ l/s/m} > 7 \text{ l/s/m}$$

(B) Considering upper armor and crest freeboard $A_c[\text{m}] = R_c[\text{m}] = 19.0 - 4.5 = 14.5$, $A_c/R_c = 1$, $I_{rp} = (2/3)/(2\pi \times 9.5/[9.8 \times 18^2])^{1/2} = 4.8$, $R_c/H_{m0} = (19.0 - 4.5)/9.5 = 1.53$ and $\gamma_f = 0.46$.

$$Q_B = \frac{q}{\sqrt{gH_{m0}^3}} = 0.2 \times \exp\left(0.53 \times 4.9 - 3.27 \times \frac{14.5}{14.5} - \frac{2.16}{0.46} \times \frac{14.5}{9.5}\right) = 0.79 \times 10^{-4}$$

$$q_B[\text{m}^3/\text{s}/\text{m}] = (9.8 \times 9.5^3)^{0.5} Q_B = 91.7 Q_B = 91.7 \times 0.79 \times 10^{-4} = 7.2 \times 10^{-3} \rightarrow 7.2 \text{ l/s/m} > 7 \text{ l/s/m}$$

(C) Considering upper armor and crest freeboard $A_c[\text{m}] = R_c[\text{m}] = 18.0 - 4.5 = 13.5$, $A_c/R_c = 1$, $I_{rp} = (2/3)/(2\pi \times 9.5/[9.8 \times 18^2])^{1/2} = 4.9$, $R_c/H_{m0} = (18.0 - 4.5)/9.5 = 1.42$ and $\gamma_f = 0.44$.

$$Q_C = \frac{q}{\sqrt{gH_{m0}^3}} = 0.2 \times \exp\left(0.53 \times 4.9 - 3.27 \times \frac{13.5}{13.5} - \frac{2.16}{0.44} \times \frac{13.5}{9.5}\right) = 0.95 \times 10^{-4}$$

$$q_C[\text{m}^3/\text{s}/\text{m}] = (9.8 \times 9.5^3)^{0.5} Q_C = 91.7 Q_C = 91.7 \times 0.95 \times 10^{-4} = 8.7 \times 10^{-3} \rightarrow 8.7 \text{ l/s/m} > 7 \text{ l/s/m}$$

The crest elevations (R_c referring to LWL) $R_c[\text{m}] = 20$ (A), 19 (B) and 18 (C) generate mean overtopping discharges $q[\text{l}/\text{m}/\text{s}] = 8.1$ (A), 7.2 (B) and 8.7 (C), slightly above the maximum value 7 l/m/s corresponding to $T_R = 100$ years. Crest elevations should be increased slightly to reduce overtopping rates below the prescribed limit (7 l/m/s).

Overtopping rates for $H_{sq}[T_R = 2 \text{ years}] = 7 \text{ m}$ and $T_p[\text{s}] = 16$ can be estimated for alternatives A, B and C as follows:

(A) Considering upper armor and crest freeboard $A_c[\text{m}] = R_c[\text{m}] = 20.0 - 4.5 = 15.5$, $A_c/R_c = 1$, $I_{rp} = (2/3)/(2\pi \times 7/[9.8 \times 16^2])^{1/2} = 5.0$, $R_c/H_{m0} = (20.0 - 4.5)/7.0 = 2.21$ and $\gamma_f = 0.50$.

$$Q_A = \frac{q}{\sqrt{gH_{m0}^3}} = 0.2 \times \exp\left(0.53 \times 5.0 - 3.27 \times \frac{15.5}{15.5} - \frac{2.16}{0.50} \times \frac{15.5}{7.0}\right)$$

$$Q_A = \frac{q}{\sqrt{gH_{m0}^3}} = 0.2 \times \exp(2.65 - 3.27 - 9.56) = 0.075 \times 10^{-4}$$

$$q_A[\text{m}^3/\text{s}/\text{m}] = (9.8 \times 7^3)^{0.5} Q_A = 58.0 Q_A = 58.0 \times 0.075 \times 10^{-4} = 0.44 \times 10^{-3} \rightarrow 0.44 \text{ l/s/m} < 1 \text{ l/s/m}$$

(B) Considering upper armor and crest freeboard $A_c[\text{m}] = R_c[\text{m}] = 19.0 - 4.5 = 14.5$, $A_c/R_c = 1$, $I_{rp} = (2/3)/(2\pi \times 7/[9.8 \times 16^2])^{1/2} = 5.0$, $R_c/H_{m0} = (19.0 - 4.5)/7 = 2.07$ and $\gamma_f = 0.46$.

$$Q_B = \frac{q}{\sqrt{gH_{m0}^3}} = 0.2 \times \exp\left(0.53 \times 5.0 - 3.27 \times \frac{14.5}{14.5} - \frac{2.16}{0.46} \times \frac{14.5}{7.0}\right) = 0.064 \times 10^{-4}$$

$$q_B[m^3/s/m]=(9.8 \times 7^3)^{0.5} Q_B=58.0 Q_B=58.0 \times 0.064 \times 10^{-4}=0.37 \times 10^{-3} \rightarrow 0.37 \text{ l/s/m} < 1 \text{ l/s/m}$$

(C) Considering upper armor and crest freeboard $A_c[m]=R_c[m]=18.0-4.5=13.5$, $A_c/R_c=1$, $I_{rp}=(2/3)/(2\pi \times 7/[9.8 \times 16^2])^{1/2}=5.0$, $R_c/H_{m0}=(18.0-4.5)/7.0=1.93$ and $\gamma_f=0.44$.

$$Q_C = \frac{q}{\sqrt{gH_{m0}^3}} = 0.2 \times \exp\left(0.53 \times 5.0 - 3.27 \times \frac{13.5}{13.5} - \frac{2.16}{0.44} \times \frac{13.5}{7.0}\right) = 0.083 \times 10^{-4}$$

$$q_C[m^3/s/m]=(9.8 \times 7^3)^{0.5} Q_C=58.0 Q_C=58.0 \times 0.083 \times 10^{-4}=0.48 \times 10^{-3} \rightarrow 0.48 \text{ l/s/m} < 1 \text{ l/s/m}$$

The crest elevations (R_c referring to LWL) $R_c[m]=20$ (A), 19 (B) and 18 (C) generate mean overtopping discharges $q[l/s/m]=0.44$ (A), 0.37 (B) and 0.48 (C), below the maximum value 1 l/s/m corresponding to $T_R=2$ years.

In order to fulfill the three overtopping limits prescribed for $T_R[\text{year}]=2, 100$ and 1000 , mean overtopping discharge for $T_R[\text{year}]=100$ is the most critical condition. Minimum crest elevations (R_c referring to LWL) are:

$R_c[m]=20.4$ (double-layer cube armor)

$R_c[m]=19.1$ (single-layer Cubipod[®] armor)

$R_c[m]=18.5$ (double-layer Cubipod[®] armor)

$$Q_A = \frac{q}{\sqrt{gH_{m0}^3}} = 0.2 \times \exp\left(0.53 \times 4.9 - 3.27 \times \frac{15.9}{15.9} - \frac{2.16}{0.50} \times \frac{15.9}{9.5}\right) = 0.74 \times 10^{-4}$$

$$q_A[m^3/s/m]=(9.8 \times 9.5^3)^{0.5} Q_A=91.7 Q_A=91.7 \times 0.74 \times 10^{-4}=6.8 \times 10^{-3} \rightarrow 6.8 \text{ l/s/m} < 7 \text{ l/s/m}$$

$$Q_B = \frac{q}{\sqrt{gH_{m0}^3}} = 0.2 \times \exp\left(0.53 \times 4.9 - 3.27 \times \frac{14.6}{14.6} - \frac{2.16}{0.46} \times \frac{14.6}{9.5}\right) = 0.75 \times 10^{-4}$$

$$q_B[m^3/s/m]=(9.8 \times 9.5^3)^{0.5} Q_B=91.7 Q_B=91.7 \times 0.75 \times 10^{-4}=6.9 \times 10^{-3} \rightarrow 6.9 \text{ l/s/m} < 7 \text{ l/s/m}$$

$$Q_C = \frac{q}{\sqrt{gH_{m0}^3}} = 0.2 \times \exp\left(0.53 \times 4.9 - 3.27 \times \frac{14.0}{14.0} - \frac{2.16}{0.44} \times \frac{14.0}{9.5}\right) = 0.74 \times 10^{-4}$$

$$q_C[m^3/s/m]=(9.8 \times 9.5^3)^{0.5} Q_C=91.7 Q_C=91.7 \times 0.74 \times 10^{-4}=6.7 \times 10^{-3} \rightarrow 6.7 \text{ l/s/m} < 7 \text{ l/s/m}$$

7.6. Design of toe berm

The toe berm usually has the minimum hydraulic stability at LWL. According to the criterion given by Grau (2008), and considering Equation 6.1 and Figure 6.5, $h_s[m]=30$ and $1.5 \times 11.0=16.5 < h_t[m] < 27$ ($0.4 < h_t/h_s < 0.9$).

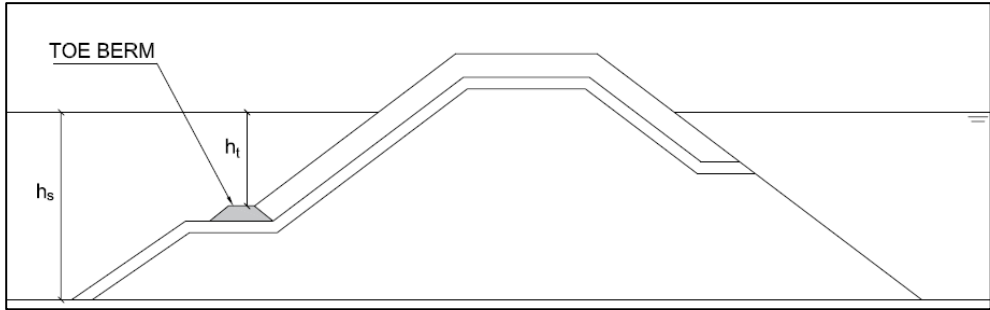


Figure 6.5 Sketch of breakwater in a deep water area.

Equation 6.1 can be used because $0.4 < h_t/h_s < 0.9$. Using 6-tonne rocks for the toe berm (2% volume in quarry), the nominal diameter is

$$D_{n50}[m] = \left(\frac{6.0}{2.700} \right)^{1/3} = 1.30$$

Considering $N_{od}=0.5$ (start of damage), the safety factor to destruction of toe berm is $(4.0/0.5)^{0.15}=1.37$.

$$\frac{H_s}{\Delta D_{n50}} = \left(2 + 6.2 \left(\frac{h_t}{h_s} \right)^{2.7} \right) N_{od}^{0.15} \Rightarrow \frac{11.0}{\left(\frac{2.700}{1.025} - 1 \right) \times 1.30} = \left(2 + 6.2 \left(\frac{h_t}{30} \right)^{2.7} \right) 0.5^{0.15}$$

$$5.18 = \left(2 + 6.2 \left(\frac{h_t}{30} \right)^{2.7} \right) 0.90 \rightarrow \frac{h_t}{30} = \left(\frac{\left(\frac{5.18}{0.90} - 2 \right)}{6.2} \right)^{\frac{1}{2.7}} = 0.83 \rightarrow h_t[m]=24.9$$

Considering $N_{od}=1.0$ (lower than moderate damage), $N_{od}^{0.15}=1.0$, the safety factor to destruction of toe berm is $(4.0/1.0)^{0.15}=1.23$.

$$5.18 = \left(2 + 6.2 \left(\frac{h_t}{30} \right)^{2.7} \right) 1.00 \rightarrow \frac{h_t}{30} = \left(\frac{\left(\frac{5.18}{1.00} - 2 \right)}{6.2} \right)^{\frac{1}{2.7}} = 0.78 \rightarrow h_t[m]=23.4$$

In this case, the 6-tonne toe berm should be placed near the sea bottom ($h_t[m]>23.4$); it would be necessary to use concrete units for elevated toe berms (e.g. $h_t[m]>17$). Ele-

vated toe berms reduce the cost of the armor (less concrete is used), but may increase the total cost if concrete units are required.

(A) It is reasonable to design an elevated toe berm with concrete units for a double-layer 169-tonne cube armor, because this armor also requires a concrete underlayer (e.g. double-layer 16-tonne cube underlayer). For instance, a 35-tonne cube toe berm with $h_t[m] > 17$ on a 16-tonne underlayer (see Figure 6.5).

(B) A single-layer 72-tonne Cubipod[®] armor requires a double-layer rock underlayer of $3.5 < W[t] < 7.0$ (6% volume in quarry). The toe berm ($W[t]=6$) is better placed on the rocky sea bottom, although 72-tonne Cubipod[®] units are larger than needed when placed in the deepest locations ($h[m] < 16$).

(C) A double-layer 33-tonne Cubipod[®] armor requires a double-layer rock underlayer of $1.5 < W[t] < 3.5$ (10% volume in quarry). The toe berm ($W[t]=6$) is better placed on the rocky sea bottom, although 33-tonne Cubipod[®] units are larger than needed when placed in the deepest locations ($h[m] < 16$).

7.7. Design of core and filter layers

Considering the rock size distribution obtained from the quarry and the general filter rule ($10 < W_i/W_{i+1} < 20$), the rock sizes of layers of the three alternatives are:

(A) Double-layer cube armored breakwater

Armor: $W=169$ -tonne cubes, $D_n[m]=4.13$, armor thickness $e_0[m]=2D_n=8.3$ and porosity $p=0.37$ (safety factors to IDa and IDe are reduced if $p=0.41 > 0.37$).

Underlayer: $W/10 \approx 16$ -tonne cubes, $D_n[m]=1.88$, $e_1[m]=2D_n=3.8$ and $p=0.41$

Second filter layer: 1-tonne quarry stones, $D_n[m]=0.72$, $e_2[m]=2D_n=1.5$ and $p=0.37$

Core: quarry-run $0.005 < W[t] < 0.050$, $p=0.34$

Toe berm: 35-tonne cubes, $D_n[m]=2.44$, $e_{toe}[m]=3D_n=7.3$, toe berm width $B[m]=4D_n=9.8 \approx 10$

(B) Single-layer Cubipod[®] armored breakwater

Armor: $W=72$ -tonne Cubipods, $D_n[m]=3.10$, $e_0[m]=1D_n=3.1$ and $p=0.415$

Underlayer: $W/20 \approx 3.5$ -tonne quarry stones, $D_n[m]=1.09$, $e_2[m]=2D_n=2.2$ and $p=0.38$

Second filter layer: 0.3-tonne quarry stones, $D_n[m]=0.48$, $e_2[m]=3D_n=1.5$ and $p=0.36$

Core: quarry-run $0.005 < W[t] < 0.050$, $p=0.34$

Toe berm: 6-tonne quarry stones, $D_n[m]=1.30$, $e_{toe}[m]=2D_n=2.6$, toe berm width $B[m]=4D_n=5.2$

(C) Double-layer Cubipod[®] armored breakwater

Armor: $W=33$ -tonne Cubipods, $D_n[m]=2.40$, $e_0[m]=2D_n=4.8$ and $p=0.420$

Underlayer: $W/15\approx 2$ -tonne quarry stones, $D_n[m]=0.90$, $e_2[m]=2D_n\approx 2.0$ and $p=0.38$

Second filter layer: 0.3-tonne quarry stones, $D_n[m]=0.48$, $e_2[m]=3D_n=1.5$ and $p=0.36$

Core: quarry-run $0.005 < W[t] < 0.050$, $p=0.34$

Toe berm: 6-tonne quarry stones, $D_n[m]=1.30$, $e_{toe}[m]=3D_n=3.9$, toe berm width $B[m]=4D_n=5.2$

When the preliminary breakwater design is completed, the volume of different sizes of materials must be compared to the rock size distribution at the quarry. Stone sizes or layer thicknesses may be modified to efficiently exploit the quarry.

7.8. Design of crown wall

Equations 3.2 and 3.3 can be used to estimate the horizontal and vertical forces which may cause sliding or overturning of the crown wall (see Figure 3.6). The design should consider a friction factor between the crown wall and bedding layer $0.5 < \mu = 0.6 < 0.7$ and safety factors 1.2 for sliding and overturning (see ROM 0.5-05, 2008). Crown walls can be built-up on a relatively permeable bedding layer placed on the core crest; the maximum crown wall base elevation (w_c) and minimum crown wall height (h_f) are conditioned by the armor and filter layers.

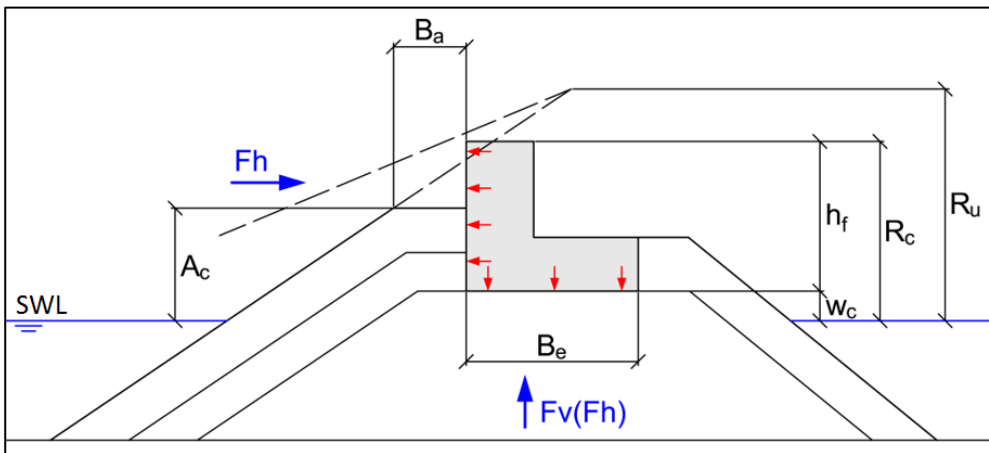


Figure 3.6 Scheme of horizontal and vertical up-lift forces acting on the crown wall.

(A) Crown wall elevation is $R_c[m]=20.4$ (referring to LWL) and cumulative layer thickness is $e_0[m]+e_1[m]+e_2[m]=8.3+3.8+1.5=13.6$. Maximum crown wall base elevation is $w_c[m]=20.4-13.6=6.8$ and elevation at HWL is $6.8-4.5=2.3$ meters. This eleva-

tion is too low to guarantee safety for personnel and terrestrial equipment during the construction phase. Core crest elevation during the construction phase may be raised to $w_c[m]=6.8+1.5=8.3$ (3.8-meter elevation at HWL) and the top 1.5-meter layer substituted later by uniform permeable material. Crown wall height is $h_f[m]=20.4-8.3=12.1$

(B) Crown wall elevation is $R_c[m]=19.1$ (referring to LWL) and cumulative layer thickness is $2xe_0[m]+e_1[m]+e_2[m]=2 \times 3.1+2.2+1.5=9.9$ (the berm of the armor layer crest should be two layers of Cubipods, with a width $B_a \geq 3D_n$, at the front of the crown wall). The maximum crown wall base elevation is $w_c[m]=19.1-9.9=9.2$ and elevation at HWL is $9.2-4.5=4.7$ meters (safe enough for personnel and terrestrial equipment during construction phase). The crown wall height is $h_f[m]=19.1-9.2=9.9$.

(C) Crown wall elevation is $R_c[m]=18.5$ (referring to LWL) and cumulative layer thickness is $e_0[m]+e_1[m]+e_2[m]=4.8+2.0+1.5=8.3$. Maximum crown wall base elevation is $w_c[m]=18.5-8.3=10.2$ and elevation at HWL is $10.2-4.5=5.7$ meters. Crown wall height is $h_f[m]=18.5-10.2=8.3$.

For design storm ($T_R[\text{year}]=1000$, $H_s[m]=11.0$, $T_p[s]=19$), $T_{01}[s] \approx T_p/1.2=16$ and $h_s[m]=30.0+4.5=34.5$.

$$I_{r_m} = \tan \alpha / \sqrt{2\pi H_s / (g T_{01}^2)} = \frac{\left(\frac{2}{3}\right)}{\sqrt{\frac{(2\pi \times 11.0)}{(9.8 \times 16^2)}}} = 4.0$$

$$L_m = \frac{g T_{01}^2}{2\pi} \tanh\left(\frac{2\pi h_s}{L_m}\right) = \frac{9.8 \times 16^2}{2\pi} \tanh\left(\frac{2\pi \times 34.5}{L_m}\right) \rightarrow L_m[m]=267$$

$$R_u[m] = \min(2.58H_s \leftrightarrow 1.34H_s I_{r_m}^{0.55}) = 28.4$$

(A) The forces on crown wall are greatest at HWL ($\Delta h[m]=4.5$). Equations 3.2 to 3.5 can be used to estimate the safety factors for crown wall sliding and overturning if $0.31 < \gamma_f(R_u/R_c) < 0.94$, $0.07 < (R_c - A_c)/h_f < 0.59$, $0.01 < w_c/h_f < 0.27$ and $3.1 < (L_m/B_a)^{0.5} < 6.5$. Mass densities of concrete and sea water are $\rho_c[t/m^3]=2.400$ and $\rho_w[t/m^3]=1.025$, respectively.

$R_c[m]=A_c=20.4-4.5=15.9$, $\cot\alpha=1.5$, $\gamma_f=0.50$ for double-layer cube armor, $H_s[m]=11.0$, $w_c[m]=3.8$, $h_f[m]=12.1$, $B_c[m]=8$, $B_a[m]=3D_n=3 \times 4.13 \approx 12.5$, and $g[m/s^2]=9.81$. The applicability limits are $0.31 < \gamma_f(R_u/R_c)=0.89 < 0.94$, $(R_c - A_c)/h_f=0$, $w_c/h_f=0.31$ and $3.1 < (L_m/B_a)^{0.5}=4.0 < 6.5$. In this case, not all variables fall within the range of applicability, but all variables are within or near the range of applicability; for preliminary designs higher safety factors than those prescribed are used.

$$\frac{Fh}{0.5\rho_w g h_f^2} = \left(-1.29 + 1.80 \frac{\gamma_f R_u}{R_c} + 0.93 \left(\frac{R_c - A_c}{h_f} \right) + 0.16 \sqrt{\frac{L_m}{B_a}} \right)^2$$

$$\left(-1.29 + 1.80 \frac{\gamma_f R_u}{R_c} + 0.93 \left(\frac{R_c - A_c}{h_f}\right) + 0.16 \sqrt{\frac{L_m}{B_a}}\right)^2 = 1.1149$$

$$0.5 \rho_w g h_f^2 = 736 \text{ kN/m}$$

$$Fh[\text{kN/m}] = 1.1149 \times 736 = 821$$

$$\frac{Fv(Fh)}{0.5 \rho_w g h_f B_e} = \left(-0.86 + 0.75 \frac{\gamma_f R_u}{R_c} + 0.41 \left(\frac{R_c - A_c}{h_f}\right) + 0.17 \sqrt{\frac{L_m}{B_a}} - 0.9 \frac{w_c}{h_f}\right)^2$$

$$\left(-0.86 + 0.75 \frac{\gamma_f R_u}{R_c} + 0.41 \left(\frac{R_c - A_c}{h_f}\right) + 0.17 \sqrt{\frac{L_m}{B_a}} - 0.9 \frac{w_c}{h_f}\right)^2 = 0.0976$$

$$0.5 \times \rho_w \times g \times h_f \times B_e = 487 \text{ kN/m}$$

$$Fv(Fh)[\text{kN/m}] = 0.0976 \times 487 = 47$$

Considering a crown wall with $h_f[\text{m}] = 12.1$, $B_a[\text{m}] = 3D_n = 3 \times 4.13 = 12.5$, and $B_e[\text{m}] = 8.0$ the other dimensions are estimated to guarantee that $SF(\text{sliding}) > 1.20$ (see Figure 7.2).

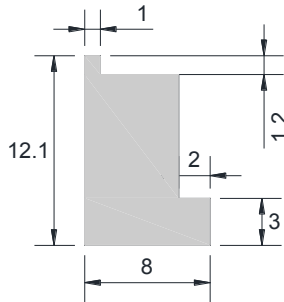


Figure 7.2 Cross section of the crown wall for a double-layer cube armored breakwater.

$$We [\text{kN/m}] = 9.81 \times 2.4 \times (12.1 \times 1 + 10.9 \times 5 + 3 \times 2) = 9.81 \times 174 = 1709$$

$$SF(\text{sliding}) = \mu [We - Fv(Fh)] / Fh = 0.6 [1709 - 47] / 821 = 1.21 > 1.20$$

$$M(Fh) = 0.55 h_f Fh = 0.55 \times 12.1 \times 821 = 5,462 \text{ mkN/m}$$

$$M(Fv(Fh)) = \frac{2}{3} (B_e) Fv(Fh) = \frac{2}{3} \times 8 \times 47 = 253 \text{ mkN/m}$$

$$M(We) - M(Fv(Fh)) = 9.81 \times 2.4 \times ((12.1 \times 7.5) + (54.5 \times 4.5) + (6 \times 1)) - 253 = 7,799 \text{ mkN/m}$$

According to ROM 0.5-05 (2008):

$$SF(\text{overturning}) = [M(We) - M(Fv(Fh))] / M(Fh) = 7,799 / 5,462 = 1.43 > 1.2$$

Figure 7.3 shows the cross section of a double-layer cube armored breakwater trunk with toe berm (dimensions in meters).

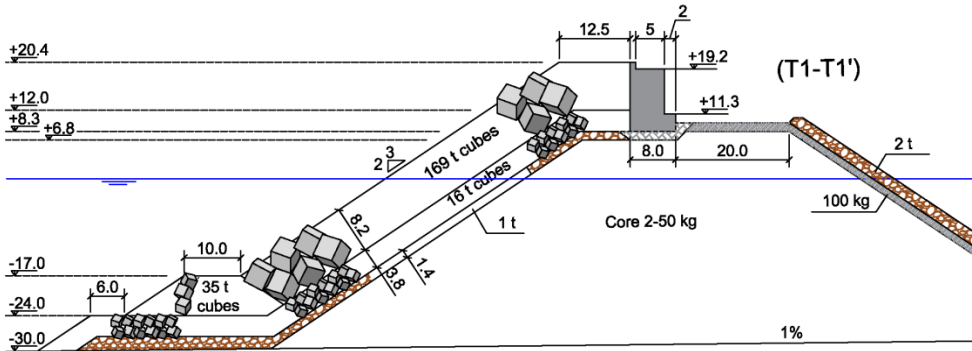


Figure 7.3 Cross section of a double-layer cube armored breakwater trunk with toe berm.

Although this alternative is stable, the lowest parts of the breakwater (toe berm and filters) require an excessive amount of concrete compared to the conventional cross section recommended by SPM (1975). On a rocky sea bottom, the alternative A without a toe berm illustrated in Figure 7.4 (dimensions in meters) is easier to build and requires less concrete.

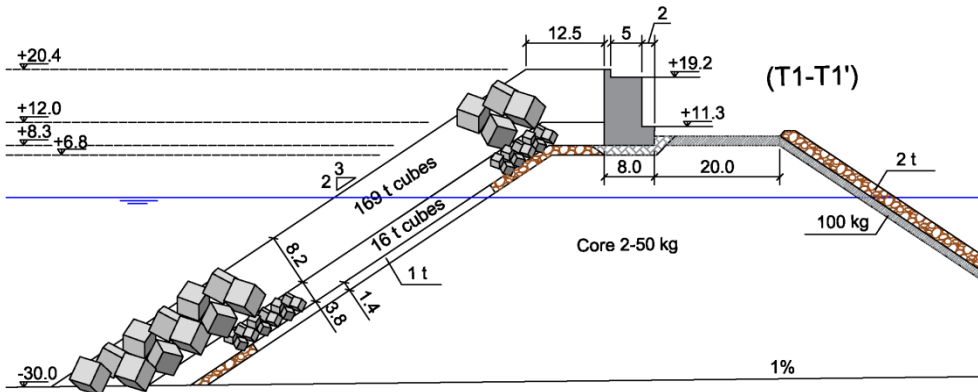


Figure 7.4 Cross section of a double-layer cube armored breakwater trunk without toe berm.

(B) The forces on the crown wall are greatest at HWL ($\Delta h[m]=4.5$). Equations 3.2 to 3.5 can be used to estimate the safety factors for crown wall sliding and overturning if $0.31 < \gamma_f(R_u/R_c) < 0.94$, $0.07 < (R_c - A_c)/h_f < 0.59$, $0.01 < w_c/h_f < 0.27$ and $3.1 < (L_m/B_a)^{0.5} < 6.5$.

Mass densities of concrete and sea water are $\rho_r[t/m^3]=2.400$ and $\rho_w[t/m^3]=1.025$, respectively.

$R_c[m]=A_c=19.1-4.5=14.6$, $\cot\alpha=1.5$, $\gamma_f=0.46$ for a single-layer Cubipod[®] armor, $H_s=11.0$, $w_c=9.2-4.5=4.7$, $h_f[m]=19.1-9.2=9.9$, $B_c[m]=8$, $B_a[m]=4D_n=4 \times 3.1 \approx 12.5$, and $g[m/s^2]=9.81$. The applicability limits are $0.31 < \gamma_f(R_u/R_c) = 0.89 < 0.94$, $(R_c - A_c)/h_f = 0$, $w_c/h_f = 0.47$ and $3.1 < (L_m/B_a)^{0.5} = 4.6 < 6.5$. In this case, not all variables fall within the range of applicability, but all variables are within or near the range of applicability; for preliminary designs, safety factor higher than those prescribed are used.

$$\frac{Fh}{0.5\rho_wgh_f^2} = \left(-1.29 + 1.80 \frac{\gamma_f R_u}{R_c} + 0.93 \left(\frac{R_c - A_c}{h_f} \right) + 0.16 \sqrt{\frac{L_m}{B_a}} \right)^2$$

$$\left(-1.29 + 1.80 \frac{\gamma_f R_u}{R_c} + 0.93 \left(\frac{R_c - A_c}{h_f} \right) + 0.16 \sqrt{\frac{L_m}{B_a}} \right)^2 = 1.121$$

$$0.5\rho_wgh_f^2 = 493[kN/m]$$

$$Fh[kN/m]=553$$

$$\frac{Fv(Fh)}{0.5\rho_wgh_fB_e} = \left(-0.86 + 0.75 \frac{\gamma_f R_u}{R_c} + 0.41 \left(\frac{R_c - A_c}{h_f} \right) + 0.17 \sqrt{\frac{L_m}{B_a}} - 0.9 \frac{w_c}{h_f} \right)^2$$

$$\left(-0.86 + 0.75 \frac{\gamma_f R_u}{R_c} + 0.41 \left(\frac{R_c - A_c}{h_f} \right) + 0.17 \sqrt{\frac{L_m}{B_a}} - 0.9 \frac{w_c}{h_f} \right)^2 = 0.029$$

$$0.5\rho_wgh_fB_e = 398[mkN/m]$$

$$Fv(Fh)[kN/m]=0.029 \times 398 = 11$$

Considering a crown wall with $h_f[m]=9.9$, $B_a[m]=4D_n=4 \times 3.1=12.5$, and $B_c[m]=8.0$ the other dimensions are estimated to ensure that $SF(\text{sliding}) > 1.20$ (see Figure 7.5).

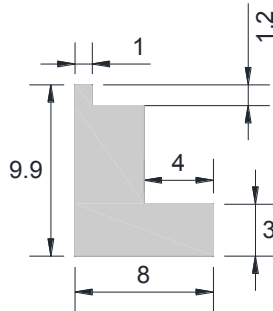


Figure 7.5 Cross section of the crown wall for a single-layer Cubipod[®] armored breakwater.

$$We \text{ [kN/m]} = 9.81 \times 2.4 \times (9.9 \times 1 + 8.7 \times 3 + 3 \times 4) = 9.81 \times 115.2 = 1130$$

$$SF(\text{sliding}) = \mu [We - F_v(F_h)] / F_h = 0.6 [1130 - 11] / 553 = 1.21 > 1.20$$

$$M(F_h) = 0.55 h_f F_h = 0.55 \times 9.9 \times 553 = 3,009 \text{ mkN/m}$$

$$M(F_v(F_h)) = \frac{2}{3} (B_e) F_v(F_h) = \frac{2}{3} \times 8 \times 11 = 61 \text{ mkN/m}$$

$$M(We) - M(F_v(F_h)) = 9.81 \times 2.4 \times ((9.9 \times 7.5) + (8.7 \times 3 \times 5.5) + (3 \times 4 \times 2)) - 61 = 5,632 \text{ mkN/m}$$

According to ROM 0.5-05 (2008):

$$SF(\text{overturning}) = [M(We) - M(F_v(F_h))] / M(F_h) = 5,632 / 3,009 = 1.87 > 1.2$$

Figure 7.6 illustrates Alternative B (cross section of a single-layer Cubipod[®] armored breakwater trunk).

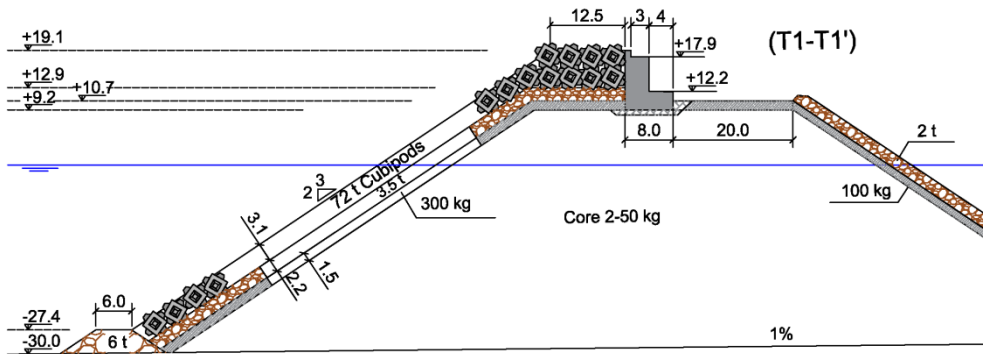


Figure 7.6 Cross section of a single-layer Cubipod[®] armored breakwater trunk.

(C) The forces on the crown wall are greatest at HWL ($\Delta h[m]=4.5$). Equations 3.2 to 3.5 can be used to estimate the safety factors for crown wall sliding and overturning if $0.31 < \gamma_f(R_u/R_c) < 0.94$, $0.07 < (R_c - A_c)/h_f < 0.59$, $0.01 < w_c/h_f < 0.27$ and $3.1 < (L_m/B_a)^{0.5} < 6.5$. Mass densities of concrete and sea water are $\rho_c[t/m^3]=2.400$ and $\rho_w[t/m^3]=1.025$, respectively.

$R_c[m]=A_c=18.5-4.5=14.0$, $\cot\alpha=1.5$, $\gamma_f=0.44$ for a double-layer Cubipod[®] armor, $H_s=11.0$, $w_c=10.2-4.5=5.7$, $h_f[m]=18.5-10.2=8.3$, $B_e[m]=8$, $B_a[m]=5 \times 2.4 \approx 12.5$, and $g[m/s^2]=9.81$. The applicability limits are $0.31 < \gamma_f(R_u/R_c)=0.93 < 0.94$, $(R_c - A_c)/h_f = 0$, $w_c/h_f = 0.69$ and $3.1 < (L_m/B_a)^{0.5} = 4.6 < 6.5$. In this case, not all variables fall within the range of applicability, but all variables are within or near the range of applicability; for preliminary designs, safety factors higher than those prescribed are used.

$$\frac{Fh}{0.5\rho_wgh_f^2} = \left(-1.29 + 1.80 \frac{\gamma_f R_u}{R_c} + 0.93 \left(\frac{R_c - A_c}{h_f} \right) + 0.16 \sqrt{\frac{L_m}{B_a}} \right)^2$$

$$\left(-1.29 + 1.80 \frac{\gamma_f R_u}{R_c} + 0.93 \left(\frac{R_c - A_c}{h_f} \right) + 0.16 \sqrt{\frac{L_m}{B_a}} \right)^2 = 1.272$$

$$0.5\rho_wgh_f^2 = 346 [kN/m]$$

$$Fh [kN/m] = 1.272 \times 346 = 441$$

$$\frac{Fv(Fh)}{0.5\rho_wgh_fB_e} = \left(-0.86 + 0.75 \frac{\gamma_f R_u}{R_c} + 0.41 \left(\frac{R_c - A_c}{h_f} \right) + 0.17 \sqrt{\frac{L_m}{B_a}} - 0.9 \frac{w_c}{h_f} \right)^2$$

$$\left(-0.86 + 0.75 \frac{\gamma_f R_u}{R_c} + 0.41 \left(\frac{R_c - A_c}{h_f} \right) + 0.17 \sqrt{\frac{L_m}{B_a}} - 0.9 \frac{w_c}{h_f} \right)^2 = 0.00005$$

$$0.5\rho_wgh_fB_e = 334 [mkN/m]$$

$$Fv(Fh) [kN/m] = 0.00005 \times 334 = 0.02$$

Considering a crown wall with $h_f [m] = 8.3$, $B_a [m] = 5D_n = 5 \times 2.4 \approx 12.5$ and $B_e [m] = 8.0$ the other dimensions are estimated to guarantee that $SF(\text{sliding}) > 1.20$ (see Figure 7.7).

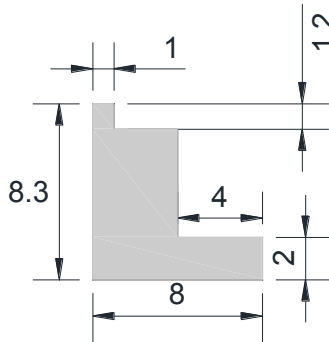


Figure 7.7 Cross section of a crown wall for a double-layer Cubipod[®] armored breakwater.

$$W_e [kN/m] = 9.81 \times 2.4 \times (8.3 \times 1 + 7.1 \times 3 + 2 \times 4) = 9.81 \times 90.2 = 885$$

$$SF(\text{sliding}) = \mu [W_e - Fv(Fh)] / Fh = 0.6 [885 - 0.02] / 441 = 1.21 > 1.20$$

$$M(Fh) = 0.55h_f Fh = 0.55 \times 8.3 \times 441 = 2,012 mkN/m$$

$$M(F_v(F_h)) = \frac{2}{3}(B_c)F_v(F_h) = \frac{2}{3} \times 8 \times 0.02 = 0.1 \text{ mkN/m}$$

$$M(We)-M(F_v(F_h)) = 9.81 \times 2.4 \times ((8.3 \times 7.5) + (21.3 \times 5.5) + (8 \times 2)) - 0.1 = 4,600 \text{ mkN/m}$$

According to ROM 0.5-05 (2008):

$$SF(\text{overturning}) = [M(We)-M(F_v(F_h))]/M(F_h) = 4,600/2,012 = 2.29 > 1.2$$

Figure 7.8 illustrates Alternative C (cross section of a double-layer Cubipod[®] armored breakwater trunk).

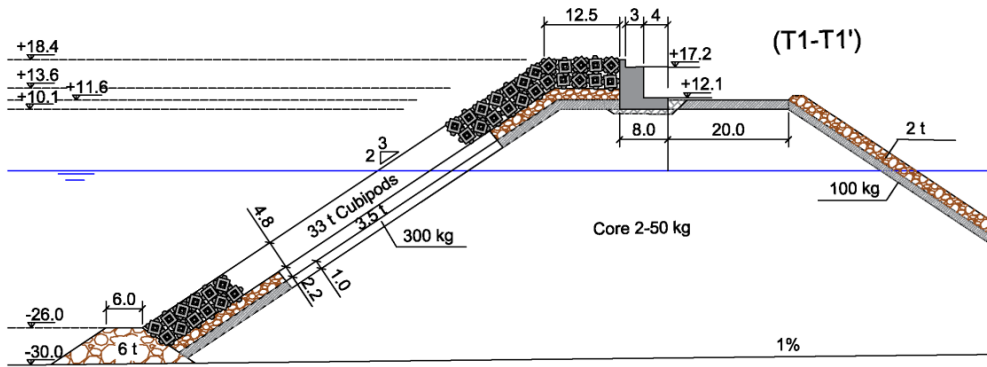


Figure 7.8 Cross section of a double-layer Cubipod[®] armored breakwater trunk.

7.9. Estimated construction costs and optimum alternative

Once the cross sections of the main trunk for the three alternative solutions (A, B and C) are defined, it is convenient to estimate construction costs. The three alternatives are feasible, but one or two alternatives may be disregarded for economic reasons.

In order to describe the 3.5-km long breakwater of this example, several cross sections are given for different water depths. Water depth and design storm will change along the breakwater with the size of the armor units, filters, crown wall, etc. Nevertheless, for cost-comparison purposes, it may be assumed that the breakwater cost (root, change of alignment, main trunk and roundhead) may be roughly approximated to 80% of breakwater length with the cross section of the main trunk. In this case, 80% \times 3,500=2,800 meters.

Volume of materials required for Alternative A (Figure 7.4):

In this example, cube armor porosity at prototype scale is assumed to be $p=0.41$, as recommended by SPM (1984). However, the stability coefficient $K_D=6.0$ and safety factors given in Table 2.3 were obtained from 2-D small scale model tests with armor

porosity $p=0.37$, and higher armor porosity leads to lower hydraulic stability (see Medina et al., 2014). If armor porosity is $p=0.41 > 0.37$, concrete consumption (directly proportional to $\Phi=2[1-p]$) is reduced by $6.3\%=1-([1-0.41]/[1-0.37])$ and the stability number (directly proportional to $\Phi^{1.2}=[2(1-p)]^{1.2}$) of the armor layer is reduced by $7.6\%=1-([1-0.41]/[1-0.37])^{1.2}$. Safety factors to IDa and IDe given in Table 7.1 will be lower at prototype scale if armor porosity increases.

Concrete for 169-tonne cubes ($n_c=2$ and $p=0.41 \rightarrow \Phi=n_c(1-p)=1.18 < 1.26$):

$$f_{ctk}[\text{MPa}]=2.1(D_n/4.00)=2.1(4.13/4.00)=2.2; f_{ck}[\text{MPa}]=(f_{ctk}(D_n)/0.21)^{3/2}=34$$

$$\text{Volume: } V=n_c(1-p)D_nA=1.18 \times 4.13 \times 2,800 \times (12.5 + [16.2 + 30.0] \times [1 + 1.5^2]^{0.5}) = 1,306,905 \text{ m}^3 \text{ (18,560 units, each weighing 169-tonne)}$$

Concrete for 16-tonne cubes ($\Phi=1.18 < 1.26$):

$$f_{ctk}=1.5 \text{ MPa}; f_{ck}=20 \text{ MPa}$$

$$\text{Volume: } V=n_c(1-p)D_nA=1.18 \times 1.88 \times 2,800 \times (10 + [10.1 + 30.0] \times [1 + 1.5^2]^{0.5}) = 511,717 \text{ m}^3 \text{ (76,758 16-tonne units)}$$

Concrete for crown wall:

$$f_{ck}=20 \text{ MPa}$$

$$\text{Volume: } 2,800 \times (12.1 \times 1 + 10.9 \times 5 + 3 \times 2) = 203,280 \text{ m}^3$$

Quarry stones (lee-side armor, filters and core):

$$\text{Volume: } (1-0.36) \times 2,800 \times (8.3 + 30.0) \times ([10 + 8 + 20] + [8.3 + 30.0] \times [1 + 1.5^2]^{0.5}) = 7,346,973 \text{ m}^3$$

$$\text{Weight: } 2.7 \times 7,346,973 = 19,836,828 \text{ t} = 19.84 \times 10^6 \text{ t}$$

Construction costs for Alternative A (Figure 7.4):

Using Equations 1.1 to 1.4

$$V_B[\text{m}^3]=1,306,905+511,717=1,818,622$$

$$W_B[\text{t}]=(169 \times 1,306,905) + (16 \times 511,717) / 1,818,622 = 125.9$$

$$\text{HOR}[\text{€}/\text{m}^3]=([65 \times 1,306,905] + [60 \times 511,717]) / 1,818,622 = 63.6$$

$$\ln(1,818,622 \times 123.1) = 19.25$$

$$C_B \left[\frac{\text{€}}{\text{m}^3} \right] = (205 + 63.6) + 0.75 \left[10^5 \left(\frac{1}{(19.25)} \right)^2 - 10^4 \left(\frac{1}{(19.25)} \right) \right] = 81.4$$

Total cost for Alternative A (armor and crown wall):

$$1,818,622 \times 81.4 + 203,280 \times 60 = 160.2 \text{ M€}$$

Assuming a unit cost of 8 €/tonne for quarry materials (lee-side armor, filters and core), the estimated total cost is:

$$\text{Cost(A)}=160.2+(8 \times 19.8)=160.2+158.7=319 \text{ M€}$$

Volume of materials required for Alternative B (Figure 7.6):

Concrete for a 72-tonne single-layer Cubipod[®] armor ($n_c=1$ and $p=0.41 \rightarrow \Phi=0.59$):

$$f_{ctk}[\text{MPa}]=2.1(D_n/4.00)=2.1(3.1/4.00)=1.63 \text{ MPa}; f_{ck}[\text{MPa}]=(f_{ctk}(D_n)/0.21)^{3/2}=22$$

$$\text{Volume: } 0.59 \times 2,800 \times 3.1 \times (12.5+1.25+[14.5+27.4] \times [1+1.5^2]^{0.5})=511.2 \cdot 10^3 \text{ m}^3 \text{ (17,000 units)}$$

Concrete for crown wall:

$$f_{ck}=20 \text{ MPa}$$

$$\text{Volume: } 2,800 \times (9.9 \times 1 + 8.7 \times 3 + 3 \times 4) = 134.4 \cdot 10^3 \text{ m}^3$$

Quarry stones (lee-side armor, filters and core):

$$\text{Volume: } (1-0.36) \times 2,800 \times [(12.9+30) \times (16+8+20) + [12.9+30] \times [1+1.5^2]^{0.5}) = 9,328,160 \text{ m}^3$$

$$\text{Weight: } 2.7 \times 9,328,160 = 25,2 \cdot 10^6 \text{ t}$$

Toe berm rock:

$$\text{Weight: } 2.7 \times (1-0.38) \times 2,800 \times (11 \times 2.6) = 134 \cdot 10^3 \text{ t}$$

Construction costs for Alternative B (Figure 7.6):

Using Equations 1.1 to 1.4

$$V_C[\text{m}^3]=511,200 \quad W_C[\text{t}]=72 \quad \text{HOR}[\text{€/m}^3]=61 \quad \ln(511,200 \times 72)=17.43$$

$$C_C \left[\frac{\text{€}}{\text{m}^3} \right] = (265 + 61) + 1.00 \left[10^5 \left(\frac{1}{17.43} \right)^2 - 10^4 \left(\frac{1}{17.43} \right) \right] = 82.6$$

Total cost for Alternative B (armor and crown wall):

$$511,200 \times 82.6 + 134,400 \times 60 = 50.6 \text{ M€}$$

Assuming a unit cost of 12 €/tonne for toe berm rocks and 8 €/tonne for other quarry materials (lee-side armor, filters and core), the estimated total cost is:

$$\text{Cost(B)}=50.6+(12 \times 0.134)+(8 \times 25.2)=253.7 \text{ M€}.$$

Volume of materials required for Alternative C (Figure 7.8):

Concrete for 33-tonne single-layer Cubipod® armor ($n_c=2$ and $p=0.415 \rightarrow \Phi=1.17$):

$f_{ck}=20$ MPa

Volume: $1.17 \times 2,800 \times 2.4 \times (12.5 + [16.0 + 27.5] \times [1 + 1.5^2]^{0.5}) = 713.6 \cdot 10^3 \text{ m}^3$ (51,900 units)

Concrete for crown wall:

$f_{ck}=20$ MPa

Volume: $2,800 \times (8.3 \times 1 + 7.1 \times 3 + 2 \times 4) = 105.3 \cdot 10^3 \text{ m}^3$

Quarry stones (lee-side armor, filters and core):

Volume: $(1 - 0.36) \times 2,800 \times [(13.6 + 30) \times (10 + 8 + 20) + [13.6 + 30] \times [1 + 1.5^2]^{0.5}] = 9,110,177 \text{ m}^3$

Weight: $2.7 \times 9,110,177 = 24,6 \cdot 10^6 \text{ t}$

Toe berm rock:

Weight: $2.7 \times (1 - 0.38) \times 2,800 \times (12 \times 4.0) = 225 \cdot 10^3 \text{ t}$

Construction costs for Alternative C (Figure 7.8):

Using Equations 1.1 to 1.4

$V_c[\text{m}^3]=713,600$ $W_c[\text{t}]=33$ $\text{HOR}[\text{€}/\text{m}^3]=60$ $\ln(713,600 \times 33)=16.97$

$$C_c \left[\frac{\text{€}}{\text{m}^3} \right] = (265 + 60) + 1.00 \left[10^5 \left(\frac{1}{16.97} \right)^2 - 10^4 \left(\frac{1}{16.97} \right) \right] = 83.5$$

Total cost for Alternative C (armor and crown wall):

$713,600 \times 83.5 + 105,300 \times 60 = 65.9 \text{ M€}$

Assuming a unit cost of 12 €/tonne for toe berm rocks and 8 €/tonne for other quarry materials (lee-side armor, filters and core), the estimated total cost is:

$\text{Cost}(C) = 65.9 + (12 \times 0.225) + (8 \times 24.6) = 265.3 \text{ M€}$

The most influential characteristics affecting logistics and construction cost are summarized in Table 7.2. Alternative A (double-layer cube armored breakwater) should be disregarded because it involves the highest construction cost, the highest energy and carbon footprint (more than 3.5-fold the amount of concrete consumed in Alternative B), the highest number of units to be placed (more than 5.5-fold the number of concrete units needed for Alternative B), and the largest unit to be placed (more than double that in Alternative B). Additionally, the core crest (working platform during construction) is the lowest ($w_c[\text{m}]=3.8$).

Table 7.2 Cost and logistic characteristics of alternatives A, B and C.

Alternative	Figure	Cost [M€]	Concrete [Mm ³]	#units [x10 ³]	Wmax [t]	w _c [m]
A	7.4	319	1.819	95.3	169	3.8
B	7.6	254	0.516	17.2	72	4.7
C	7.8	265	0.714	51.9	33	5.7

Compared to Alternative B, Alternative C (the double-layer Cubipod[®] armored breakwater) has a higher core crest ($w_c[m]=5.7>4.7$) and requires a smaller crawler crane to place the Cubipods ($W[t]=33<72$); however, the construction cost is higher (4%), the concrete consumption is higher (38%) and the number of units to be placed on the breakwater is three times higher. Alternative B (the single-layer Cubipod[®] armored breakwater) is the best alternative because it has the lowest costs, the lowest environmental impact (lower energy and carbon footprint) and the least restrictive logistic conditions (40% smaller block yard and about half the armor unit placement time).

Optimum alternative: B - Figure 7.6 (single-layer Cubipod[®] armored breakwater).

7.10. Roundhead design

Once the optimum alternative for the main trunk has been selected, the corresponding roundhead will be designed. Sections 2.4 and 2.5 characterize the hydraulic stability for single- and double-layer Cubipod[®] roundheads. Two alternatives for the roundhead are considered: B1 (single-layer Cubipod[®] armored roundhead) and B2 (double-layer Cubipod[®] armored roundhead). If the roundhead slope $\cot\alpha = 1.5$, Equation 2.2, Table 2.4 and Figure 2.8 can be used to estimate the weight of the Cubipods on the roundhead, considering the global safety factors given in Table 7.1.

Table 2.4 Safety factors for double-layer cube and Cubipod[®] armors in trunk and roundhead.

Design K_D and global safety factors					Initiation of Damage (IDa)		Initiation of Destruction (IDe)	
Part	Unit	K_D	# layers	slope	SF(IDa5%)	SF(IDa50%)	SF(IDE5%)	SF(IDE50%)
Trunk	Cube	6.0	2	3/2	0.67	0.86	1.05	1.35
	Cubipod [®]	28.0	2	3/2	0.82	0.99	1.09	1.40
Round-head	Cube	5.0	2	3/2	0.88	1.13	1.17	1.40
	Cubipod [®]	7.0	2	3/2	0.99	1.18	1.19	1.36

Table 7.1 Safety factors for single- and double-layer trunk and roundhead Cubipod® armors.

Global safety factors		IDa	IDe
Part	# layers	SF(IDa50%)	SF(IDe5%)
Trunk	double-layer	0.90	1.10
	single-layer	1.20	1.30
Roundhead	double-layer	1.10	1.25
	single-layer	1.15	1.30

Considering the design storms at water depth $h_s[m]=30$:

Initiation of Damage (IDa, $T_R[\text{year}]=100$): $H_s[m]=9.5$ and $T_p[s]=18$

Initiation of Destruction (IDe, $T_R[\text{year}]=1000$): $H_s[m]=11.0$ and $T_p[s]=19$

For the preliminary design of double-layer Cubipod® armored roundheads, Equation 2.2 with $K_D=7.0$ can be used:

$$N_{sd}(B2) = \frac{H_{sd}}{\Delta D_n} = (K_D \cot \alpha)^{1/3} = (7.0 \times 1.5)^{1/3} = 2.19$$

Initiation of Damage (IDa):

$$(B2): \quad H_{sd}[m] = 2.19(\Delta D_n) = 2.19 \times \left(\frac{2.400}{1.025} - 1 \right) \times D_n = 2.19 \times 1.34 \times D_n = 9.5$$

$$D_n(B2_IDa) = \frac{9.5}{2.93} \times \frac{1.10}{1.18} = 3.02m$$

Initiation of Destruction (IDe):

$$(B2): \quad H_{sd}[m] = 2.19(\Delta D_n) = 2.19 \times \left(\frac{2.400}{1.025} - 1 \right) \times D_n = 2.93 \times D_n = 11.0$$

$$D_n(B2_IDe) = \frac{11.0}{2.93} \times \frac{1.25}{1.19} = 3.94m > 3.02m$$

$$W[t] = 2.400 \times (3.94)^3 = 147$$

$$SF(B2_IDa50\%) = 1.10 \times \frac{3.94}{3.02} = 1.44$$

(B2) A double-layer 147-tonne Cubipod[®] armor in the roundhead has SF(IDE5%)=1.25 and SF(IDa50%)=1.44, in agreement with the minimum safety factors indicated in Table 7.1.

Figure 7.9 illustrates Alternative B2 (cross section of the double-layer Cubipod[®] armored roundhead). A double-layer 147-tonne Cubipod[®] armor requires a 10-tonne ($W_0/10 > W_1 > W_0/20$) single-layer Cubipod[®] filter on double-layer rock filters.

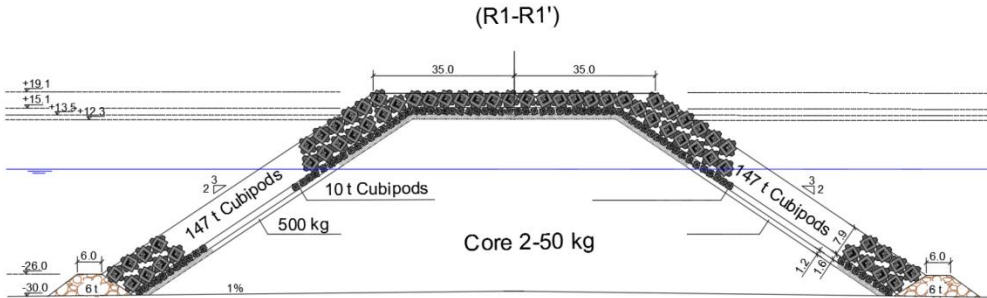


Figure 7.9 Cross section of double-layer Cubipod[®] armored roundhead (Alternative B2).

For the preliminary design of single-layer Cubipod[®] armored roundheads, Equation 2.2 with $K_D=5.0$ can be used

$$N_{sd}(B1) = \frac{H_{sd}}{\Delta D_n} = (K_D \cot \alpha)^{1/3} = (5.0 \times 1.5)^{1/3} = 1.96$$

$$s_{op}(IDa) = H_{m0}/L_{op}(IDa) = 9.5/(g18^2/2\pi) = 0.019 \quad s_{op}(IDE) = 11/(g19^2/2\pi) = 0.020$$

The values for $s_{op} \approx 0.020$ in Figure 2.8 correspond to

$$SF(IDE5\%) \approx 2.4/1.96 = 1.22 \text{ and}$$

$$SF(IDa50\%) > SF(IDE50\%) \approx 2.7/1.96 = 1.38$$

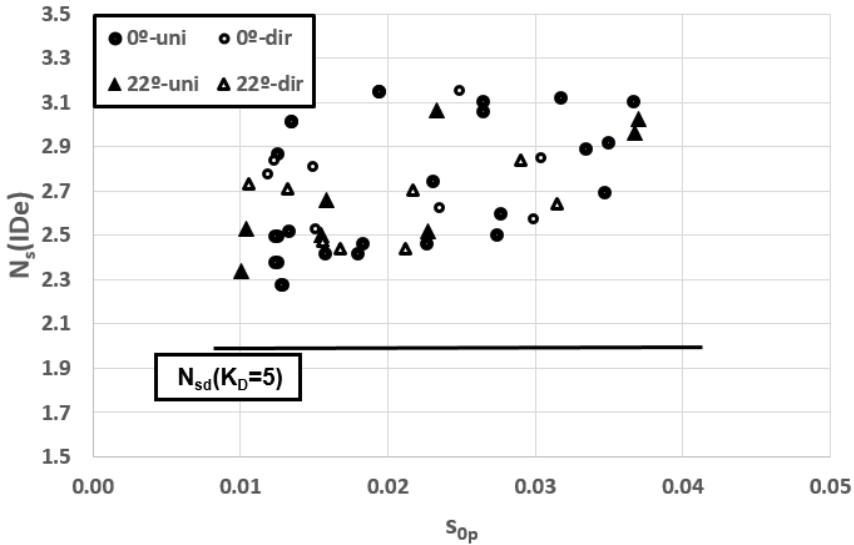


Figure 2.8 Stability numbers to IDE for single-layer Cubipod® armored roundheads.

Initiation of Damage (IDa):

$$(B1): H_{sd}[m] = 1.96(\Delta D_n) = 1.96 \times \left(\frac{2.400}{1.025} - 1 \right) \times D_n = 1.96 \times 1.34 \times D_n = 9.5$$

$$D_n(B1_IDa) < \frac{9.5}{2.63} \times \frac{1.15}{1.38} = 3.01m$$

Initiation of Destruction (IDe):

$$(B1): H_{sd}[m] = 1.96(\Delta D_n) = 1.96 \times \left(\frac{2.400}{1.025} - 1 \right) \times D_n = 2.63 \times D_n = 11.0$$

$$D_n(B1_IDe) = \frac{11.0}{2.63} \times \frac{1.30}{1.22} = 4.46m > 3.01m$$

$$W[t] = 2.400 \times (4.46)^3 = 213$$

$$SF(B1_IDa50\%) > 1.15 \times \frac{4.46}{3.01} = 1.70$$

(B1) A single-layer 213-tonne Cubipod® armor in the roundhead has SF(IDE5%)=1.30 and SF(IDa50%)>1.70, in agreement with the minimum safety factors indicated in Table 7.1.

The armor unit size can be reduced if high density concrete is used; however, high density aggregates are usually very expensive. Heavy units require adequate equipment

for placement; crawler cranes similar to a LIEBHERR LR 11350 (maximum load 1,350 t at radius 12.0 m and maximum load torque 22,000 tm) can place 213-tonne (emerged units) at 80 meters (approx. 18,000 tm < 22,000 tm) and 135-tonne (submerged units) at 120 meters (approx. 16,000 tm < 22,000 tm). Figure 7.10 shows Alternative B1 (cross section of the double-layer Cubipod[®] armored roundhead). A single-layer 217-tonne Cubipod[®] armor requires a 15-tonne ($W_0/10 > W_1 > W_0/20$) single-layer Cubipod[®] filter on double-layer rock filters.

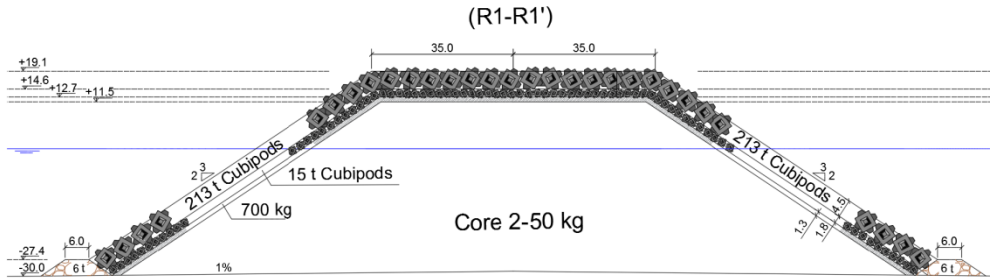


Figure 7.10 Cross section of single-layer Cubipod[®] armored roundhead (Alternative B1).

Figure 7.11 shows the plan view of the transitions and roundhead corresponding to Alternative B1. Armor thickness changes in the breakwater and transitions are required (see Section 6.5).

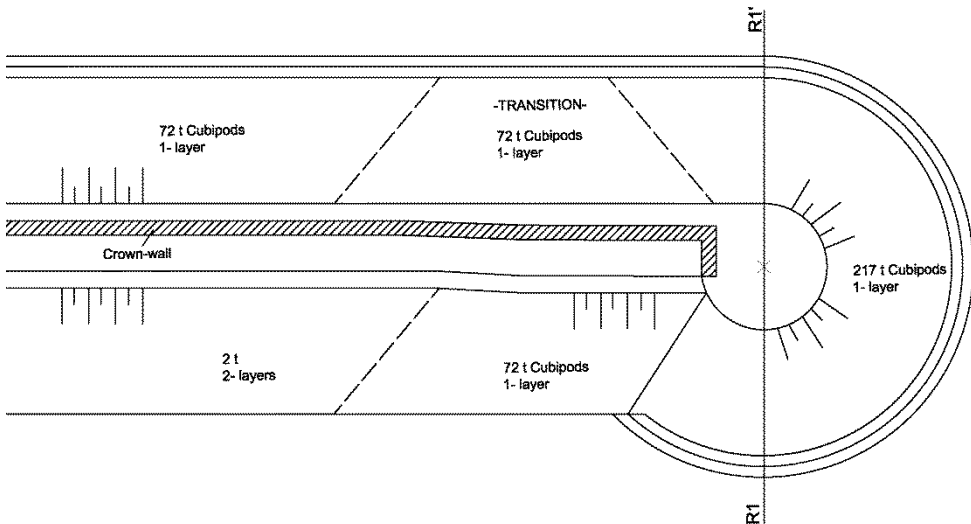


Figure 7.11 Plan view of the transitions for a single-layer Cubipod[®] armored roundhead.

Alternatives B2 (Figure 7.9) and B1 (Figure 7.10) can be compared from the economic and logistic points of view.

Volume of concrete for Alternative B2 (Figure 7.9):

Concrete for 147-tonne double-layer Cubipod[®] armor ($\Phi=1.17$):

$$f_{ck}=31 \text{ MPa (HOR[€/m}^3]=63$$

Considering $\frac{3}{4}$ of the lateral area and the smaller base area of a truncated cone:

$$\text{Volume B2: } [1.17/2] \times [(2 \times 4.0 + 1.6) \times (3/4) \pi (99 + 35) \times 77] + [\pi \times 35^2 \times (4.0 + 1.6)] = 147,268 \text{ m}^3 \approx 150 \cdot 10^3 \text{ m}^3$$

$$\text{Total cost for Alternative B2: } 63 \times 150 \cdot 10^3 \approx 9.45 \text{ M€}$$

Volume of concrete for Alternative B1 (Figure 7.10):

Concrete for 213-tonne double-layer Cubipod[®] armor ($\Phi=0.59$):

$$f_{ck}=(45/4.0)^{3/2}=38 \text{ MPa (HOR[€/m}^3]=66$$

$$\text{Volume B2: } [0.59] \times [(4.5 + 1.9) \times (3/4) \pi (99 + 35) \times 77] + [\pi \times 35^2 \times (4.5 + 1.9)] = 106,340 \text{ m}^3 \approx 110 \cdot 10^3 \text{ m}^3$$

$$\text{Total cost for Alternative B1: } 66 \times 110 \cdot 10^3 \approx 7.26 \text{ M€}$$

Alternative B2 has a higher cost (30%) and concrete consumption as well as a larger number of units to be placed (80%); nevertheless, unit size is smaller (easy control of internal temperatures due to heat generation during concrete curing) and a slightly smaller crawler crane (if available) could be used.

7.11. Cubipod[®] armor design in breaking conditions

The water depth of the toe of the main trunk and roundhead at LWL is $h_s[m]=30$ (non-breaking conditions); however, most of the root of the breakwater ($0 < h_s[m] < 30$) is in depth-limited wave breaking conditions, and the hydraulic stability is qualitatively different than that described in Section 7.4. When maximum wave height attacking the structure is limited by water depth (see Section 2.6), Equations 2.3 to 2.5 can be used for a preliminary design of the armor layer. For instance, the cross section of the breakwater trunk at $h_s[m]=10$ (LWL) can be defined as follows:

$$\text{Maximum water depth at HWL: } h_s[m]=10+4.5=14.5$$

$$B \text{ (Equation 2.5): } D_n > h/6.2\Delta = h_s(1+3 \tan\beta)/(6.2\Delta)=14.5 \times (1+0.12)/(6.2 \times 1.34)=1.95 \text{ m}$$

$$D_n(B_IDe)=1.95 \times \frac{1.30}{1.30}=1.95$$

$$W[t]=2.400 \times (1.95)^3 = 18$$

A single-layer 18-tonne Cubipod® armor in the trunk at $h_s[m]=10$ (LWL) has a $SF(IDE5\%)>1.30$ because oblique wave attack is less damaging than perpendicular wave attack, in agreement with the minimum safety factors listed in Table 7.1.

Filter layer: $W_1[t]=2.0$, $D_{n50}[m]=(2.0/2.7)^{1/3}=0.74$

Overtopping at the root of the breakwater is significantly lower than that estimated for the main trunk (see Section 7.5). For practical purposes, EurOtop (2007) recommended using an obliquity factor, $\gamma_\beta=1-0.0033|\theta[^\circ]|$, to take into account the reduction in overtopping rates when waves attack the breakwater with an obliquity angle $\theta[^\circ]\neq 0$. The breakwater root forms a 70° angle with the main trunk, and waves attack the structure ($h_s[m]=10$ at LWL) with an angle $\theta\approx 70^\circ-9^\circ=61^\circ$; thus, $\gamma_\beta=1-0.0033|\theta[^\circ]|\approx 1-0.0033\times(61)=0.80$. Therefore, crest freeboard can be lowered significantly along the root of the breakwater.

The depth-limited significant wave heights at $h_s[m]=14.5$ (HWL) can be estimated according to the simplified method proposed by CIRIA, CUR, CETMEF (2007):

$T_R[\text{year}]=100$ (crest design): $H_{m0}[m]\approx 9.5$, $T_p[s]=18$, $s_{0p}=H_{m0}/L_{0p}=0.019$.

$h/L_{0p}=14.5/(9.8\times 18^2/2\pi)=0.029$ and $\tan\beta=0.04$ ($h_s[m]=10.0$ at LWL)

$H_s/h\approx 0.65$ corresponds to $s_{0p}=0.019$, $h/L_{0p}=0.029$ and $\tan\beta=0.04$

$H_s[m]\approx 0.65\times 14.5=9.4$

Waves are approximately Rayleigh-distributed in non-breaking conditions (main trunk) and truncated or composited Rayleigh-distributed in depth-limited wave breaking condition (see Battjes and Groenendijk, 2000). Therefore, the use of significant wave heights estimated for depth-limited wave breaking conditions in overtopping predictors (valid for non-breaking conditions) such as Equation 3.1 will provide conservative estimations for wave overtopping.

Crest freeboard (Alternative B-main trunk) at HWL:

$R_c[m]=19.1-4.5=14.6$.

Crest freeboard (Alternative B-root) at HWL and $h_s[m]=10$:

$R_c[m]=14.6\times 0.8=11.7\approx 12.0$

Crest elevation is lowered 2.6 meters. $A_c[m]=R_c[m]=16.5-4.5=12.0$, $\gamma_\beta=0.80$, $A_c/R_c=1$, $Ir_p=(2/3)/(2\pi\times 9.4/[9.8\times 18^2])^{1/2}=4.8$, $R_c/H_{m0}=12.0/9.4=1.28$ and $\gamma_f=0.46$.

$$Q = \frac{q}{\sqrt{gH_{m0}^3}} = 0.2 \exp\left(0.53 Ir_p - 3.27 \frac{A_c}{R_c} - \frac{2.16}{\gamma_f} \frac{R_c}{H_{m0}}\right) \quad 3.1$$

$$Q = \frac{q}{\sqrt{gH_{m0}^3}} = 0.2 \exp\left(0.53 \times 4.8 - 3.27 \frac{12.0}{12.0} - \frac{1}{0.80} \frac{2.16}{0.46} \frac{12.0}{9.4}\right) = 0.55 \times 10^{-4}$$

$$q[m^3/s/m] = (9.8\times 9.4^3)^{0.5} Q = 90.2 \quad Q = 90.2 \times 0.55 \times 10^{-4} = 49.6 \times 10^{-4} \rightarrow 5.0 \text{ l/s/m} < 7 \text{ l/s/m}$$

Equation 6.1 is not strictly applicable (oblique waves and depth-limited breaking conditions) for toe berm designs; nevertheless, using 6-tonne rocks for the toe berm (2% volume in quarry), the nominal diameter according to Equation 6.1 would be:

$$D_{n50}[m] = \left(\frac{6.0}{2.700} \right)^{1/3} = 1.30$$

$$\frac{H_s}{\Delta D_{n50}} = \frac{9.4}{1.63 \times 1.30} = 4.4 \approx \left(2 + 6.2 \left(\frac{h_t}{h_s} \right)^{2.7} \right) N_{od}^{0.15} = \left(2 + 6.2 \left(\frac{7.4}{10.0} \right)^{2.7} \right) 0.5^{0.15} = 4.3$$

Oblique waves and depth-limited breaking conditions significantly increase the uncertainty of the hydraulic stability estimation for the toe berm, but a preliminary design can be considered validated with the corresponding small-scale physical tests. Figure 7.12 shows the cross section of the trunk at $h_s[m]=10$ (LWL).

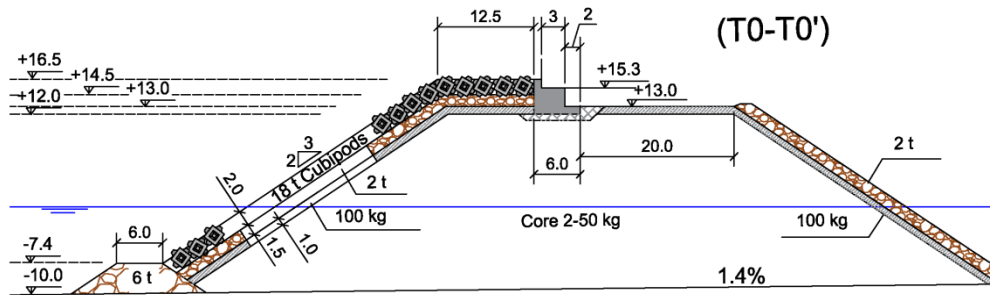


Figure 7.12 Cross section of single-layer Cubipod[®] armored trunk at $h_s[m]=10$ (LWL).

7.12. Small-scale tests for validation and design optimization

The preliminary design described above should be validated and optimized with the corresponding small-scale physical tests. Preliminary designs using *Cubipod[®] Manual 2016* are mostly based on standard non-breaking, non-overtopping tests without wave obliquity. The root of the breakwater (oblique waves in depth-limited breaking conditions), curved trunk (specific radius) and roundhead (specific geometry) may behave differently than expected. The preliminary design must be validated and optimized to reduce construction costs and provide a reliable final design. Furthermore, different phases of the breakwater construction can be tested to reduce the risk of failure during construction.

In this case, 3D physical tests are highly recommended to validate and optimize: (1) breakwater root, (2) curved trunk, (3) main trunk and (4) roundhead. Hydraulic stability of toe berm and armor, pressure on crown wall and overtopping rates can be measured with one or several small-scale models, depending on the facilities available. The breakwater covers an area of approximately 1.5 km x 2.5 km; with a typical 1/50 scale,

it would be necessary to use a very large wave basin (larger than 40.0x60.0x1.5 meters with a 60m-long wavemaker) to test a single model. If the breakwater is very large, as in this case, it is usually more efficient to test different parts of the breakwater in smaller facilities.

Reducing the scale, the size of the model and the facility can also be reduced; however, in order to avoid significant scale effects in armor hydraulic stability, small-scale armor units must be larger than $D_n[\text{cm}]=3.0$ (see Frostick et al., 2011).

The following armoring along the breakwater is assumed: (1a) double-layer 6-tonne rocks, (1b) single-layer 18-tonne Cubipods, (1c) single-layer 40-tonne Cubipods, (2) single-layer 72-tonne Cubipods in curved trunk, (3) single-layer 72-tonne Cubipods in main trunk, and (4) single-layer 213-tonne Cubipods in roundhead. The smaller armor units are the rocks used at the root of the breakwater (1a) with $D_{n50}[\text{m}]=1.30$. The smaller scale is 1/45 for the root of the breakwater. 18-tonne Cubipods (1b) with $D_n[\text{m}]=1.95$ require a scale higher than 1/65, while the minimum scale for the curved and main trunk ($W[t]=72$ and $D_n[\text{m}]=3.10$) is 1/100.

If a wave basin with dimensions 40.0x30.0x1.5 meters (30 m-long wavemaker) is available, the breakwater root and curved trunk (Model 1) can be modelled at a 1/50 scale (Froude's similarity). The main trunk and roundhead (Model 2) may also be modelled at a 1/50 scale in the same facility. The number of models and scales should be adapted to the characteristics of the available test facilities.

The wave characteristics must be determined once the models and scale are selected; for instance, two models at 1/50 scale: (1) root and curved trunk, and (2) main trunk and roundhead. In this case, three design storms at the toe of the main trunk and roundhead are prescribed for armor hydraulic stability and overtopping ($T_R[\text{year}]=2, 100$ and 1000) with $H_s[\text{m}]=7.0, 9.5$ and 11.0 , and $T_p[\text{s}]=16, 18$ and 19 , respectively. Waves at the toe of the structure should exceed the 1000-year return period wave storm, with the maximum safety factor of the corresponding model; in this case, at prototype scale, $H_s[\text{m}]=11.0$ and $T_p[\text{s}]=19$ with $\text{SF}(\text{IDe}5\%)=1.30$. It is also convenient to test the models with water levels and wave storm characteristics in the neighborhood of the design storms. Considering a tidal range $\text{HWL-LWL}=\Delta h[\text{m}]=4.5$ and a 1/50 scale, the wave characteristics of the models may be:

Prototype H_s : $6.0 < H_s[\text{m}] < 14.5 = 1.30 \times 11.0$

Model: $H_s[\text{cm}]=12, 14, 16, 18, 20, 22, 24, 26, 28, 30$, etc.

Prototype T_p : $16=6.0 \times 7.0^{0.5}$, $18=5.8 \times 9.5^{0.5}$ and $19=5.7 \times 11.0^{0.5}$

Model: $T_p[\text{s}]=(6.0, 5.8 \text{ and } 5.7) \times (H[\text{cm}]/100)^{0.5}$

Runs of 1000 unidirectional random waves with JONSWAP ($\gamma=3.3$) spectrum

Prototype water levels: $\text{LWL}[\text{m}]=0.0$, $\text{HWL}[\text{m}]=4.5$ and $\text{HWL1}[\text{m}]=5.5$

Model: $\Delta h[\text{cm}] = 0.0, 9.0$ and 11.0

Prototype water depth at the toe: $h_s[\text{m}] = 30$ at LWL

Model: $h_s[\text{cm}] = 60$ at LWL

To prevent wave breaking at the wavemaker, the water depth at the wave generation area should be $h_s[\text{cm}] = 100 \gg 60$ at LWL. Crest elevation at prototype scale is $R_c[\text{m}] = 19.1$, which corresponds to $R_c[\text{cm}] = 38.2$; a reasonable depth for the wave basin would be higher than $150 \text{ cm} (> 100 + 38.2)$.

Each physical model (root and roundhead) can be tested with three water levels and three wave steepnesses (nine test series). Each test series will have about ten runs of 1000 random waves with increasing H_s , from $H_s[\text{cm}] = 12$ to Initiation of Destruction (IDe). Hydraulic stability of armor and toe berm, overtopping rates and pressure on crown wall should be measured to validate the design.

With the experimental design described above, each model will be tested with the design storms ($T_R[\text{year}] = 2, 100$ and 1000) and above the design storms up to IDe. Testing the models with different wave steepnesses, similar to those of the design storm, will provide valuable information to assess the breakwater performance under design storms different than those prescribed during the design phase. Design wave climate may change in time when additional wave climate information is available; this is especially true in the present climate change scenario.

Testing the models with a water level above the prescribed HWL can also provide valuable information about the breakwater performance with overtopping and forces on the crown wall. Testing the physical models around the prescribed design point provides essential information to assess the risk of failure during lifetime, considering different wave climate scenarios.

Model peak periods range $2.1 < T_p[\text{s}] < 3.1$

$$T_p[\text{s}] = 6.0 \times (12/100)^{0.5} = 2.1$$

$$T_p[\text{s}] = 5.0 \times (30/100)^{0.5} = 3.1$$

Model mean period range $1.7 < T_m[\text{s}] \approx T_p[\text{s}] / 1.2 < 2.6$

Approximate duration of runs of 1000 waves: 2000 seconds.

One or two work days are required to calibrate sensors and complete a test series. One work day may be reasonable to reconstruct the model after a test series. One week may be required to check the wave basin and sensors. One week may be required to construct each model.

A minimum of three months is required to validate two models. Additional tests are required for optimization before validation. A minimum of four months' occupation

(40 h/week) of a wave basin 40.0x30.0x1.5 meters (30 m-long wavemaker) is a reasonable estimation to optimize and validate the design of this large mound breakwater.

NOTATIONS

Symbols

a [m]	= distance between consecutive units in the first row
A_c [m]	= upper armor freeboard (crest elevation in reference to SWL)
$(a_{\min})_{mi}$ [m]	= distance between consecutive units in the first row of grid “mi” (roundheads)
b [m]	= horizontal distance between rows
B [m]	= berm width at toe berm crest
B_a [m]	= horizontal upper berm width
B_c [m]	= core crest width
B_e [m]	= crown wall base width
C_B [€/m ³]	= unit construction cost for conventional cube armor units
C_C [€/m ³]	= unit construction cost for Cubipod® armor units
C_R [-]	= H_R/H_I or $H_{sr}/H_{si}=m_{0r}/m_{0i}$ = coefficient of reflection
$\cot\alpha$ [-]	= armor slope
D_e [-]	= equivalent dimensionless damage
D_n [m]	= $(W/\gamma_r)^{1/3}$ = equivalent cube side length or nominal diameter
D_{ni} [m]	= $(W_i/\gamma_i)^{1/3}$ = nominal diameter of quarry stones in layer “i”
D_{n50} [m]	= nominal diameter of quarry stones
e_i [m]	= thickness of layer “I”
f_{ck} [MPa]	= characteristic compressive strength
$f_{ct,k}$ [MPa]	= characteristic tensile strength
f_p [s ⁻¹]	= peak frequency
f_{0p} [s ⁻¹]	= deep water peak frequency
F_h [kN/m]	= unit maximum horizontal force
F_v [kN/m]	= $(F_v(F_h))$ = unit up-lift vertical force corresponding to the wave generating the maximum horizontal force

g [m/s ²]	= 9.81 m/s ² = gravity acceleration
h [m]	= water depth
h_t [m]	= water depth at toe berm crest
h_c [m]	= drop height measured from the lowest point of the unit to be dropped in the free-fall tests
h_e [m]	= equivalent drop height corresponding to prototype free-fall tests
h_{ec} [m]	= critical equivalent height corresponding to prototype free-fall tests
h_f [m]	= crown wall height
h_s [m]	= water depth at breakwater toe
H [m]	= regular wave height
H_{inc} or H_I [m]	= incident wave height (regular waves)
H_{m0} [m]	= $4(m_0)^{0.5}$ = significant wave height
H_R [m]	= reflected wave height (regular waves)
H_s [m]	= significant wave height
H_{sd} [m]	= design significant wave height
H_{si} [m]	= H_{m0i} = significant incident wave height
H_{sr} [m]	= H_{m0r} = significant reflected wave height
HOR [€/m ³]	= unit cost of the concrete supplied
HWL [m]	= High Water Level
HWL1 [m]	= 1.0 meter above HWL
Ir [-]	= $\tan\alpha/(H_I/L_0)^{0.5}$ = Iribarren's number (regular waves)
Ir_m [-]	= $\tan\alpha/(H_{m0}/L_{01})^{0.5}$ = Iribarren's number using H_{m0} and T_{01}
Ir_p [-]	= $\tan\alpha/(H_{m0}/L_{0p})^{0.5}$ = Iribarren's number using H_{m0} and T_p
k [rad/m]	= $2\pi/L$ = wave number
kh [-]	= $2\pi h/L$ = relative water depth
K_D [-]	= stability coefficient
L [m]	= $gT^2 \tanh(2\pi h/L)/2\pi$ = wave length
L_b [m]	= breakwater length
L_m [m]	= $gT_{01}^2 \tanh(2\pi h/L_{01})/2\pi$ = local wave length corresponding to T_{01}

L_0 [m]	= $gT^2/2\pi$ = deep water wave length
L_{01} [m]	= $gT_{01}^2 \tanh(2\pi h/L_{01})/2\pi$ = wave length corresponding to T_{01}
L_{0p} [m]	= $gT_p^2/2\pi$ = deep water wave length corresponding to T_p
LWL [m]	= Low Water Level
m	= cube size index (m=1, 2,..., M)
mi	= grid number (mi=1,2,3,...)
M	= number of different cube unit sizes
M(Fh) [kN]	= unit overturning moment due to Fh
M(Fv(Fh)) [kN]	= unit overturning moment due to Fv(Fh)
n	= Cubipod [®] size index (n=1, 2, ..., N)
n_c	= 1 or 2= number of armor layers
n_f	= number of rows placed in each grid
n_{mi}	= number of rows which can be completed within the grid “mi”
n_r	= number of repetitions of free-fall tests from the same drop height h_c
N	= number of different Cubipod [®] unit sizes
N_{od}	= toe berm damage (number of rocks lost in a D_{n50} width)
N_s [-]	= $H_s/(\Delta D_n)$ = stability number
N_{sd} [-]	= $H_{sd}/(\Delta D_n)$ = design stability number
$N_s(\text{IDa})$	= stability number corresponding to Initiation of Damage
$N_s(\text{IDa}5\%)$	= stability number corresponding to Initiation of Damage with only a 5% probability of not being surpassed
$N_s(\text{IDa}50\%)$	= median value of the stability number to Initiation of Damage
$N_s(\text{IDe})$	= stability number corresponding to Initiation of Destruction
$N_s(\text{IDe}5\%)$	= stability number corresponding to Initiation of Destruction with only a 5% probability of not being surpassed
$N_s(\text{IDe}50\%)$	= median value of the stability number to Initiation of Destruction
N_w	= number of waves
p [-]	= $1-(\Phi/n_c)$ = armor porosity
q [$\text{m}^3/\text{s}/\text{m}$]	= unit overtopping rate

Q [-]	= dimensionless overtopping rate
R [m]	= radius of roundhead or curved trunk
R_c [m]	= crest freeboard (crest elevation referred to SWL)
R_{mi} [m]	= radius of the first row of the grid “mi”
R_{rh} [m]	= initial roundhead radius
R_u [m]	= run-up elevation referring to SWL
R_{uv} [m]	= visual run-up
s_{0p} [-]	= H_{m0}/L_{0p} = deep water wave steepness
$S(n\Delta t)$ [kN/m]	= $(W_e - F_v(n\Delta t))\mu - F_h(n\Delta t)$ = crown wall sliding safety margin failure function
S_d [kN/m]	= $\min[S(n\Delta t)]$ = minimum $S(n\Delta t)$
S_1 [kN/m]	= $(W_e - F_v(F_h))\mu - F_h$ = sliding safety margin corresponding to the maximum horizontal force, $F_h = \max(F_h(n\Delta t))$
SF(IDa)	= $N_s(IDa)/N_{sd}$, safety factor for IDa
SF(IDe)	= $N_s(IDe)/N_{sd}$, safety factor for IDE
t [unit]	= tonne (force or mass)
T [s]	= wave period (regular waves)
T_m [s]	= mean period
T_p [s]	= $1/f_p$ = peak period
T_{0p} [s]	= $1/f_{0p}$ = deep water peak period
T_R [year]	= return period
T_{01} [s]	= m_0/m_1 = mean orbital period
V [m ³]	= total volume of concrete used in the armor
V_B [m ³] units	= total volume of concrete used in the armor to manufacture cube units
V_C [m ³]	= total volume of concrete used in the armor to manufacture Cubipods
V_m [m ³]	= total volume of cubes corresponding to size “m” ($m=1, 2, \dots, M$)
V_n [m ³]	= total volume of Cubipods corresponding to size “m” ($n=1, 2, \dots, N$)
w_c [m]	= crown wall base elevation
W [t] = W_0 [t]	= armor unit weight

W_{50} [t]	= median weight of quarry stones
W_B [t]	= weight of cube units
W_C [t]	= weight of Cubipod [®] units
W_e [kN/m]	= crown wall unit weight
W_i [t]	= median weight of quarry stones of filter layer “i”
W_m [t]	= cube unit weight corresponding to size “m” (m=1, 2, ..., M)
W_n [t]	= Cubipod [®] unit weight corresponding to size “n” (n=1, 2, ..., N)
α [rad or °]	= angle of structure slope
β [-]	= bottom slope
γ_f [-]	= roughness factor
γ_i [t/m ³]	= specific weight of the units in layer i
γ_r [t/m ³]	= specific weight of concrete or quarry stones
γ_w [t/m ³]	= specific weights of water
γ_β [-]	= obliquity factor
Δ [-]	= $(\gamma_r/\gamma_w)-1$ = relative submerged mass density
Δh [m]	= tidal range (HWL-LWL)
θ [°]	= wave obliquity
μ [-]	= friction coefficient between crown wall and rocky bedding layer
ρ_r [t/m ³]	= concrete or quarry stone mass density
ρ_w [t/m ³]	= water mass density
σ [-]	= directional spreading
Φ [-]	= $n_c(1-p)$ = packing density

Acronyms

AAU	= <i>Aalborg University</i> (Denmark)
AD	= Anvil Drop
CDTI	= <i>Centro para el Desarrollo Tecnológico Industrial</i> , Spanish Ministry of Economy and Competitiveness.

CEPYC	= <i>Centro de Estudios de Puertos y Costas</i> belonging to the <i>Centro de Estudios y Experimentación de Obras Públicas</i> (CEDEX), Spanish Ministry of Public Works and Transport.
De	= Destruction
EAD	= Extreme Anvil Drop
ED	= Edge Drop
EED	= Extreme Edge Drop
GPS	= Global Positioning System
IDa	= Initiation of Damage
IDe	= Initiation of Destruction
IH Cantabria	= <i>Instituto de Hidráulica Ambiental de Cantabria</i> (Santander, Spain)
INHA	= <i>Instituto de Hidrodinámica Aplicada</i> (P.T. del Vallés, Spain)
LPC	= <i>Laboratorio de Puertos y Costas de la UPV</i> (Valencia, Spain)
MSE	= Mean Squared Error
OHL	= <i>Obrascón Huarte Lain</i> Group
PCT	= Patent Cooperation Treaty
RD	= Random Drop
RLM	= Relative Loss of Mass
rMSE	= Relative Mean Squared Error
SATO	= <i>Sociedad Anónima de Trabajos y Obras</i> (OHL Group)
SF	= Safety Factor
SPTO	= Spanish Patent and Trademark Office
SWL	= Still Water Level
UDC	= <i>Universidade da Coruña</i> (Spain)
UPM	= <i>Universidad Politécnica de Madrid</i> (Spain)
UPV	= <i>Universitat Politècnica de València</i> (Spain)
Var	= Variance

REFERENCES

- Battjes, J.A. and Groenendijk, H.W. (2000). “Wave height distributions on shallow waters”. *Coastal Engineering*, 40, 161-182.
- Bruce, T., Van del Meer, J., Allsop, W., Franco, L., Kortenhaus, A., Pullen, T. and Schüttrumpf, H. (2009). “Overtopping performance of different armour units for rubble mound breakwaters”. *Coastal Engineering*, 56(2), 166-179.
- Burcharth, H. F., Howell, G. L. and Liu, Z. (1991). “On the determination of concrete armour unit stresses including specific results related to dolosse”. *Coastal Engineering*, 15(1-2), 107-165.
- Burcharth, H.F., Andersen, T.L. and Medina, J.R. (2010). “Stability of Cubipod armoured roundheads in short crested waves”. *Proc. of 32nd Int. Conf. on Coastal Engineering*, ASCE, 32(2010), structures.39
- Burcharth, H.F., Maciñeira-Alonso, E. and Noya-Arquero, F. (2015). “Design, construction and performance of the main breakwater of the new outer port at Punta Langosteira, La Coruña, Spain”. In *Design of Coastal Structures and Sea Defences*, Y.C. Kim (Ed.), Series on Coastal and Ocean Engineering Practice: Vol. 2, World Scientific, Singapore, 23-76.
- CIRIA, CUR, CETMEF (2007). *The Rock Manual. The use of rock in hydraulic engineering (2nd edition)*. C683, CIRIA, London.
- Corredor, A., Torres, R., Miñana, J.V., Fernández, E., Menéndez, C.F., Santos, M., Gómez-Martín, M.E., Goumy, R. and Medina, J.R. (2008). “CUBÍPODO: Estudios de estabilidad hidráulica 2D y 3D, estudio del remonte y rebase, diseño del encofrado y ensayos de caída de prototipos”. *III Congreso Nacional de la Asociación Técnica de Puertos y Costas: Innovación en la construcción y explotación portuaria*, Puertos del Estado, 187-211 (in Spanish).
- Corredor, A., Santos, M., Gómez-Martín, M.E. and Medina, J.R. (2012). “Placement of Cubipod Armor Units in San Andrés Breakwater (Port of Málaga, Spain)”. *Proc. of 33rd Int. Conf. on Coastal Engineering*, ASCE, 33(2012), structures.6.
- Corredor, A., Santos, M., Peña, E., Maciñeira, E., Gómez-Martín, M.E. and Medina, J.R. (2013). “Designing and constructing Cubipod armored breakwaters in the ports of Málaga and Punta Langosteira (Spain)”. *Coasts, Marine Structures and Breakwaters 2013. From Sea to Shore - Meeting the Challenges of the Sea*, ISBN: 9780727759757, ICE Publishing.
- EHE-08 (2008). *Instrucción de hormigón estructural*. Ministerio de la Presidencia, España. REAL DECRETO 1247/2008, de 18 de julio, por el que se aprueba la

- instrucción de hormigón estructural (EHE-08). B.O.E. Nº 203 del 22/08/2008 (in Spanish).
- EurOtop (2007). *European Manual for the Assessment of Wave Overtopping*. Eds. Pullen, T. Allsop, N.W.H. Bruce, T., Kortenhuis, A., Schüttrumpf, H. and Van der Meer, J.W. Retrieved 05/25/2016 from www.overtopping-manual.com.
- Frostick, L.E., McLelland, S.J. and Mercer, T.G. (Eds.) (2011). *Users Guide to Physical Modelling and Experimentation: Experience of the HYDRALAB Network*. CRC Press/Balkema, Leiden, The Netherlands.
- Goda, Y. (2010). Reanalysis of regular and random breaking wave statistics. *Coastal Engineering*, 52 (1), 71–106.
- Gómez-Martín, M.E and Medina, J.R. (2014). “Heterogeneous packing and hydraulic stability of cube and Cubipod armor units”. *J. Waterway, Port, Coastal, Ocean Eng.*, 140(1), 100-108.
- Gómez-Martín, M.E. (2015). *Análisis de la evolución de averías en el manto principal de diques en talud formado por escolleras, cubos y Cubípodos*. PhD Thesis. Universitat Politècnica de València. doi:10.4995/Thesis/10251/59231 (in Spanish).
- Grau, J.I. (2008). “Avances en la construcción de Diques de Abrigo en España”, in *Libro del III Congreso Nacional de la Asociación Técnica de Puertos y Costas*, Organismo Público Puertos del Estado, Madrid, 13-60 (in Spanish).
- Hanzawa, M., Kato, T., Kishira, Y., Ozawa, Y., Niidome, Y., Murakami, T., Ono, A., Hidaka, K., Yoshida, H. and Tanaka, I. (2006). “Fully reinforced 80t Dolos and sloping top caisson in Hososhima Port”. *Proc. 30th Int. Conf. on Coastal Engineering*, ASCE, 4805-4814.
- Herrera, M.P. and Medina, J.R. (2015). “Toe berm design for very shallow waters on steep sea bottoms”. *Coastal Engineering*, 103, 67-77.
- Hudson, R.Y. (1959). “Laboratory investigations of rubble-mound breakwaters”. *Journal of Waterways and Harbors Division*, 89(WW3), 93-121.
- Iribarren, R. (1938). *Una fórmula para el cálculo de diques de escollera*. Ed. M. Bermejillo Usabiaga (Pasajes), July 1938 (in Spanish).
- Lomónaco, P., Vidal, C., Medina, J.R. and Gómez-Martín, M.E. (2009). “Evolution of damage on roundheads protected with cube and Cubipod armour units”. *Proc. Coastal, Marine Structures and Breakwaters 2009*, ICE-Thomas Telford Ltd., Vol. 1, 169-180+186-188.
- Medina, J.R., González-Escrivá, J.A., Garrido, J.M. and De Rouck, J. (2002). “Overtopping analysis using neural networks”. *Proc. 28th Int. Conf. on Coastal Engineering*, ASCE, 2165-2177.

- Medina, J.R., Gómez-Martín, M.E, Corredor, A. and Santos, M. (2010). “Diseño de diques en talud con el manto principal de cubípodos”. *Revista de Obras Públicas*. Colegio de Ingenieros de Caminos, Canales y Puertos. Madrid. 157(3515), 37-52 (in Spanish).
- Medina, J.R., Gómez-Martín, M.E, Corredor, A., Torres, R., Miñana, J.V., Fernández, E., Menéndez, C.F. and Santos, M. (2011). “Prototype drop tests of cube and Cubipod armor units”. *Journal of Waterway, Port, Coastal and Ocean Engineering*, 137(2), 54-63.
- Medina, J.R. and Gómez-Martín, M.E. (2012). “ K_D and safety factors of concrete armor units”. *Proc. 33rd Int. Conf. on Coastal Engineering*, ASCE, 33(2012), structures.29.
- Medina, J.R., Molines, J. and Gómez-Martín, M.E. (2014). “Influence of armour porosity on the hydraulic stability of cube armour layers”. *Ocean Engineering*, 88(2014), 289-297.
- Molines, J. (2009). *Estabilidad de espaldones de diques en talud con mantos de cubos y Cubípodos. Aplicación al dique de abrigo en Gandia (Valencia)*. Final Degree Project ETSICCP de la Universidad Politécnica de Valencia, Sept. 2009 (in Spanish).
- Molines, J. (2010). *Estabilidad de los espaldones de diques en talud con mantos de cubos y Cubípodos*. Premio Modesto Vigueras 2010, Asociación Técnica de Puertos y Costas, Madrid (in Spanish).
- Molines, J. (2011). “Stability of crownwall of cube and Cubipod armoured mound breakwaters”. *PIANC On Course E-Magazine* N° 144-2011, 29-43.
- Molines, J. and Medina, J.R. (2015). “Calibration of overtopping roughness factors for concrete armor units in non-breaking conditions using the CLASH database”. *Coastal Engineering*, 96, 62-70.
- Molines, J. (2016). *Wave overtopping and crown wall stability of cube and Cubipod-armored mound breakwaters*. PhD Thesis. Universitat Politècnica de València. doi:10.4995/Thesis/10251/62178.
- Muttray, M., Reedijk, J.S., Vos-Rovers, I. and Bakker, P. (2005). “Placement and structural strength of Xbloc® and other single layer armour units”. *ICE Coastlines, Structures and Breakwaters*. London, April 2005.
- Pardo, V., Herrera, M.P., Molines, J. and Medina, J.R. (2014). “Placement tests, porosity and randomness of cube and Cubipod armor layer”. *J. Waterway, Port, Coastal, Ocean Eng.*, 140(5), 04014017.
- Pardo, V. (2015). *Análisis de las mallas de colocación y la porosidad de los mantos monopaca y bicapa de Cubípodos en troncos y morros de dique en talud*. PhD

- Thesis. Universitat Politècnica de València. doi:10.4995/Thesis/10251/58608 (in Spanish).
- ROM 0.0-01 (2002). *ROM 0.0 General procedure and requirements in the design of harbor and maritime structures*. Ente Público de Puertos del Estado, Ministerio de Fomento, Madrid (Spain).
- ROM 0.5-05 (2008). *ROM 0.5-05 Geotechnical recommendations for the design of maritime and harbour works*. Ente Público de Puertos del Estado. Ministerio de Fomento (Spain).
- Smolka, E., Zarranz, G. and Medina, J.R. (2009). “Estudio Experimental del Rebase de un Dique en Talud de Cubípodos”. *Libro de las X Jornadas Españolas de Costas y Puertos*, Universidad de Cantabria-Adif Congresos, 803-809 (in Spanish).
- SPM (1975). *Shore Protection Manual*, U.S. Army Coastal Engineering Research Center, Fort Belvoir, Virginia.
- SPM (1984). *Shore Protection Manual*, U.S. Army Engineer Waterways Experiment Station, Coastal and Hydraulics Laboratory, Vicksburg, Mississippi.
- Van der Meer, J.W. (1998). “Geometrical Design of Coastal Structures” in *Seawalls, dikes and revetments*. K.W. Pilarczyk (Ed.). Balkema, Rotterdam.
- Van der Meer, J.W. and Sigurdarson, S. (2014). “Geometrical design of berm breakwaters”. *Proc. 34th Int. Conf. on Coastal Engineering*, 1(34), structures.25.
- Van Gent, M.R.A. and Van der Werf, I.M. (2015). “Rock toe stability of rubble mound breakwaters”. *Coastal Engineering*, 83, 166–176.

FIGURES

Figure 1.1 Six-tonne Cubipod [®] units in the San Andrés Breakwater of the Port of Málaga (Spain).....	2
Figure 1.2 Twenty five-tonne Cubipod [®] units in the Western Breakwater of the Outer Port of A Coruña at Punta Langosteira (Spain).	3
Figure 1.3 Fifteen-tonne cube and sixteen-tonne Cubipod [®] units in the Port of Alicante (Spain).	4
Figure 1.4 Mound breakwater protected by a single-layer Cubipod [®] armor.	5
Figure 1.5 Construction of a Cubipod [®] armored mound breakwater.....	7
Figure 1.6 View of a quarry at Punta Langosteira (Spain).....	8
Figure 1.7 Concrete being poured into the molds to manufacture 25-tonne Cubipod [®] units.	10
Figure 1.8 SATO-designed formwork to manufacture 7-m ³ (16-tonne) Cubipod [®] units.	13
Figure 1.9 Five-level stacking of Cubipod [®] units (Port of Málaga, Spain).	14
Figure 1.10 Breakwater cross section used in the parametric study of construction costs (Corredor et al., 2008).	15
Figure 1.11 Classification of armor construction costs ($L_b[m]=1000$, $h_t[m]=15$, $W[t]=20$).	16
Figure 2.1 Units for single-layer armoring.	22
Figure 2.2 Schematic representation of N_{sd} and safety factors.	23
Figure 2.3 Stability numbers corresponding to IDa and IDe (2-layer cube and Cubipod [®] armors).....	25
Figure 2.4 Stability numbers to IDa and IDe observed for single- and double-layer Cubipod [®] armor trunks.	29
Figure 2.5 3D models of roundheads protected with double-layer Cubipod [®] armors: (a) IH Cantabria, (b) AAU.....	33
Figure 2.6 N_s (IDa) and N_s (IDe) of double-layer cube and Cubipod [®] armors in roundhead.....	34

Figure 2.7a Double roundhead 3D model with single-layer Cubipod [®] armor tested at UDC.	37
Figure 2.11 Schematic cross section of a breakwater in breaking conditions.	44
Figure 3.1 Cross section of 2D model used in overtopping tests (dimensions in cm).	46
Figure 3.2 Dimensionless visual run-up R_{uv}/H_{inc} corresponding to double-layer cube, single- and double-layer Cubipod [®] armors (regular waves).	47
Figure 3.3 Dimensionless visual run-up R_{uv}/H_{inc} observed for double-layer cube and Cubipod [®] armors (regular waves).	49
Figure 3.4 Dimensionless visual run-up R_{uv}/H_{inc} corresponding to double-layer cube and single-layer Cubipod [®] armors (regular waves).	51
Figure 3.5 Example of measured F_h and $F_v(F_h)$ on a double-layer cube armor model.	53
Figure 3.6 Scheme of horizontal and vertical up-lift forces acting on the crown wall.	54
Figure 3.7 Measured coefficient of reflection $C_R(kh)=H_R/H_I$ (regular waves).	59
Figure 3.8 Proportion of measured reflected energy $C_R^2(kh)=(H_R/H_I)^2$ (regular waves).	60
Figure 3.9 Measured coefficient of reflection $C_R(kh)=H_R/H_I$ (regular waves).	60
Figure 4.1 Steel-reinforced concrete overturning platform (10.0x7.5x0.9 m).	65
Figure 4.2 Cubipods dropped on the rigid free-fall platform (5.0x5.0x1.15 m).	67
Figure 4.3 Free-fall tests (AD, ED and RD) and extreme free-fall tests (EAD and EED).	67
Figure 4.4 Sixteen-tonne Cubipod [®] unit being dropped onto four Cubipods in an extreme free-fall test, $h_c[m]=9.5$ (EED).	68
Figure 4.5 Relative loss of mass (RLM) for armor units dropped onto a rigid platform.	69
Figure 4.6 Minimum characteristic tensile and compressive strengths for massive armor units.	70

Figure 5.1 Vertical molds and bases to manufacture 45-tonne (19 m ³) Cubipod [®] units (Port of Punta Langosteira, Spain).....	74
Figure 5.2 Double pressure clamps handling Cubipod [®] units in the block yard.....	74
Figure 5.3 Five-level stacked Cubipod [®] units in the block yard of the Port of Málaga (Spain).....	75
Figure 5.4 Cubipod [®] block yard with gantry cranes (Port of Punta Langosteira, Spain).....	75
Figure 5.5 Block yard of 3-tonne Cubipod [®] units handled with a forklift (Marina Bay D’Alger, Algeria).....	76
Figure 5.6 Block yard of 6-tonne Cubipod [®] units handled by a boom truck (Port of Las Palmas, Spain).....	76
Figure 5.7 Molds and production line of 25-tonne (10.6 m ³) Cubipods (Port of Punta Langosteira, Spain).....	77
Figure 5.8 Vertical molds and bases to manufacture 6-tonne (2.6 m ³) Cubipod [®] units (Port of Las Palmas, Spain).....	78
Figure 5.9 Block yard and production line of 6-tonne (2.6 m ³) Cubipods (Port of Las Palmas, Spain).....	79
Figure 5.10 Main dimensions of Cubipod [®] units (front/side/top view).....	80
Figure 5.11 Extensive Cubipod [®] block yard with wheeled cranes at the Port of Málaga (Spain).....	81
Figure 5.12 Stacking Cubipods in “open” and “closed” arrangements.....	82
Figure 5.13 Schematic plan view of an intensive block yard with gantry crane.....	82
Figure 5.14 Loading Cubipods onto a platform to be transported to the placement site.....	83
Figure 6.1 Twenty-five-tonne single-layer Cubipod [®] armor protecting the Southern Breakwater at Punta Langosteira (A Coruña, Spain).....	86
Figure 6.2 Placing Cubipods in San Andrés Breakwater (Port of Málaga, Spain).....	87
Figure 6.3 Mound breakwater cross section with toe berm and scour protection apron.....	88
Figure 6.4 Single-layer Cubipod [®] armored breakwater with toe berm and crown wall.....	89
Figure 6.5 Sketch of breakwater in deep water.....	89

Figure 6.6 Sketch of breakwater cross section with toe berm.	90
Figure 6.7 Fixed and progressive placement grids.	92
Figure 6.8 Realistic armor placement. Straight trunk.	92
Figure 6.9 Coupled grids to place Cubipods on roundheads.	95
Figure 6.10 Small-scale realistic placement of Cubipods in trunk and roundhead.	96
Figure 6.11 Reference area to measure the armor porosity in the roundhead.	96
Figure 6.12 Transition single-to-double Cubipod® armor.	98
Figure 6.13 Single-layer Cubipod® armor advancing on the first layer of Cubipods.	98
Figure 7.1 Breakwater plan view.	102
Figure 7.2 Cross section of the crown wall for a double-layer cube armored breakwater.	114
Figure 7.3 Cross section of a double-layer cube armored breakwater trunk with toe berm.	115
Figure 7.4 Cross section of a double-layer cube armored breakwater trunk without toe berm.	115
Figure 7.5 Cross section of the crown wall for a single-layer Cubipod® armored breakwater.	116
Figure 7.6 Cross section of a single-layer Cubipod® armored breakwater trunk.	117
Figure 7.7 Cross section of a crown wall for a double-layer Cubipod® armored breakwater.	118
Figure 7.8 Cross section of a double-layer Cubipod® armored breakwater trunk.	119
Figure 7.9 Cross section of double-layer Cubipod® armored roundhead (Alternative B2).	125
Figure 7.10 Cross section of single-layer Cubipod® armored roundhead (Alternative B1).	127
Figure 7.11 Plan view of the transitions for a single-layer Cubipod® armored roundhead.	127
Figure 7.12 Cross section of single-layer Cubipod® armored trunk at $hs[m]=10$ (LWL).	130

TABLES

Table 1.1 Minimum characteristic compressive and tensile strengths at 28 days for concrete to manufacture cube and Cubipod [®] armor units.	11
Table 2.1 K_D and safety factors associated with different concrete armor units.	24
Table 2.2 Safety factors of double-layer cube and Cubipod [®] armor trunks.	26
Table 2.3 Safety factors to IDa and IDe (percentiles 5% and 50%) for single- and double- layer Cubipod [®] armors (trunk).	30
Table 2.4 Safety factors for double-layer cube and Cubipod [®] armors in trunk and roundhead.	35
Table 4.1 Minimum characteristic compressive and tensile strengths at 28 days to manufacture cube and Cubipod [®] concrete armor units.	72
Table 7.1 Safety factors for single- and double-layer trunk and roundhead armors. ...	104
Table 7.2 Cost and logistic characteristics of alternatives A, B and C.	123

CUBIPOD® MANUAL 2016

JOSEP R. MEDINA | M. ESTHER GÓMEZ-MARTÍN

Cubipod® Manual 2016 provides basic criteria for preliminary design of mound breakwaters protected with single -or double- layer Cubipod® armors. Economic, logistic and environmental factors are analyzed to guide the designers in the preliminary design phase of a breakwater. The economic cost of a large mound breakwater usually depends critically on the geometry of the concrete unit used for the armor layer. Each geometry (cube, Cubipod®, Tetrapod, etc.) and placement pattern (random, specific, ordered, etc.) can be used for single-layer armoring, double-layer armoring or both. Each armor design alternative, with a different packing density, has a different hydraulic performance and logistic constraints. Although some general rules and comments are applicable to other armor units, *Cubipod® Manual 2016* is focused on the use of Cubipod® units in conventional mound breakwaters.

